A NEW EIGHTEEN PARAMETER TRIANGULAR ELEMENT FOR GENERAL PLATE AND SHELL ANALYSIS

by

TERRANCE WILLIAM BEARDEN

B.A.Sc. (1974)

The University of Manitoba

A THESIS SUBMITTED IN PARTIAL FULFILMENT OF
THE REQUIREMENTS FOR THE DEGREE OF
MASTER OF APPLIED SCIENCE

in the Department
of
CIVIL ENGINEERING

We accept this thesis as conforming
to the required standard

The University of British Columbia

April, 1976

© Terrance William Bearden, 1976

In presenting this thesis in partial fulfilment of the requirements for an advanced degree at the University of British Columbia, I agree that the Library shall make it freely available for reference and study. I further agree that permission for extensive copying of this thesis for scholarly purposes may be granted by the Head of my Department or by his representatives. It is understood that copying or publication of this thesis for financial gain shall not be allowed without my written permission.

T.W. Bearden

Department of Civil Engineering

The University of British Columbia
2075 Wesbrook Place
Vancouver, Canada
V6T 1W5

April, 1976

ABSTRACT

The purpose of this investigation was to develop an eighteen parameter flat triangular finite element for analyzing plate and shell structures. The development of the element was accomplished by combining a plate bending element with a new plane stress element. The well known nine parameter triangle using the normal displacement and two slopes at each vertex was used for the plate bending element. This element contains an incomplete cubic for the normal displacement. For the in-plane element, complete cubics were used initially for the displacements and then various constraints were imposed to reduce the number of generalized co-ordinates to nine, namely the two in-plane displacements and an in-plane rotation at each vertex. One of the constraints, namely that the included angle at each vertex was invariant, destroyed the completeness of the element. However, the element was compatible in the plane.

A patch-type test of the in-plane element showed that it could not represent all constant strain states exactly. However, the errors were small. The complete element was then tested on a plane stress cantilever beam, a square plate subjected to membrane stresses only, a cylindrical shell, a spherical shell and a non-prismatic folded plate structure. In all cases, reasonable engineering accuracy was achieved with modest grids of elements. Thus it was concluded that the incompleteness of the in-plane element was not too important.

Finally, a compatible beam element was formulated and tested to supplement the triangular element. The beam element formulation included unsymmetric crosssections.

TABLE OF CONTENTS

LIST OF TABLES

LIST OF FIGURES

LIST OF SYMBOLS

Symbols	Definition
A	Area of triangle
{A}	Column vector of polynomial coefficients
a,b,c	Element dimension, Figure 3.5
a_i	Coefficients of the displacement polynomials, Equation 3.2
[B]	Strain-displacement matrix
C_j, S_j	Cosine & sine of the angle α, Figure 3.1
C.L.	Centre line
C.S.T.	Constant strain triangle formulation
[D]	Elasticity matrix
E	Modulus of elasticity of the material being modelled & that of the finite elements
e	Eccentricity, Figure 5.2
Eqn.	Equation
F(m,n)	Modified Euler's beta function, Eqn. 3-33
{F}	Load vector
Fig.	Figure
G	Shear modulus of elasticity
IN.	Inches
I_y, I_{yz}, I_z	Moment of inertias
J	Polar moment of inertia
[K]	Stiffness matrix
ℓ_i	Area co-ordinates used in the linear strain triangle
L	Length of beam stiffener element
L_i	Area co-ordinates used in plate bending formulation

L.S.T.	Linear strain triangle
N	Number of sub-divisions (grid refinement)
N_i	Shape functions used in the plate bending formulation
N_x, N_y, N_{xy} $N_\theta\ N_\phi\ N_{\theta\phi}$	Membrane stresses
{P}	Load vector
r_1, r_2, r_3	Length of element's sides
r_y, r_z	Radii of curvature
[T]	Transformation matrix ex. Equation 3-28
U	Strain Energy
u, v	Displacements in the x & y direction, respectively
$\ddot{u}_{nij}$	Normal displacement at node i to node j
$\ddot{u}_{nk}$	Normal displacement at node k
$\ddot{u}_{tij}$	Tangential displacement at node i to node j
$\ddot{u}_{tk}$	Tangential displacement at node k
$\ddot{w}$	Normal out of x,y plane displacement
W_i, W_e	Internal & external work
x,y,z	Global cartesian co-ordinates
α	Angle tangent to element side & axis, Figure 3.1
$\{\delta\}$	Deflection vector
$\{\varepsilon\}$	Strain vector
ξ, ζ	Local co-ordinates, Figure 3.5
$\{\sigma\}$	Stress vector
θ, ϕ	Angle, Figure 6.12
$[\lambda]$	Direction cosine matrix
γ_i	Shear strain at node i

ν	Poisson's ratio
ω	Rotation
$\backsimeq$	Corresponds to

Subscripts

A	With respect to polynomial coefficients
b	Flexural action (bending)
c	Centroid of element
G	Global co-ordinate system
L	Local co-ordinate system
P	Membrane action (plane stress)
x,y,ξ,ζ	Denote derivatives of displacement with respect to x,y,ξ,ζ
δ	With respect to the actual degree of freedom

Superscript

T	Denotes transposition of rows and columns of a matrix

Special Symbols

[ ]	Denotes a matrix
{ }	Denotes a column vector

ACKNOWLEDGEMENTS

The author would like to express his appreciation to his advisor, Dr. M. D. Olson for his assistance, encouragement and for reading and checking the entire thesis.

Also, the author would like to thank Dr. N. D. Nathan for his assistance.

The author would like to extend his thanks to Sarah Dahabieh for typing the manuscript.

I am also very grateful to the Defence Research Board and the National Research Council for their financial assistance.

CHAPTER 1

INTRODUCTION

The method of finite elements originated about twenty years ago in the field of engineering and has since developed immensely. The basic idea behind the method is that a solution region can be approximated by replacing it with an assemblage of descrete elements. The finite element procedure reduces the problem to one of a finite number of unknowns by dividing the solution region into elements and by expressing the unknown field in terms of assumed approximating functions within each element. The approximating or interpolation functions used herein are defined in terms of the values of the displacement field variables at specific points called nodes. These nodal variables are the unknowns which are solved for. The interpolation functions cannot be chosen arbitrarily because certain compatibility conditions have to be satisfied. The accuracy of the solution depends not only on the size of elements used but also on the interpolation functions incorporated. One major advantage of the finite element method is that the force - displacement or stiffness characteristics of each element can be computed and then the elements assembled to represent the stiffness of the overall structure.

When choosing the interpolation functions that are to be incorporated in deriving an element's stiffness characteristics, discretion has to be used. The higher the order of the functions used the more complex the formulation becomes and the problem size increases greatly demanding more computer memory to be utilized. However if the polynomials are very low in order then accuracy can be lost even though a great many elements can be used in the analysis. It is desired to develop a relatively low order triangular finite element in plane stress which when combined with a triangular plate bending element, can be used to model shell and folded plate structures with reasonable accuracy and economy. Starting with complete cubic polynomials to represent the two in-plane displacements and an in-plane rotation at each node of the plane stress element, various constraints are then introduced to reduce the number of degrees of freedom to nine for the element. This element was then combined with the well known Zienkiewicz nine parameter plate bending triangular element which uses a cubic polynomial for the normal displacement.

A computer program employing the new eighteen degree of freedom triangular finite element was developed. Various shell structures and a folded plate one were analyzed and results were compared with analytical solutions. Subsequently a twelve degree of freedom unsymmetrical beam stiffener element was formulated so that stiffened plate and stiffened shell structures could also be modeled.

CHAPTER 2

GENERAL INFORMATION

2.1 Finite Element Technique: The assumptions used in the finite element method herein are:

1) The element's thickness is uniform.
2) The material is elastic, isotropic and homogeneous.
3) Elements are assumed to be connected only at node points.
4) Relation between forces and deformations is linear.
5) Small deflection theory is assumed from plate theory; therefore there isn't any coupling of the in-plane and bending actions.

2.1.1 Description of Method - Displacement Approach: Using the potential energy (P.E.) principle, we assume a displacement field within the element. For equilibrium, the P.E. is a minimum and the internal work (strain energy) is equivalent to the work done by the external forces acting on the element. From this approach the stiffness characteristics of the element can be defined. This is illustrated below:

The stresses in a continuum are expressed in terms of strains

$$\{ \sigma \} = [D] \{ \varepsilon \} \qquad 2 - 1$$

where $\{ \sigma \}$ = Stress Vector

$[D]$ = Elasticity Matrix

$\{ \varepsilon \}$ = Strain Vector

The strains at any point within an element can be described in terms of the nodal displacements as

$$\{ \varepsilon \} = [B] \{ \delta \} \qquad 2 - 2$$

where $\{ \delta \}$ = nodal displacement vector

$[B]$ = strain-displacement matrix.

assuming a virtual displacement $\{\delta\}^*$ at the nodes, the external work W_e done by the nodal loads $\{ P\}$ is:

$$W_e = \{ \delta \}^{*T} \{ P \} \qquad 2\text{-}3$$

Similarly the internal work W_i done by the element when subjected to the virtual displacement is:

$$W_i = \int_{vol.} \{ \varepsilon \}^{*T} \{ \sigma \} \, dvol. \qquad 2\text{-}4$$

substituting equations 2-1 and 2-2 into 2-4 yields

$$W_i = \int \{\delta \}^{*T} [B]^T [D] [B] \{ \delta \} \, dvol. \qquad 2\text{-}5$$

equating the internal work with the external work yields

$$\{ \delta \}^{*T} \{ P \} = \{ \delta \}^{*T} \int_{vol} [B]^T [D] [B] \, dvol \{ \delta \} \qquad 2\text{-}6$$

then for an arbitrary virtual displacement $\{ \delta \}^*$

$$\{ P \} = \int_{vol} [B]^T [D] [B] \, dvol \{ \delta \} \qquad 2\text{-}7$$

and $\{ P \} = [K] \{ \delta \}$ 2-8

So

$$[K] = \int_{vol} [B]^T [D] [B] \, dvol. \qquad 2\text{-}9$$

where $[K]$ = element stiffness matrix

CHAPTER 3

DERIVATION OF THE ELEMENT'S PROPERTIES

3.1 General Information:

A triangular element is used because its shape affords easy application to many types of problems where rectangular elements could not be used. For example modelling odd shaped objects and desiring subsequent grid refinements in regions of high stress gradients. This is illustrated later with a non-prismatic folded plate roof and various shell roofs. It is assumed that the behavior of a continuously curved surface can be adequately represented by the behavior of a surface built up of small, flat elements. From plate theory small deflections are assumed so that the in-plane and bending actions are assumed uncoupled within each flat element.

It is desired to make the finite element as near to being compatible as possible. A compatible element is one which satisfies sufficient inter-element continuity requirements that the total potential energy in the structure converges monotonically towards a minimum as the mesh of finite elements is progressively refined(7). The potential energy is a minimum when; among all the kinematically admissible displacements, those satisfying the equilibrium conditions make the potential energy stationary. The definition of compatibility may also be expressed as follows; if a dependent variable in a structure enters the energy expression with highest derivative of order $q > 0$, then the $(q - 1)$ derivative of that variable must be continuous between adjacent compatible elements(7). For plate bending, the highest derivative is two so the first derivative of the normal displacement or the slope must be continuous. The element to be compatible must have continuous slopes (rotations) and displacements for modelling plate and shell structures. For in plane or membrane action, the highest derivative is one, so only the displacements and not the slopes have to be continuous for compatibility.

Convergence to the correct minimum potential energy is obtained if the polynomials are complete to order P. Where P is the maximum derivative in the energy expression. Only completeness to order P is necessary for convergence. The finite element described herein is the result of combining an in-plane and a plate bending element. For the in-plane portion the highest derivative in the energy expression is one, so only complete first order polynomials in u and v are required to ensure convergence of the potential energy. The energy expression for plate bending has highest derivatives of order two. Then at least a complete quadratic polynomial must be used for the normal displacement to ensure convergence.

3.2 In-Plane Element Formulation:

As mentioned earlier it is desired to combine a 9 degree of freedom triangular plane stress element with the well known Zienkiewicz 9 parameter plate bending triangular element to represent folded plate and shell structures. So the two displacements u and v and an in-plane rotation are used at each node to define the plane stress finite element. (refer to fig. 3.5)

Beginning with complete cubic polynomials for each of the two in-plane displacements, constraints are introduced to force the displacement parallel to an edge to vary only linearly along that edge and to force the included angle at each vertex to remain fixed. Condensation of the remaining two degrees of freedom then yields the 9 parameter element.

Then proceding as mentioned above, the 9 x 9 stiffness matrix in local co-ord is developed:

Starting with complete cubic polynomials:

$$u = a_1 + a_2\xi + a_3\zeta + a_4\xi^2 + a_5\xi\zeta + a_6\zeta^2 + a_7\xi^3 + a_8\xi^2\zeta + a_9\xi\zeta^2 + a_{10}\zeta^3 \qquad 3\text{-}1$$

$$V = a_{11} + a_{12}\xi + a_{13}\zeta + a_{14}\xi^2 + a_{15}\xi\zeta + a_{16}\zeta^2 + a_{17}\xi^3 + a_{18}\xi^2\zeta + a_{19}\xi\zeta^2 + a_{20}\zeta^3 \qquad 3\text{-}2$$

But constraints are to be introduced to force the displacement parallel to an edge to vary linearly along it, so, u can be rewritten omitting the squared and cubic terms in ξ only. (for side one).

$$u = a_1 + a_2\xi + a_3\zeta + a_4\xi\zeta + a_5\zeta^2 + a_6\xi^2\zeta + a_7\xi\zeta^2 + a_8\zeta^3 \qquad 3\text{-}1a$$

In series notation:

$$u = \sum_{i=1}^{8} a_i\, \xi^{mi}\, \zeta^{pi} \qquad 3\text{-}1b$$

$$V = \sum_{i=1}^{10} a_{i+8}\, \xi^{li}\, \zeta^{ni} \qquad 3\text{-}2a$$

where

$$\{m\}^T = \langle 0\ 1\ 0\ 1\ 0\ 2\ 1\ 0 \rangle$$
$$\{p\}^T = \langle 0\ 0\ 1\ 1\ 2\ 1\ 2\ 3 \rangle$$
$$\{l\}^T = \langle 0\ 1\ 0\ 2\ 1\ 0\ 3\ 2\ 1\ 0 \rangle$$
$$\{n\}^T = \langle 0\ 0\ 1\ 0\ 1\ 2\ 0\ 1\ 2\ 3 \rangle$$

So initially we begin with 18 parameters and wish to reduce these to 9.

First Reduction: Force a displacement parallel to an edge to vary linearly along it. (refer to fig. 3.1)

let $s = \sin\alpha$

$c = \cos\alpha$

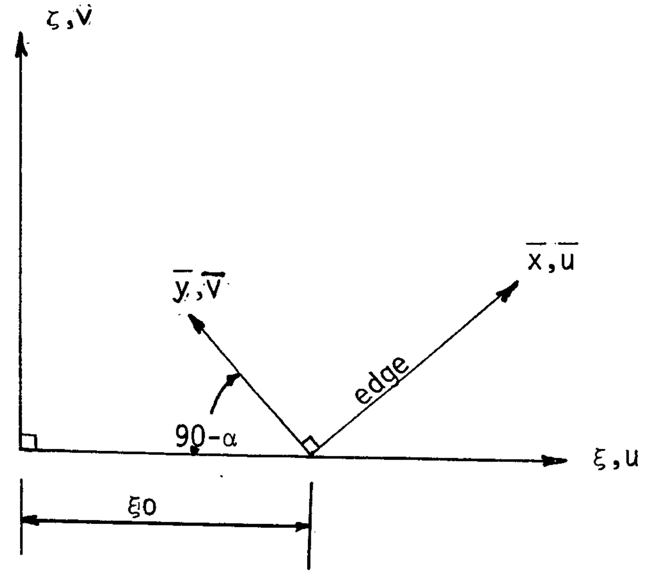

Fig. 3.1 Co-ordinate Systems

then

$$\bar{u} = uc + vs \qquad\qquad 3\text{-}3$$
$$\bar{v} = -us + vc$$

also

$$\xi = \xi_o + \bar{x}c - \bar{y}s \qquad\qquad 3\text{-}4$$
$$\zeta = \bar{x}s + \bar{y}c$$

Referring to equations 1b and 2a and substituting equations 4 then;

$$u = \sum_{i=1}^{8} a_i \,(\xi_o + \bar{x}c - \bar{y}s)^{ni}\,(\bar{x}s + \bar{y}c)^{pi} \qquad \text{3-1c}$$

and

$$v = \sum_{i=1}^{10} a_{i+8}\,(\xi_o + \bar{x}c - \bar{y}s)^{li}\,(\bar{x}s + \bar{y}c)^{ni} \qquad \text{3-2b}$$

but

$\bar{u} = uc + vs$ from equations 3

so the tangential displacement along an edge is $\bar{u}$

$$\bar{u} = c\,[\sum_{i=1}^{8} a_i\,(\xi_o + \bar{x}c - \bar{y}s)^{ni}\,(\bar{x}s + \bar{y}c)^{pi}] + $$

$$+ s\,[\sum_{i=1}^{10} a_{i+8}(\xi_o + \bar{x}c - \bar{y}s)^{li}\,(\bar{x}s + \bar{y}c)^{ni}] \qquad \text{3-5}$$

and we are interested in $\bar{u}$ along an edge,

where $\bar{y} = 0$ therefore

$$\bar{u} = c\,[\sum_{i=1}^{8} a_i\,(\xi_o + \bar{x}c)^{mi}\,(\bar{x}s)^{pi}] + s\,[\sum_{i=1}^{10} a_{i+8}\,(\xi_o + \bar{x}c)^{li}\,(\bar{x}s)^{ni}] \qquad \text{3-6}$$

For $\bar{u}$ to vary linearly along an edge, we want the squared and cubic terms of $\bar{x}$ to vanish:

<u>Squared terms:</u>

$$sc^2a_{12} + cs\,(ca_4 + sa_{13}) + s^2\,(ca_5 + sa_{14}) +$$

$$+ s3c^2\xi_o\,a_{15} + cs2\xi_o\,(ca_6 + sa_{16}) +$$

$$+ s^2\xi_o\,(ca_7 + sa_{17}) = 0 \qquad \text{3-7}$$

Cubic Terms:

$$sc^3 a_{15} + c^2 s\ (ca_6 + sa_{16}) + s^2 c\ (ca_5 + sa_{17}) +$$
$$+ s^3\ (ca_8 + sa_{18}) = 0 \qquad 3\text{-}8$$

Note:

Equations 7 and 8 are constraint equations for sides 2 and 3 of the element. Therefore actually 4 constraints are applied, leaving 5 parameters to be removed to yield the 9 desired.

The cos α and sin α (c and s) should actually be subscripted where j = 1, 2, 3 (side number).

Table 3.1 Trigonometric relations for the Element

Side j	Cj	Sj	ξo_j
1	1	0	0
2	$-a/r_2$	c/r_2	a
3	b/r_3	c/r_3	-b

where

$r_1 = a + b$, $r_2 = \sqrt{a^2 + c^2}$, $r_3 = \sqrt{b^2 + c^2}$ are the lengths of the 3 sides of the elements.

In-Plane Rotations:

Define the rotation of one side of the element to be

$$\omega = \frac{\partial \bar{V}}{\partial \bar{x}}$$

where

$$\frac{\partial \bar{V}}{\partial \bar{x}} = \frac{\partial \xi}{\partial \bar{x}} \frac{\partial \bar{V}}{\partial \xi} + \frac{\partial \zeta}{\partial \bar{x}} \frac{\partial \bar{V}}{\partial \zeta}$$

from equations 4 and 3

$$\frac{\partial \xi}{\partial x} = c \qquad \frac{\partial \zeta}{\partial \bar{x}} = s$$

therefore

$$\frac{\partial \bar{V}}{\partial \bar{x}} = c \frac{\partial \bar{V}}{\partial \xi} + s \frac{\partial \bar{V}}{\partial \zeta}$$

$$= c \left(- u_\xi s + V_\xi c \right) + s \left(- u_\zeta s + V_\zeta c \right) \qquad 3\text{-}9$$

where

$$u_\xi = \frac{\partial u}{\partial \xi}, \text{ etc.}$$

from equations 1b and 2 a :

$$u_\xi = \sum_{i=1}^{8} a_i m_i \xi^{mi-1} \zeta^{pi} , \qquad V_\xi = \sum_{i=1}^{10} a_{i+8} \, li \xi^{li-1} \zeta^{ni}$$

$$u_\zeta = \sum_{i=1}^{8} a_i p_i {}^{mi} \; {}^{pi-1} , \qquad V_\zeta = \sum_{i=1}^{10} a_{i+8} \, ni \xi^{li} \zeta^{ni-1}$$

then

$$\frac{\partial \bar{v}}{\partial \bar{x}} = c_j \left[- s_j \sum_{i=1}^{8} a_i m_i \xi^{mi-1} \zeta^{pi} + c_j \sum_{i=1}^{10} a_{i+8} \; li \, \xi^{li-1} \zeta^{ni} \right] +$$

$$+ s_j \left[- s_j \sum_{i=1}^{8} a_i p_i \xi^{ni} \zeta^{pi-1} + c_j \sum_{i=1}^{10} a_{i+8} \; n_i \xi^{li} \zeta^{ni-1} \right] \qquad 3\text{-}10$$

for the jth side of the element

<u>Define:</u> The rotation at a node to be the average of the 2 side rotations at the node (refer to fig. 3.2)

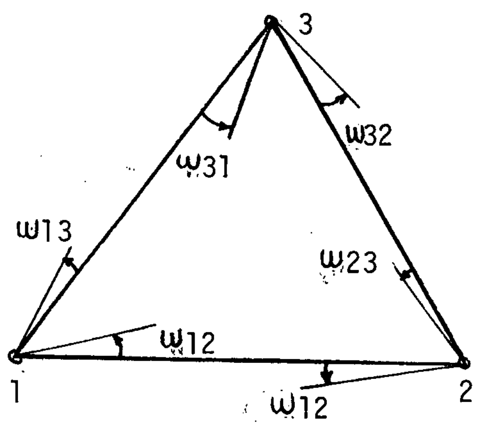

Fig. 3.2 Rotations for an Element

$$\omega_1 = \frac{\omega_{12} + \omega_{13}}{2}$$

$$\omega_2 = \frac{\omega_{21} + \omega_{23}}{2} \qquad 3\text{-}11$$

$$\omega_3 = \frac{\omega_{32} + \omega_{31}}{2}$$

Rotation at node (1):

Co-ordinates $(\xi_1, \zeta_1) = (-b, 0)$

$$\omega_{12} = a_{10} - 2a_{12}b + 3a_{15}b^2 \qquad 3\text{-}12$$

$$\omega_{13} = \frac{-bca_2}{r_3^2} + \frac{b^2}{r_3^2}(a_{10} - 2a_{12}b + 3a_{15}b^2) +$$

$$\frac{-c^2}{r_3^2}(a_3 - a_4 b + a_6 b^2) + \frac{bc}{r_3^2}(a_{11} - a_{13}b + a_{16}b^2) \qquad 3\text{-}13$$

then

$$\omega_1 = \frac{-bc}{r_3^2} a_2 + a_{10}\left(\frac{b^2}{r_3^2} + 1\right) - 2ba_{12}\left(1 + \frac{b^2}{r_3^2}\right) + 3a_{15}b^2\left(1 + \frac{b^2}{r_3^2}\right) +$$

$$-\frac{c^2}{r_3^2}(a_3 - a_4 b + a_6 b^2) + \frac{bc}{r_3^2}(a_{11} - a_{13}b + a_{16}b^2)] * \frac{1}{2}$$

3-14

Rotation at node (2):

$(\xi_2, \zeta_2) = (a, 0)$

$$\omega_{21} = a_{10} + 2a_{12}a + 3a_{15}a^2 \qquad 3\text{-}15$$

$$\omega_{23} = \frac{ac}{r_2^2} a_2 + \frac{a^2}{r_2^2}(a_{10} + 2a_{12}a + 3a_{15}a^2) +$$

$$-\frac{c^2}{r_2^2}(a_3 + a_4 a + a_6 a^2) - \frac{ca}{r_2^2}(a_{11} + a_{13}a + a_{16}a^2)$$

3-16

then

$$\omega_2 = [\, \frac{ac}{r_2^2} a_2 + a_{10} \left(1 + \frac{a^2}{r_2^2} \right) + 2aa_{12} \left(1 + \frac{a^2}{r_2^2} \right) + 3a^2 a_{15} \left(1 + \frac{a^2}{r_2^2} \right) +$$

$$- \frac{c^2}{r_2^2} (a_3 + a_4 a + a_6 a^2) - \frac{ca}{r_2^2} (a_{11} + a_{13} a + a_{16} a^2)] * \frac{1}{2}$$

3-17

Rotations at node (3):

$$(\xi_3, \zeta_3) = (o, c)$$

$$\omega_{32} = \frac{ac}{r_2^2} (a_2 + a_4 c + a_7 c^2) + \frac{a^2}{r_2^2} (a_{10} + a_{13} c + a_{17} c^2) +$$

$$- \frac{c^2}{r_3^2} (a_3 + 2a_5 c + 3a_8 c^2) - \frac{ca}{r_2^2} (a_{11} + 2a_{14} c + 3a_{18} c^2)$$

3-18

$$\omega_{31} = - \frac{bc}{r_3^2} (a_2 + a_4 c + a_7 c^2) + \frac{b^2}{r_3^2} (a_{10} + a_{13} c + a_{17} c^2) +$$

$$- \frac{c^2}{r_3^2} (a_3 + 2a_5 c + 3a_8 c^2) + \frac{bc}{r_3^2} (a_{11} + 2a_{14} c + 3a_{18} c^2)$$

3-19

then

$$\omega_3 = [\, c \left(\frac{a}{r_2^2} - \frac{b}{r_3^2} \right) (a_2 + a_4 c + a_7 c^2) + \left(\frac{a^2}{r_2^2} + \frac{b^2}{r_3^2} \right)$$

$$(a_{10} + a_{13} c + a_{17} c^2) - c^2 \left(\frac{1}{r_2^2} + \frac{1}{r_3^2} \right) (a_3 + 2a_5 c + 3a_8 c^2) +$$

$$+ c \left(\frac{b}{r_3^2} - \frac{a}{r_2^2} \right) (a_{11} + 2a_{14} c + 3a_{18} c^2)] * \frac{1}{2} \qquad 3\text{-}20$$

Shear Strains:

Shear strain is normally defined as the change in angle from a right angle but since our element's sides are not initially at right angles to one another, we have to redefine the shear strains as:

Define

$\gamma \equiv$ The difference of the side rotations at a node.

So

$$\gamma_1 = \frac{\omega_{12} - \omega_{13}}{2} \qquad 3\text{-}21a$$

$$\gamma_2 = \frac{\omega_{23} - \omega_{21}}{2} \qquad 3\text{-}21b$$

$$\gamma_3 = \frac{\omega_{31} - \omega_{32}}{2} \qquad 3\text{-}21c$$

Shear strain at node (1) is:

From equations 12, 13 substituted into equation 21a, yields

$$\gamma_1 \equiv [\frac{bc}{r_3^2} a_2 + a_{10} (1 - \frac{b^2}{r_3^2}) - 2a_{12}b (1 - \frac{b^2}{r_3^2}) + + 3a_{15}b^2 (1 - \frac{b^2}{r_3^2}) + \frac{c^2}{r_3^2} (a_3 - a_4 b + a_6 b^2) - \frac{bc}{r_3^2} (a_{11} - a_{13}b + a_{16}b^2)] \frac{1}{2} \qquad 3\text{-}22$$

Shear strain at node (2):

From equations 15 and 16 substituted into equation 21b gives

$$\gamma_2 = [- \frac{ac}{r_2^2} a_2 + a_{10} (1 - \frac{a^2}{r_2^2}) \pm 2aa_{12} (1 - \frac{a^2}{r_2^2}) +$$

$$+ 3a^2 a_{15} \left(1 - \frac{a^2}{r_2^2} \right) + \frac{c^2}{r_2^2} \left(a_3 + a_4 a + a_6 a^2 \right) + \frac{ca}{r_2^2}$$

$$\left(a_{11} + a_{13} a + a_{16} a^2 \right)] * \frac{1}{2} \qquad 3\text{-}23$$

<u>Shear Strain at node (3):</u>

Substitute equations 18 and 19 into 21c yields:

$$\gamma_3 = [\, c \left(\frac{a}{r_2^2} + \frac{b}{r_3^2} \right) \left(a_2 + a_4 c + a_7 c^2 \right) + \left(\frac{a^2}{r_2^2} - \frac{b^2}{r_3^2} \right)$$

$$\left(a_{10} + a_{13} c + a_{17} c^2 \right) + c^2 \left(\frac{1}{r_3^2} - \frac{1}{r_2^2} \right) \left(a_3 + 2a_5 c + 3a_8 c^2 \right) +$$

$$- c \left(\frac{a}{r_2^2} + \frac{b}{r_3^2} \right) \left(a_{11} + 2a_{14} c + 3a_{18} c^2 \right)] * \frac{1}{2} \qquad 3\text{-}24$$

<u>Summarizing</u> the generalized displacement vector is:

$$\{\delta\} = \left\langle \underbrace{u_1, v_1, w_1, u_2, \ldots w_3}_{\text{9 desired degrees of freedom}},\ \underbrace{u_c, v_c}_{\text{centroidal degrees of freedom to be statically condensed later.}},\ \underbrace{\gamma_1, \gamma_2, \gamma_3}_{\text{shear strains set to 0}},\ \underbrace{0, 0}_{\text{square \& cubic side 2}},\ \underbrace{0, 0}_{\text{square \& cubic side 3}} \right\rangle$$

<u>Note:</u>

The nodal shear strains are all set to zero later.

$$\gamma_1 = \gamma_2 = \gamma_3 = 0$$

Transformation matrix relating the degree of freedom to the polynomial coefficients is:

$$\underset{18 \times 1}{\{ \delta \}} = \underset{18 \times 18}{[T]} \underset{18 \times 1}{\{ A \}} \qquad 3\text{-}25$$

where

$[T]$ = Transformation matrix

$$\{ A \} = \begin{Bmatrix} a_1 \\ a_2 \\ \cdot \\ \cdot \\ \cdot \\ a_{18} \end{Bmatrix}$$

The transformation matrix is written out in full on next page (Table 3.2)

where

- c_i s_i are sine and cosine of angle α for side i
- B, C and A are dimensions of the element
- r_1, r_2, r_3 are the lengths of the 3 sides of the element.

TABLE 3.2: TRANSFORMATION MATRIX FOR PLANE STRESS ELEMENT (1)

$\underset{9,1}{\overset{1,1}{\Big[}} T \underset{9,9}{\overset{1,9}{\Big]}} =$

	a_1	a_2	a_3	a_4	a_5	a_6	a_7	a_8	a_9
u_1	1	$-B$							
U_1									1
θ_{z1}		$-\frac{BC}{2r_3^2}$	$-\frac{C^2}{2r_3^2}$	$\frac{C^2B}{2r_3^2}$		$-\frac{C^2B^2}{2r_3^2}$			
u_2	1	A							
U_2									1
θ_{z2}		$\frac{AC}{2r_2^2}$	$-\frac{C^2}{2r_2^2}$	$-\frac{AC^2}{2r_2^2}$		$-\frac{A^2C^2}{2r_2^2}$			
u_3	1		C		C^2			C^3	
U_3									1
θ_{z3}		$\frac{C}{2}\left(\frac{A}{r_2^2}-\frac{B}{r_3^2}\right)$	$-\frac{C^2}{2}\left(\frac{1}{r_2^2}+\frac{1}{r_3^2}\right)$	$\frac{C^2}{2}\left(\frac{A}{r_2^2}-\frac{B}{r_3^2}\right)$	$-C^3\left(\frac{1}{r_2^2}+\frac{1}{r_3^2}\right)$		$\frac{C^3}{2}\left(\frac{A}{r_2^2}-\frac{B}{r_3^2}\right)$	$-\frac{3C^4}{2}\left(\frac{1}{r_2^2}+\frac{1}{r_3^2}\right)$	

TABLE 3.2: TRANSFORMATION MATRIX FOR PLANE STRESS ELEMENT (CONT'D) (2)

$\left[T\right]_{9,10\quad 9,18}^{1,10\quad 1,18} =$

a_{10}	a_{11}	a_{12}	a_{13}	a_{14}	a_{15}	a_{16}	a_{17}	a_{18}
$-B$		B^2			$-B^3$			
$(\frac{B^2}{r_3^2}+1)\frac{1}{2}$	$\frac{BC}{2r_3^2}$	$-B(1+\frac{B^2}{r_3^2})$	$\frac{-B^2C}{2r_3^2}$		$\frac{3B^2}{2}(1+\frac{B^2}{r_3^2})$	$\frac{B^3C}{2r_3^2}$		
A	A^2			A^3				
$(1+\frac{A^2}{r_2^2})\frac{1}{2}$	$-\frac{CA}{2r_2^2}$	$A(1+\frac{A^2}{r_2^2})$	$-\frac{CA^2}{2r_2^2}$		$\frac{3}{2}A^2(1+\frac{A^2}{r_2^2})$	$-\frac{CA^3}{2r_2^2}$		
	C			C^2				C^3
$\frac{1}{2}(\frac{A^2}{r_2^2}+\frac{B^2}{r_3^2})$	$\frac{C}{2}(\frac{B}{r_3^2}-\frac{A}{r_2^2})$		$\frac{C}{2}(\frac{A^2}{r_2^2}+\frac{B^2}{r_3^2})$	$C^2(\frac{B}{r_3^2}-\frac{A}{r_2^2})$			$\frac{C^2}{2}(\frac{A^2}{r_2^2}+\frac{B^2}{r_3^2})$	$\frac{3}{2}C^3(\frac{B}{r_3^2}-\frac{A}{r_2^2})$

TABLE 3.2: TRANSFORMATION MATRIX FOR PLANE STRESS ELEMENT (CONT'D) (3)

$${}^{10,1}_{18,1}\left[T\right]^{10,9}_{18,9} =$$

u_c	1	$\frac{(A-B)}{3}$	$\frac{C}{3}$	$\frac{C}{3}\frac{(A-B)}{3}$	$\frac{C^2}{9}$	$\left(\frac{A-B}{3}\right)^2\frac{C}{3}$	$\frac{C^2}{9}\left(\frac{A-B}{3}\right)$	$\frac{C^3}{27}$	
U_c									1
γ_1		$\frac{BC}{2r_3^2}$	$\frac{C^2}{2r_3^2}$	$-\frac{BC^2}{2r_3^2}$		$\frac{B^2C^2}{2r_3^2}$			
γ_2		$-\frac{AC}{2r_2^2}$	$\frac{C^2}{2r_2^2}$	$\frac{AC^2}{2r_2^2}$		$\frac{A^2C^2}{2r_2^2}$			
γ_3		$\frac{C}{2}\left(\frac{A}{r_2^2}+\frac{B}{r_3^2}\right)$	$\frac{C^2}{2}\left(\frac{1}{r_3^2}-\frac{1}{r_2^2}\right)$	$\frac{C^2}{2}\left(\frac{A}{r_2^2}+\frac{B}{r_3^2}\right)$	$C^3\left(\frac{1}{r_3^2}-\frac{1}{r_2^2}\right)$		$\frac{C^3}{2}\left(\frac{A}{r_2^2}+\frac{B}{r_3^2}\right)$	$\frac{3C^4}{2}\left(\frac{1}{r_3^2}-\frac{1}{r_2^2}\right)$	
0				$C_2^2 S_2$	$C_2 S_2^2$	$C_2^2 S_2 2A$	$C_2 S_2^2 A$		
0						$C_2^3 S_2$	$C_2^2 S_2^2$	$C_2 S_2^3$	
0				$C_3^2 S_3$	$C_3 S_3^2$	$-C_3^2 S_3 2B$	$-C_3 S_3^2 B$		
0						$C_3^3 S_3$	$C_3^2 S_3^2$	$C_3 S_3^3$	

$$ {}^{10,10}_{8,10}\left[\,T\,\right]^{10,18}_{18,18} = $$

$\frac{A-B}{3}$	$\frac{C}{3}$	$\frac{(A-B)}{3}^2$	$\frac{(A-B)}{3}\frac{C}{3}$	$\frac{C^2}{9}$	$\frac{(A-B)}{3}^3$	$\frac{(A-B)}{3}^2\frac{C}{3}$	$\frac{(A-B)}{3}\frac{C^2}{9}$	$\frac{C^3}{27}$
$(1-\frac{B^2}{r_3^2})\frac{1}{2}$	$\frac{-BC}{2r_3^2}$	$-B(1-\frac{B^2}{r_3^2})$	$\frac{B^2C}{2r_3^2}$		$\frac{3}{2}B^2(1-\frac{B^2}{r_3^2})$	$-\frac{B^3C}{2r_3^2}$		
$\frac{1}{2}(1-\frac{A^2}{r_2^2})$	$\frac{CA}{2r_2^2}$	$A(1-\frac{A^2}{r_2^2})$	$\frac{CA^2}{2r_2^2}$		$\frac{3}{2}A^2(1-\frac{A^2}{r_2^2})$	$\frac{CA^3}{2r_2^2}$		
$(\frac{A^2}{r_2^2}-\frac{B^2}{r_3^2})\frac{1}{2}$	$-\frac{C}{2}(\frac{A}{r_2^2}+\frac{B}{r_3^2})$		$\frac{C}{2}(\frac{A^2}{r_2^2}-\frac{B^2}{r_3^2})$	$-C^2(\frac{A}{r_2^2}+\frac{B}{r_3^2})$			$\frac{C^2}{2}(\frac{A^2}{r_2^2}-\frac{B^2}{r_3^2})$	$\frac{-3C^3}{2}(\frac{A}{r_2^2}+\frac{B}{r_3^2})$
		$S_2C_2^2$	$C_2S_2^2$	S_2^3	$3S_2C_2^2 2A$	$C_2S_2^2 2A$	S_2^3A	
					$S_2C_2^3$	$C_2^2S_2^2$	$S_2^3C_2$	S_2^4
		$S_3C_3^2$	$C_3S_3^2$	S_3^3	$-3S_3C_3^2B$	$-C_3S_3^2 2B$	$-S_3^3B$	
					$S_3C_3^3$	$C_3^2S_3^2$	$S_3^3C_3$	S_3^4

Stiffness Matrix:

The elemental stiffness matrix can be obtained from the strain energy. In plane stress the energy expression is:

$$U = \frac{Et}{2(1-\nu^2)} \iint_{\substack{\Delta \\ \text{area of} \\ \text{element}}} [\, u_\xi^{\,2} + v_\zeta^{\,2} + 2\nu u_\xi v_\zeta + \frac{1-\nu}{2}(u_\zeta + v_\xi)^2 \,]\, d\xi\, d\zeta \qquad 3\text{-}26$$

where E is Young's modulus, t is the plate thickness and ν is Poisson's ratio.

Equations 1b and 2a are substituted into equation 26 and the integrations are carried out to yield the quadratic strain energy form

$$U^e = \frac{Et}{2(1-\nu^2)} \{A\}^T [\bar{K}_A] \{A\} \qquad 3\text{-}27$$

know $\{\delta\} = [T]\{A\}$

then

$$\{A\} = [T]^{-1}\{\delta\} \qquad 3\text{-}28$$

putting equation 28 in 27 yields

$$U^e = \frac{1}{2}\frac{Et}{(1-\nu^2)}\Big[[T]^{-1}\{\delta\}\Big]^T [\bar{K}_A]\, [T]^{-1}\{\delta\} \qquad 3\text{-}29$$

Equate the strain energy to the external work done by the loads $\{P\}$:

$$\{P\}\{\delta\}^T = \frac{1}{2}\frac{Et}{(1-\nu^2)}\{\delta\}^T \Big[[T]^{-1T}[K_A]\,[T]^{-1}\Big]\{\delta\}$$

3-30

and $\{P\} = [K_\delta]\{\delta\}$

then

$$\underset{11 \times 11}{[K_\delta]} = \underset{11 \times 18}{[s]^{-1^T}} \underset{18 \times 18}{[K_A]} \underset{18 \times 11}{[s]^{-1}} \qquad 3\text{-}31$$

where

$\underset{18 \times 11}{[s]^{-1}}$ is the first 11 columns of $\underset{18 \times 18}{[T]^{-1}}$ since $\gamma_1 = \gamma_2 = \gamma_3 = 0$ and the square and cubic terms of sides 2 and 3 are set to zero.

3.2.1 Integrating the Stiffness Matrix

The entries of the stiffness matrix $[K_\delta]$ may be determined in closed form. First a formula for the integral

$$\int_\Delta \int \xi^m \zeta^n \, d\varepsilon \; d\zeta = F(m, n) \qquad 3\text{-}32$$

taken over the area of the element is obtained (4)

where

$$F(m, n) = c^{n+1} \left\{ a^{m+1} - (-b)^{m+1} \right\} \frac{m!\, n!}{(m+n+2)!} \qquad 3\text{-}33$$

When equations 1b and 2a are substituted into equation 26 and we incorporate the symmetry requirement, the result in closed form is;

$$\begin{aligned} K_{ij} = {} & m_i m_j F(m_i + m_j - 2, p_i + p_j) + n_i n_j F(l_i + l_j, n_i + n_j - 2) \\ & + \frac{1-v}{2} [p_i p_j F(m_i + m_j, p_i + p_j - 2) + l_i l_j F \\ & (l_i + l_j - 2, n_i + n_j)] + [\frac{1-v}{2} p_j l_i + v m_j n_i] F \\ & (m_j + l_i - 1, p_j + n_i - 1) + [\frac{1-v}{2} p_i l_j + v m_i n_j] F \\ & (m_i + l_j - 1, p_i + n_j - 1) \end{aligned} \qquad 3\text{-}34$$

where m_i and p_i run from 1 to 8 and l_i and n_i run from 1 to 10, as defined following equation 2a.

3.2.2 Condensation of Centroidal Degrees of Freedom:

Since the centroidal displacements u_c and v_c lie inside the element, these displacements will be unaffected when the elements are joined together to represent the structure. Therefore we may solve for them before the elements are joined together, without affecting the final result.

Minimizing the potential energy in one element:

$$\underset{11 \times 11}{[K_\delta]}\ \underset{11 \times 1}{[\delta']} = \left[\begin{array}{c|c} \underset{9 \times 9}{K_{11}} & \underset{9 \times 2}{K_{12}} \\ \hline \underset{2 \times 9}{K_{21}} & \underset{2 \times 2}{K_{22}} \end{array}\right] \left\{\begin{array}{c} \underset{9 \times 1}{\delta_1} \\ \hline \underset{2 \times 1}{\delta_2} \end{array}\right\} = \left\{\begin{array}{c} \underset{9 \times 1}{P_1} \\ \hline \underset{2 \times 1}{P_2} \end{array}\right\} \qquad 3\text{-}35$$

Evaluating:

$$K_{11}\,\delta_1 + K_{12}\,\delta_2 = P_1 \qquad 3\text{-}36$$

$$K_{21}\,\delta_1 + K_{22}\,\delta_2 = P_2 \qquad 3\text{-}37$$

Solving for δ_2 in equation 37

$$\delta_2 = K_{22}^{-1}\,(P_2 - K_{21}\delta_1)$$

Equation 36 becomes

$$K_{11}\delta_1 + K_{12}K_{22}^{-1}\,(P_2 - K_{21}\delta_1) = P_1$$

Or

$$\delta_1 (K_{11} - K_{12}K_{22}^{-1} K_{21}) = P_1 - K_{12}K_{22}^{-1} P_2\delta_2 \qquad 3\text{-}38$$

and

$$P^* = K^* \delta_1 \qquad 3\text{-}39$$

Therefore $\{ P \}^* = P_1 - K_{12}K_{22}^{-1} P_2$

and

$$\underset{9 \times 9}{[K]^*} = K_{11} - K_{12}K_{22}^{-1} K_{21} \qquad 3\text{-}40$$

where $\{ P \}^*$ and $[K]^*$ are the final load vector and stiffness matrix for the nine degree of freedom plane stress element.

3.2.3 Characteristics of the Plane Stress Element

The tangential displacement along an edge is continuous for a linear variation. The other in-plane displacement normal to each edge varies cubically along the edge. At the nodes of the element the rotation is continuous but it is not continuous along the element's sides. Because of the restriction $\gamma_1 = \gamma_2 = \gamma_3 = 0$, the element is not complete but the approximation affects the element's performance only slightly as will be illustrated later in some numerical applications. Inter-element compatibility (C^o) is easily achieved.

3.3 Bending Element Formulation:

The Zienkiewicz nine parameter plate bending triangular element is used with the nine parameter plane stress element. Nine degree of freedom would imply that a complete cubic be used for out of plane displacements W. However a difficulty arises as the full cubic expansion contains ten terms and any omission has to be made arbitrarily. To retain a certain symmetry of appearance (isotropy) all ten terms could be retained and two coefficients made equal to limit the number of unknowns to nine. Several such possibilities have been investigated but a much more serious problem occurs. The transformation matrix becomes singular for certain orientations of the triangle sides. This happens for instance, when two sides of the triangle are parallel to the x and y axes. O. C. Zienkiewicz pointed out that difficulties of such asymmetry can be avoided by the use of area co-ordinates (9). R.D. Cook also pointed out that invariance could be achieved by the use of area co-ordinates (2).

The nine terms of a cubic expression are formed by the products of all possible cubic term combinations (9) in area co-ord.;

$$W = \sum_{i=1}^{9} w_i N_i \qquad 3\text{-}41$$

<u>where</u> : N_i = shape functions and are defined as follows:

$$N_i = L_1 + L_1^2 L_2 + L_1^2 L_3 - L_1 L_2^2 - L_1 L_3^2$$

$$N_2 = - b_1 \ (L_1^2 L_2 + \tfrac{1}{2} L_1 L_2 L_3) + b_2 \ (L_3 L_1^2 + \tfrac{1}{2} L_1 L_2 L_3)$$

$$N_3 = - c_3 \ (L_1^2 L_2 + \tfrac{1}{2} L_1 L_2 L_3) + c_2 \ (L_3 L_1^2 + \tfrac{1}{2} L_1 L_2 L_3)$$

$$N_4 = L_2 + L_2^2 L_3 + L_2^2 L_1 - L_2 L_3^2 - L_2 L_1^2$$

$$N_5 = - b_1 \ (L_2^2 L_3 + \tfrac{1}{2} L_1 L_2 L3) + b_3 \ (L_1 L_2^2 + \tfrac{1}{2} L_1 L_2 L_3)$$

$$N_6 = - c_1 \ (L_2^2 L_3 + \tfrac{1}{2} L_1 L_2 L_3) + c_3 \ (L_1 L_2^2 + \tfrac{1}{2} L_1 L_2 L_3)$$

$$N_7 = L_3 + L_3^2 L_1 + L_3^2 L_2 - L_3 L_1^2 - L_3 L_2^2$$

$$N_8 = - b_2 \left(L_3^2 L_1 + \frac{1}{2} L_1 L_2 L_3 \right) + b_1 \left(L_2 L_3^2 + \frac{1}{2} L_1 L_2 L_3 \right)$$

$$N_9 = - c_2 \left(L_3^2 L_1 + \frac{1}{2} L_1 L_2 L_3 \right) + c_1 \left(L_2 L_3^2 + \frac{1}{2} L_1 L_2 L_3 \right) \qquad 3 - 42$$

L_i = Triangular or area co-ordinates

Effectively then an incomplete cubic in w is used.

where

$$\begin{array}{ll} b_1 = y_2 - y_3 & c_1 = x_3 - x_2 \\ b_2 = y_3 - y_1 & c_2 = x_1 - x_3 \\ b_3 = y_1 - y_2 & c_3 = x_2 - x_1 \end{array} \qquad 3\text{-}42A$$

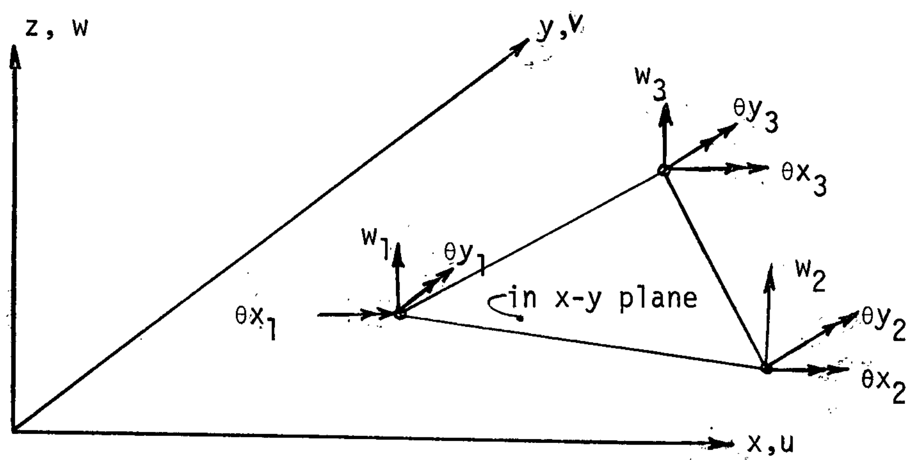

Fig. 3.3 Degrees of Freedom of the Bending Element

As shown in Fig. 3.3 the nine parameters chosen to represent the element's configuration are:

$$w_i = \left\langle w_1, \theta_{x_1}, \theta_{y_1}, w_2, \ldots \theta_{y_3} \right\rangle$$

where

$$\theta_x = \frac{\partial w}{\partial y} \qquad \text{and} \qquad \theta_y = -\frac{\partial w}{\partial x}$$

Area co-ordinates (L_1, L_2, L_3) are used since the formulation is more direct and easier. (refer to fig. 3.4)

<u>where</u> A_1 = area of triangle 3P2,etc.

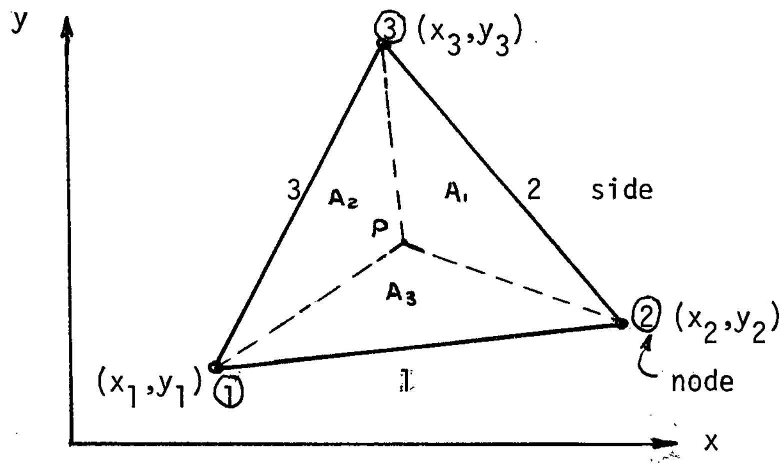

Fig. 3.4 Area Co-ordinates

<u>Then</u> $A_{TOTAL} = A_1 + A_2 + A_3$ 3-43

$$L_1 = \frac{A_1}{A_T} \qquad L_2 = \frac{A_2}{A_T} \qquad L_3 = \frac{A_3}{A_T}$$

<u>so</u>

$$L_1 + L_2 + L_3 = 1 \tag{3-44}$$

<u>Area of Element:</u> (Δ)

$$2\,\Delta = \det \begin{vmatrix} 1 & 1 & 1 \\ x_1 & x_2 & x_3 \\ y_1 & y_2 & y_3 \end{vmatrix}$$

evaluating and using equations 42A yields

$$2\,\Delta = c_2 b_1 - c_1 b_2 \tag{3-45}$$

Relationship between Cartesian and Area Co-ordinates:

We know:

$$\begin{Bmatrix} 1 \\ x \\ y \end{Bmatrix} = \begin{bmatrix} 1 & 1 & 1 \\ x_1 & x_2 & x_3 \\ y_1 & y_2 & y_3 \end{bmatrix} \begin{Bmatrix} L_1 \\ L_2 \\ L_3 \end{Bmatrix} \qquad 3\text{-}46$$

evaluating equation 46 yields

$$x = x_1L_1 + x_2L_2 + x_3L_3 \qquad 3\text{-}46b$$

$$y = y_1L_1 + y_2L_2 + y_3L_3 \qquad 3\text{-}46c$$

but from equation 44

$$L_3 = 1 - L_1 - L_2 \qquad 3\text{-}44a$$

so equations 46b and 46c using equation 44a become:

$$x = L_1C_2 - L_2C_1 + x_3 \qquad 3\text{-}47a$$

$$y = -L_1b_2 + L_2b_1 + x_3 \qquad 3\text{-}47b$$

we want:

$$\{L\} = [J]\ \{X\} \qquad 3\text{-}48$$

where $\{ L \}$ = second derivatives of the area co-ordinates (L_i)

$\{ X \}$ = second derivatives of cartesian co-ordinates

$[J]$ = Jacobian matrix

Note: second derivatives are used since strain operator has the same derivatives.

so from equation 3-48:

$$\begin{Bmatrix} \dfrac{\partial^2}{\partial L_1^2} \\[2ex] \dfrac{\partial^2}{\partial L_2^2} \\[2ex] \dfrac{\partial^2}{\partial L_1 \partial L_2} \end{Bmatrix} = [\ J\ ] \begin{Bmatrix} \dfrac{\partial^2}{\partial x^2} \\[2ex] \dfrac{\partial}{\partial y^2} \\[2ex] \dfrac{\partial^2}{\partial x \partial y} \end{Bmatrix} \qquad 3\text{-}49$$

Using the chain rule to relate the 2 co-ordinate systems:

$$\frac{\partial}{\partial L_1} = \frac{\partial x}{\partial L_1}\frac{\partial}{\partial x} + \frac{\partial y}{\partial L_1}\frac{\partial}{\partial y}$$

$$= c_2 \frac{\partial}{\partial x} - b_2 \frac{\partial}{\partial y} \qquad 3\text{-}50$$

Similarly:

$$\frac{\partial}{\partial L_2} = \frac{\partial x}{\partial L_2}\frac{\partial}{\partial x} + \frac{\partial y}{\partial L_2}\frac{\partial}{\partial y}$$

$$= - c_1 \frac{\partial}{\partial x} + b_1 \frac{\partial}{\partial y} \qquad 3\text{-}51$$

then:

$$\frac{\partial^2}{\partial L_1^2} = c_2^2 \frac{\partial^2}{\partial x^2} - 2c_2b_2 \frac{\partial^2}{\partial x \partial y} + b_2^2 \frac{\partial^2}{\partial y^2} \qquad 3\text{-}52$$

$$\frac{\partial^2}{\partial L_2^2} = c_1^2 \frac{\partial^2}{\partial x^2} - 2c_1b_1 \frac{\partial^2}{\partial x \partial y} + b_1^2 \frac{\partial^2}{\partial y^2} \qquad 3\text{-}53$$

and

$$\frac{\partial^2}{\partial L_1 \partial L_2} = - c_1c_2 \frac{\partial^2}{\partial x^2} + \left(\frac{c_1b_2 + b_1c_2}{2}\right) 2 \frac{\partial^2}{\partial x \partial y} - b_1b_2 \frac{\partial^2}{\partial y^2} \qquad 3\text{-}54$$

In matrix form, expressing equation 3-49 we obtain:

$$\left\{\begin{matrix} \dfrac{\partial^2}{\partial L_1^2} \\[2ex] \dfrac{\partial^2}{\partial L_2^2} \\[2ex] \dfrac{\partial^2}{\partial L_1 \partial L_2} \end{matrix}\right\} = \underbrace{\begin{bmatrix} c_2^2 & b_2^2 & - c_2b_2 \\[2ex] c_1^2 & b_1^2 & - c_1b_1 \\[2ex] - c_1c_2 & - b_1b_2 & \dfrac{c_1b_2 + b_1c_2}{2} \end{bmatrix}}_{[J]} \left\{\begin{matrix} \dfrac{\partial^2}{\partial x^2} \\[2ex] \dfrac{\partial^2}{\partial y^2} \\[2ex] 2\dfrac{\partial^2}{\partial x \partial y} \end{matrix}\right\} \qquad 3\text{-}49a$$

Strain-Displacement Relationship: [B]

We know:

$$\{ \varepsilon \} = \{ X \} \{ W \} \qquad 3\text{-}55$$

Where

$$\{ \varepsilon \} = \text{Strain vector} \begin{Bmatrix} \varepsilon x \\ \varepsilon y \\ \gamma xy \end{Bmatrix}$$

$$\{ W \} = \sum_{i=1}^{9} w_i N_i = \text{displacement (normal to plane)}$$

$$\quad = \{ w \} \{ N \}$$

$$\{ X \} = [J]^{-1} * \{ L \} \text{ from equation 48}$$

Then equation 3-55 can be expressed as:

$$\{ \varepsilon \} = [J]^{-1} \{ L \} \{ w \} \{ N \}$$

$$= [J]^{-1} [B] \{ N \} \qquad 3\text{-}55a$$

so

$$[B] = \{ L \} \{ N \} \qquad 3\text{-}56$$

Knowing $L_3 = 1 - L_1 - L_2$, equations 42 can be rewritten, eliminating their dependence on L_3:

$$N_1 = 3L_1^2 - 2L_1^3 - 2L_1L_2^2 - 2L_1^2L_2 + 2L_1^2L_2$$

$$N_2 = - b_3 \left(\frac{1}{2} L_1^2L_2 + \frac{1}{2} L_1L_2 - \frac{1}{2} L_1L_2^2 \right) + b_2 \left(L_1^2 - L_1^3 - \frac{3}{2} L_1^2L_2 + \right.$$
$$\left. + \frac{1}{2} L_1L_2 - \frac{1}{2} L_1L_2^2 \right)$$

$$N_3 = - c_3 \left(\frac{1}{2} L_1^2L_2 + \frac{1}{2} L_1L_2 - \frac{1}{2} L_1L_2^2 \right) + c_2 \left(L_1^2 - L_1^3 - \frac{3}{2} L_1^2L_2 + \right.$$
$$\left. + \frac{1}{2} L_1L_2 - \frac{1}{2} L_1L_2^2 \right)$$

$$N_4 = 3L_2^2 - 2L_2^3 - 2L_2L_1^2 - 2\,L_2^2L_1 + 2\,L_1L_2$$

$$N_5 = -b_1\left(L_2^2 - \frac{3}{2}L_2^2L_1 - L_2^3 + \frac{1}{2}L_1L_2 - \frac{1}{2}L_1^2L_2\right) + b_3\left(\frac{1}{2}L_1L_2^2 + \right.$$
$$\left. + \frac{1}{2}L_1L_2 - \frac{1}{2}L_1^2L_2\right)$$

$$N_6 = -c_1\left(L_2^2 - \frac{3}{2}L_2^2L_1 - L_2^3 + \frac{1}{2}L_1L_2 - L_1^2L_2\right) + c_3\left(\frac{1}{2}L_1L_2^2 + \right.$$
$$\left. + \frac{1}{2}L_1L_2 - \frac{1}{2}L_1^2L_2\right) \qquad \text{3-42a}$$

$$N_7 = 1 - 3L_1^2 - 4L_1L_2 + 4L_1^2L_2 + 2\,L_1^3 + 4L_2^2L_1 - 3L_2^2 + 2L_2^3$$

$$N_8 = -b_2\left(L_1 - 2L_1^2 - \frac{3}{2}L_2L_1 + \frac{3}{2}L_1^2L_2 + L_1^3 + \frac{1}{2}L_2^2L_1\right) +$$
$$+ b_1\left(L_2 - \frac{3}{2}L_2L_1 - 2L_2^2 + \frac{3}{2}L_1L_2^2 + \frac{1}{2}L_1^2L_2 + L_2^3\right)$$

$$N_9 = -c_2\left(L_1 - 2L_1^2 - \frac{3}{2}L_1L_2 + \frac{3}{2}L_1^2L_2 + L_1^3 + \frac{1}{2}L_2^2L_1\right) +$$
$$+ c_1\left(L_2 - \frac{3}{2}L_1L_2 - 2L_2^2 + \frac{3}{2}L_1L_2^2 + \frac{1}{2}L_1^2L_2 + L_2^3\right)$$

Now equation 3-56 can be evaluated

$$[\,B\,] = \begin{Bmatrix} \dfrac{\partial^2}{\partial L_1^2} \\[2ex] \dfrac{\partial^2}{\partial L_2^2} \\[2ex] \dfrac{\partial^2}{\partial L_1 \partial L_2} \end{Bmatrix} \left\langle N_1\,,\, N_2\,,\, N_3, \ldots N_9 \right\rangle$$

or:

$$= \begin{bmatrix} \frac{\partial^2 N_1}{\partial L_1^2} & \frac{\partial^2 N_2}{\partial L_1^2} & \cdots\cdots\cdots\cdots & \frac{\partial^2 N_9}{\partial L_1^2} \\ \frac{\partial^2 N_1}{\partial L_2^2} & \frac{\partial^2 N_2}{\partial L_2^2} & \cdots\cdots\cdots\cdots & \frac{\partial^2 N_9}{\partial L_2^2} \\ \frac{\partial^2 N_1}{\partial L_1 \partial L_2} & \frac{\partial^2 N_2}{\partial L_1 \partial L_2} & \cdots\cdots\cdots\cdots & \frac{\partial^2 N_9}{\partial L_1 \partial L_2} \end{bmatrix} \qquad 3\text{-}56a$$

This yields the [B] matrix printed on the following page. (Table 3.4).

TABLE 3.4

STRAIN-DISPLACEMENT MATRIX (BENDING ELEMENT)

$$
[\,B\,] = \left[\begin{array}{c|c|c|c|c|c|c|c|c}
6 - 12L_1 + - 4L_2 & -b_3L_2 + b_2\,(2 - 6L_1 - 3L_2) & -c_3L_2 + c_2\,(2-6L_1 - 3L_2) & -4L_2 & b_1L_2 - b_3L_2 & c_1L_2 - c_3L_2 & -6 + 12L_1 + 8L_2 & -b_2\,(-4 + 6L_1 + 3L_2) + b_1L_2 & -c_2\,(-4 + 6L_1 + 3L_2) + + c_1L_2 \\
\hline
-4L_1 & b_3L_1 - b_2\,L_1 & c_3L_1 - c_2L_1 & 6 - 4L_1 - 12L_2 & -b_1\,(2 - 3L_1 - 6L_2\,) + b_3L_1 & -c_1\,(2 - 3L_1 + -6L_2) + c_3L_1 & -6 + 8L_1 + 12L_2 & -b_2L_1 + b_1\,(-4 + 6L_2 + 3L_1) & -c_2L_1 + c_1\,(-4 + 6L_2 + + 3L_1) \\
\hline
2 - 4L_1 - 4L_2 & -b_3\,(L_1 - L_2 + \frac{1}{2}) + b_2(-3L_1 - L_2 + \frac{1}{2}) & -c_3\,(L_1-L_2 + \frac{1}{2}) + c_2\,(-3L_1-L_2 + \frac{1}{2}\,) & 2 - 4L_1 - 4L_2 & -b_1\,(-3L_2 + -L_1 + \frac{1}{2}) + b_3\,(L_2 - L_1 + \frac{1}{2}\,) & -c_1\,(-3L_2 -L_1 + \frac{1}{2}) + c_3\,(L_2-L_1 + \frac{1}{2}) & -4 + 8L_1 + 8L_2 & -b_2(3L_1+L_2+ - \frac{3}{2}) + b_1\,(L_1 + 3L_2 - \frac{3}{2}) & -c_2(3L_1+L_2 - \frac{3}{2}) + c_1\,(L_1 + 3L_2 - \frac{3}{2})
\end{array}\right]
$$

Stiffness Matrix

From the virtual work approach, as discussed in section 2.1.1, the stiffness matrix is derived from equation 2-9

$$[\,K\,] = \int_{area} [\,B\,]^T [\,D\,] \; [\,B\,] \; d\,\text{Area} \qquad 2\text{-}9$$

For plate bending, the elasticity matrix [D] is

$$[\,D\,] = \frac{Et^3}{12\,(1-\nu^2)} \begin{bmatrix} 1 & \nu & 0 \\ \nu & 1 & 0 \\ 0 & 0 & \frac{1-\nu}{2} \end{bmatrix} \qquad 3\text{-}56b$$

Then equation 2-9 can be rewritten as:

$$[\,K\,] = \int_{area} \underbrace{\left[[\,J\,]^{-1} \; [\,B\,] \right]^T \; [\,D\,] \; \left[[\,J\,]^{-1} \; [\,B\,] \right]}_{[R]} \; dA$$

$$= \sum_{i=1}^{3} [\,R\,] * \text{weight} * \text{area} \qquad 2\text{-}9b$$

A numerical integration procedure is used which is exact for the element. Since strain varies linearly so does stress. This yields a quadratic order for the stiffness. Refer to Table 3.3

where

i = side no. of the element.

TABLE 3.3:

AREA CO-ORDINATES FOR NUMERICAL INTEGRATION

Side	L_1	L_2	L_3	wt
1	$\frac{1}{2}$	$\frac{1}{2}$	0	$\frac{1}{3}$
2	0	$\frac{1}{2}$	$\frac{1}{2}$	$\frac{1}{3}$
3	$\frac{1}{2}$	0	$\frac{1}{2}$	$\frac{1}{3}$

Note: Refer to figure 3.4.

3.4 Assembling the In-Plane and Bending Element Stiffnesses

Shell and folded plate structures support their applied loadings by a coupling of in-plane resistance and bending resistance. Thus structural action may be represented by combining the in-plane stiffness with the bending stiffness. The resulting stiffness matrix in local co-ordinates treats the in-plane and bending actions as being independent of each other (uncoupled). However when the stiffness matrix is referenced to the global system coupling does result between the membrane and bending actions. When the elements modelling a body are assembled, coupling also exists between adjacent elements.

The degrees of freedom chosen to describe the in-plane action are:

$$\underset{1 \times 9}{\{ \delta_p \}^T} = \left\langle u_1 \, v_1 \, \omega_1 \, , \, u_2 \cdots \omega_3 \right\rangle$$

where $\omega = \theta_z$ (in plane rotation)

Similarly those degrees of freedom used for bending action are:

$$\underset{1 \times 9}{\{ \delta_b \}^T} = \left\langle w_1 \, , \, \theta_{x1} \, , \, \theta_{y1} \, , \, w_2 \, , \, \ldots \theta_{y3} \right\rangle$$

For the combined element (in-plane and bending), the displacement vector is to be arranged as follows:

$$\underset{1 \times 18}{\{ \delta_t \}^T} = \left\langle u_1 \, , \, v_1 \, , \, w_1 \, , \, \theta_{x1} \, , \, \theta_{y1} \, , \theta_{z1} \, , \, u_2 \, , \, \ldots \theta_{z3} \right\rangle$$

In terms of the force - displacement relationships:

<u>In-Plane</u>

$$\{ F_p \} = [K_p] \{ \delta_p \}$$

<u>Where</u> $[K_p]_{9 \times 9}$ = in-plane stiffness matrix in local co-ordinate.

<u>bending</u>:

$$\{F_b\} = [K_b]\{\delta_b\}$$

<u>where</u> $[K_b]_{9\times 9}$ = plate bending stiff-matrix in local co-ordinate.

Combined:

$\{F_L\}$ =

18 x 1

K_p^{11} 2 x 2			K_p^{12} 2 x 2			K_p^{13} 2 x 2		
	K_{b11} 3 x 3			K_{b12}			K_{b13}	
		K_p^{1} 1 x 1			K_p^{2} 1 x 1			K_p^{3} 1 x 1
K_p^{21} 2 x 2			K_p^{22} 2 x 2			K_p^{23} 2 x 2		
	K_{b21}			K_{b22}			K_{b23}	
		K_p^{4} 1 x 1			K_p^{5} 1 x 1			K_p^{6} 1 x 1
K_p^{31} 2 x 2			K_b^{32} 2 x 2			K_p^{33} 2 x 2		
	K_{b31}			K_{b32}			K_{b33}	
		K_p^{7} 1 x 1			K_p^{8} 1 x 1			K_p^{9} 1 x 1

$\{\delta_L\}$

18 x 1

18 x 18

$[K_C]$

To further clarify what has happened, here is how the bending stiffness matrix has been paritioned and addressed for use in $[\ K_L\ ]$.

$$\underset{9 \times 1}{\{\ F_b\ \}} = \underset{\begin{array}{c} 9 \times 9 \\ [\ K_b\ ] \end{array}}{\left[\begin{array}{c|c|c} K_{b\,11} \ (3 \times 3) & K_{b12} & K_{b13} \\ \hline K_{b21} & K_{b22} & K_{b23} \\ \hline K_{b31} & K_{b32} & K_{b33} \end{array}\right]} \underset{9 \times 1}{\left\{\begin{array}{c} w_1 \\ \theta_{x1} \\ \theta_{y1} \\ \hdashline w_2 \\ \theta_{x2} \\ \theta_{y2} \\ \hdashline w_3 \\ \theta_{x3} \\ \theta_{y3} \end{array}\right\}}$$

And the in-plane stiffness matrix is addressed as follows

$$\{F_p\} = \underset{[\ K_p\ ]}{\left[\begin{array}{c|c|c|c|c|c} K_{p11} & & K_{p12} & & K_{p13} & \\ \hline & K_p^{1} & & K_p^{2} & & K_p^{3} \\ \hline K_{p21} & & K_{p22} & & K_{p23} & \\ \hline & K_p^{4} & & K_p^{5} & & K_p^{6} \\ \hline K_{p31} & & K_{p32} & & K_{p33} & \\ \hline & K_p^{7} & & K_p^{8} & & K_p^{9} \end{array}\right]} \left\{\begin{array}{c} u_1 \\ v_1 \\ \hdashline \omega_1 \\ \hdashline u_2 \\ v_2 \\ \hdashline \omega_2 \\ \hdashline u_3 \\ v_3 \\ \hdashline \omega_3 \end{array}\right\}$$

Now the resultant stiffness matrix can be used.

From the stiffness method technique, the stiffness matrix for a structure is developed by summing the element stiffness matrices at the appropriate nodes. However prior to summing the element matrices, they must all be referenced to a common co-ordinate system (global or structure co-ordinate).

3.5 Co-ordinate Transformations

Each element in this study has associated with it, its own local co-ordinate system. Each system has the same orientation with respect to the element, regardless of how the element may be orientated in global co-ordinates the element displacement field is expressed in terms of local co-ordinates and as long as the displacement function used has a balanced representation of terms, then invariance will be achieved even though incomplete polynomials are used (2). Fig. 3.5 illustrates the use of local and global axes.

The local degree of freedom must be related to the global co-ordinate system so that the total structure stiffness matrix can be computed by simply summing the element stiffnesses.

Let some matrix say [λ] relate the 2 co-ordinate systems.

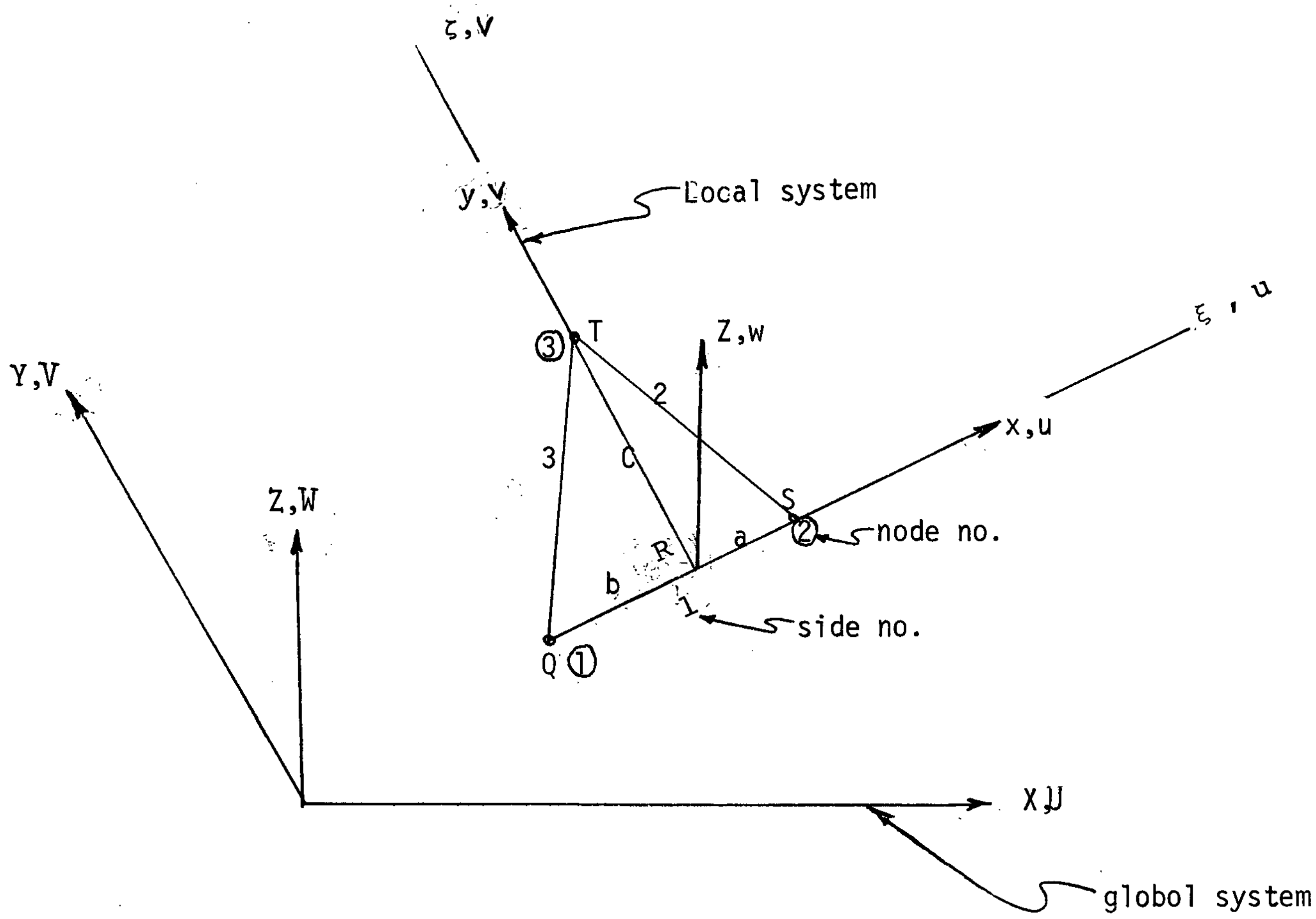

Fig. 3.5 Co-ordinate Systems

Then

$$\begin{Bmatrix} u \\ v \\ w \end{Bmatrix} = [\,\lambda\,] \begin{Bmatrix} U \\ V \\ W \end{Bmatrix} \qquad 3\text{-}57$$

and

$$\begin{Bmatrix} \theta_x \\ \theta_y \\ \theta_z \end{Bmatrix} = [\,\lambda\,] \begin{Bmatrix} \theta_X \\ \theta_Y \\ \theta_Z \end{Bmatrix} \qquad 3\text{-}57a$$

where $\langle U, V, W, \theta_X, \theta_Y, \theta_Z \rangle$ are the degrees of freedom in terms of global co-ordinates.

$\langle u, v, w, \theta_x, \theta_y, \theta_z \rangle$ are the degrees of freedom in terms of the local axes for each node of the element.

The $[\,\lambda\,]$ is merely a matrix of direction cosines:

$$[\,\lambda\,] = \begin{bmatrix} \lambda_{xX} & \lambda_{xY} & \lambda_{xZ} \\ \lambda_{yX} & \lambda_{yY} & \lambda_{yZ} \\ \lambda_{zX} & \lambda_{zY} & \lambda_{zZ} \end{bmatrix}$$

For the whole element, the transformation from global to local is:

$$
\underset{18 \times 1}{\begin{Bmatrix} u_1 \\ v_1 \\ w_1 \\ \theta_{x1} \\ \theta_{y1} \\ \theta_{z1} \\ u_2 \\ \vdots \\ \cdot \\ \cdot \\ z3 \end{Bmatrix}}
=
\underset{18 \times 1}{\begin{bmatrix} \underset{3 \times 3}{[\lambda]} & & & & & \\ & [\lambda] & & & & \\ & & \ddots & & & \\ & & \text{diagonal matrices} & & & \\ & & & \ddots & & \\ & & & [\lambda] & & \\ & & & & [\lambda] & \\ & & & & & [\lambda] \end{bmatrix}}
\underset{18 \times 1}{\begin{Bmatrix} U_1 \\ V_1 \\ W_1 \\ \theta_{X1} \\ \theta_{Y1} \\ \theta_{Z1} \\ U_2 \\ \cdot \\ \cdot \\ \cdot \\ Z3 \end{Bmatrix}}
$$

Or

$$\{ \delta_L \} = [T] \{ \delta_G \} \qquad 3\text{-}58$$

The elemental stiffness matrix in local co-ordinate is transformed to the global co-ordinate system:

$$\underset{18 \times 18}{[K_G]} = \underset{18 \times 18}{[T]^T} \underset{18 \times 18}{[K]} [T] \qquad 3\text{-}59$$

To find the direction cosine matrix [λ], consider the equation of the plane which passes through nodes 1, 2 and 3 of figure 3.5. The global co-ordinates of the three nodes are X_i Y_i Z_i for i = 1, 2, 3.

$$\det \begin{vmatrix} X - X_1 & Y - Y_1 & Z - Z_1 \\ X_2 - X_1 & Y_2 - Y_1 & Z_2 - Z_1 \\ X_3 - X_1 & Y_3 - Y_1 & Z_3 - Z_1 \end{vmatrix} = 0 \qquad \text{3-60}$$

This yields:

$$(x - x_1) [(y_2 - y_1) (z_3 - z_1) - (y_3 - y_1) (z_2 - z_1)] +$$
$$- (y - y_1) [(x_2 - x_1) (z_3 - z_1) - (x_3 - x_1) (z_2 - z_1)] +$$
$$+ (z - z_1) [(x_2 - x_1) (y_3 - y_1) - (x_3 - x_1) (y_2 - y_1) = 0$$

Or:

$$x [(y_2 - y_1) (z_3 - z_1) - (y_3 - y_1) (z_2 - z_1)] +$$
$$+ y [(x_3 - x_1) (z_2 - z_1) - (x_2 - x_1) (z_3 - z_1)] +$$
$$+ z [(x_2 - x_1) (y_3 - y_1) - (x_3 - x_1) (y_2 - y_1)] = \text{constant} \qquad \text{3-61}$$

Or

$$A X + B Y + C Z = \text{constant} \qquad \text{3-62}$$

Now relate to the X - Y axes to the direction cosines of the normal to the X - Y plane ditto are:

$$\lambda = \frac{\text{component projection}}{\text{vector length}} \qquad \text{(general)}$$

vector length is $E = \sqrt{A^2 + B^2 + C^2}$

then:

$$\lambda_{zX} = \frac{A}{E} \qquad \lambda_{zY} = \frac{B}{E} \qquad \lambda_{zZ} = \frac{C}{E} \qquad \text{3-63}$$

The direction cosines for the x axis from node 1 to 2 are:

Vector length = $a + b = l_1$

Or

$$l_1 = \sqrt{(x_2 - x_1)^2 + (y_2 - y_1)^2 + (z_2 - z_1)^2}$$

Then :

$$\lambda_{xX} = \frac{x_2 - x_1}{l_1} \qquad \lambda_{xY} = \frac{y_2 - y_1}{l_1} \qquad \lambda_{xZ} = \frac{z_2 - z_1}{l_1} \qquad 3\text{-}64$$

The direction cosines for the y axis are:

The y axis is perpendicular to both x and z so use the dot product.

This yields:

$$\lambda_{yX}\,\lambda_{xX} + \lambda_{yY}\,\lambda_{xY} + \lambda_{yZ}\,\lambda_{xZ} = 0$$

$$\lambda_{yX}\,\lambda_{zX} + \lambda_{yY}\,\lambda_{zY} + \lambda_{yZ}\,\lambda_{zZ} = 0$$

and $\lambda_{yX}^2 + \lambda_{yY}^2 + \lambda_{yZ}^2 = 1$

and the vector length is:

$$L = \sqrt{[(Y_2 - y_1)C - (z_2 - z_1)B]^2 + [(x_2 - x_1)C - (z_2 - z_1)A]^2 + [(x_2 - x_1)B - (y_2 - y_1)A]^2}$$

then

$$\lambda_{yX} = -\frac{(y_2 - y_1)C - (z_2 - z_1)B}{L}$$

$$\lambda_{yY} = \frac{(x_2 - x_1)C - (z_2 - z_1)A}{L}$$

and

$$\lambda_{yz} = \frac{-(x_2 - x_1)\, B - (y_2 - y_1)\, A}{L} \qquad 3\text{-}66$$

3.6 Element Dimensions (in terms of global co-ordinate) refer to fig. 3.5.

The length of side (1) has already been defined as l_1. The length of side (2), between nodes (2) and (3) is l_2:

$$l_2 = \sqrt{(x_3 - x_2)^2 + (y_3 - y_2)^2 + (z_3 - z_2)^2}$$

$$a = \frac{[\,(x_2 - x_3)\,(x_2 - x_1) + (y_2 - y_3)\,(y_2 - y_1) + (z_2 - z_3)\,(z_2 - z_1)\,]}{l_1}$$

So

$$b = l_1 - a$$

$$c = \sqrt{l_2^2 - a^2}$$

3.7 Summary of the Combined Element:

As a result of combining the nine parameter plane stress element with the nine parameter plate bending element, the triangular element can model the six possible movements at a node in space, namely three translations and three rotations. The displacement tangential to each side of the element varies linearly, but the normal (membrane) displacement and plate bending vary cubically along the edges. Therefore, all displacements are continuous between elements. However the bending slopes normal to the edge are not compatible except at the nodes.

As mentioned in section 3.1 if the element is to model shells and plate structures, both displacements and slopes must be continuous for the element and from element to adjacent element. However only slope continuity is satisfied at the nodes and not along the sides of the element. For slope continuity along the sides of the element, both the translations and the rotations have to be continuous. These sacrifices did not hinder the elements performance to a great extent as will be illustrated later in some numerical examples.

CHAPTER 4

STRESS COMPUTATIONS

4.1 In General:

When a structure is modelled using finite elements, the deflections of the nodes are solved from the force-deformation equation:

$$\{F\} = [K]^{*}\{\delta\} \qquad 4\text{-}1$$

where

$[K]^{*}$ = master stiffness matrix in global co-ordinate

$\{\delta\}$ = master deflection vector in global co-ordinate

The master stiffness matrix is decomposed and the nodal displacements are easily computed.

Before the stresses can be computed, this deflection vector should be transformed to the local system for each element and the in-plane movements and the bending movements separated. These have to be separated because the elasticity matrices [D] and the strain - displacement matrices [B] are different for each type of action. Even though the maximum stress at a point in a body is totally independent of any co-ordinate system used, it is convenient here to work with the local system for each element. Using equation 3-58

$$\underset{18 \times 1}{\{\delta_L\}} = \underset{18 \times 18}{[T]} \; \underset{18 \times 1}{\{\delta_G\}}$$

where [T] = transformation matrix.

Now the local solution vector of deflections can be broken down for each element as follows:

$$\begin{Bmatrix} u_1 \\ v_1 \\ w_1 \\ \theta_{x1} \\ \theta_{y1} \\ \theta_{z1} \\ u_2 \\ \cdot \\ \cdot \\ \cdot \\ \theta_{z3} \end{Bmatrix}_{18 \times 1} = \begin{Bmatrix} u_1 \\ v_1 \\ \theta_{z1} \\ u_2 \\ \cdot \\ \cdot \\ \cdot \\ \theta_{z3} \end{Bmatrix}_{9 \times 1} + \begin{Bmatrix} w_1 \\ \theta_{x1} \\ \theta_{y1} \\ w_2 \\ \cdot \\ \cdot \\ \cdot \\ \theta_{z3} \end{Bmatrix}_{9 \times 1}$$

Or

$$\{\delta_L\} = \{\delta_p\} + \{\delta_b\} \qquad 4\text{-}3$$

Now the stresses can be computed. In general, the strains are computed from equation 2-2

$$\{\varepsilon\} = [B]\ \{\delta\} \qquad 4\text{-}3a$$

where

$[B]$ = strain-displacement - matrix

and then the stresses from equation 2-1 are:

$$\{\sigma\} = [D]\{\varepsilon\}$$

The resultant stress at a node is computed by calculating the average stress of all the surrounding element conditions.

4.2 In Plane Stresses:

In the following, three different methods for approximating the stresses from the calculated displacements are presented. The first method (consistent) uses the same strain-displacement matrix as in the stiffness calculation. The second method (C.S.T) uses the strain-displacement matrix from the constant stress triangle and just ignores the rotational degree of freedom at each node. The third method (L.S.T.) uses the linear strain triangle strain-displacement matrix and involves calculating effective mid-side node displacements, thus making use of the nodal rotations.

4.2.1 Consistent Formulation:

The word consistent implies solving for the stresses in the usual manner described in the previous section, deriving the strain-displacement matrix [B] that is consistent with the element formulation of Sec. 3.2.

Having the solution vector of the in-plane displacements $\{\delta_p\}$ in local co-ordinate, we can proceed to solve for the stresses anywhere within the element.

$$\{\delta_p\} = [D_p] \{\varepsilon_p\} \qquad 4\text{-}4$$

where

$$[D_p] = \frac{E}{1 - v^2} \begin{bmatrix} 1 & v & 0 \\ v & 1 & 0 \\ 0 & 0 & \frac{1-v}{2} \end{bmatrix}$$

$$\{\sigma_p\} = \text{plane stress vector} \begin{Bmatrix} \sigma x \\ \sigma y \\ Txy \end{Bmatrix}$$

$$\{\varepsilon_p\} = \text{the strains} \begin{Bmatrix} \varepsilon x \\ \varepsilon y \\ \gamma xy \end{Bmatrix}$$

$$\{\varepsilon_p\} = [B_p] \{\delta_p\} \qquad 4\text{-}5$$

where $[B_p]$ = strain-displacement matrix.

So equation 4-4 can be expressed as:

$$\underset{3 \times 1}{\{\sigma_p\}} = \underset{3 \times 3}{[D_p]}\ \underset{3 \times 3}{[B_p]}\ \underset{3 \times 1}{\{\delta_p\}} \qquad 4\text{-}6$$

The strain-displacement matrix is formulated from the original displacement polynomials:

$$u = \sum_{i=1}^{8} a_i\, \xi^{mi}\, \zeta^{pi} \qquad 3\text{-}1b$$

$$V = \sum_{i=1}^{10} a_{i+8}\, \xi^{li}\, \zeta^{ni} \qquad 3\text{-}2a$$

where:

$$\{m\}^T = \langle 0\ 1\ 0\ 1\ 0\ 2\ 1\ 0 \rangle$$

$$\{p\}^T = \langle 0\ 0\ 1\ 1\ 2\ 1\ 2\ 3 \rangle$$

$$\{l\}^T = \langle 0\ 1\ 0\ 2\ 1\ 0\ 3\ 2\ 1\ 0 \rangle$$

$$\{n\}^T = \langle 0\ 0\ 1\ 0\ 1\ 2\ 0\ 1\ 2\ 3 \rangle$$

knowing

$$\varepsilon x = \frac{\partial u}{\partial \xi}$$

$$\varepsilon y = \frac{\partial V}{\partial \zeta} \qquad 4\text{-}7$$

$$\gamma xy = \frac{\partial u}{\partial \zeta} + \frac{\partial V}{\partial \xi}$$

Equations 4-7 can be evaluated anywhere in the element and in particular at the nodes resulting in nine strains per element.

An alternate approach of computing the plane stresses was tried in an effort to improve on the previously mentioned method. This is based on the Linear Strain Triangle approach. Also the constant Strain Triangle was computed to serve as a comparison to the validity of the results.

4.2.2 Constant Strain Formulation: (C.S.T.)

This triangular element shown in Figure 4.1 has six degrees of freedom, two per node. The element is rather limited because of its simplicity. It can only represent a constant state of strain (and stress) across the entire element. However, this element does yield stresses which can serve as an approximate check on higher order elements.

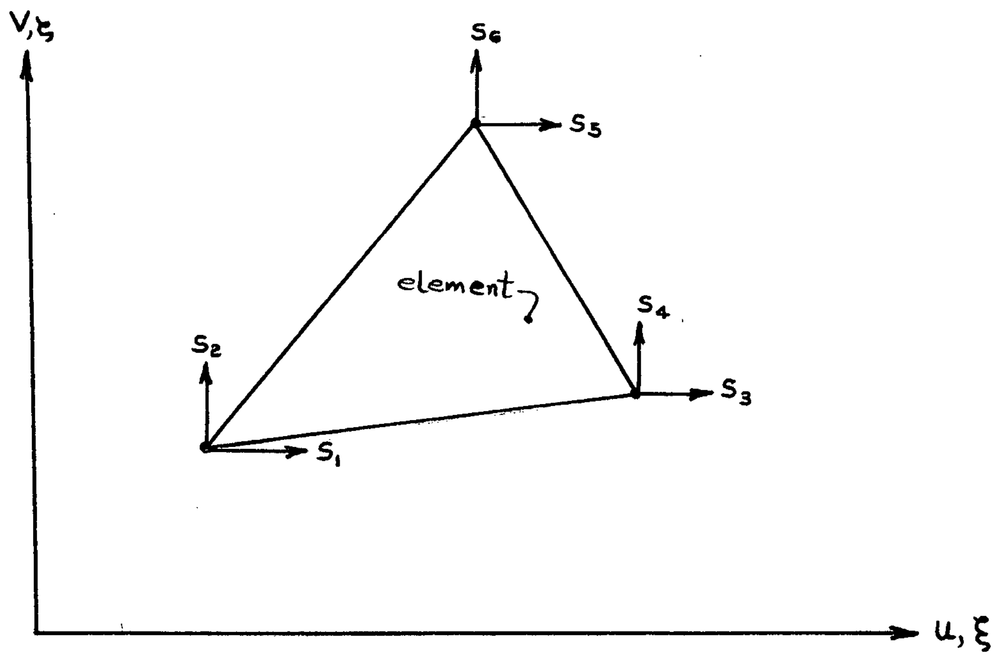

Fig. 4.1 Constant Strain-Triangle Degree of Freedom

Again we start with the solution vector in local co-ordinates $\{\delta_p\}$

$$\text{where} \quad \underset{9 \times 1}{\{\delta_p\}} = \begin{Bmatrix} u_1 \\ v_1 \\ \omega_1 \\ u_2 \\ \cdot \\ \cdot \\ \cdot \\ \omega_3 \end{Bmatrix}$$

but for the constant strain triangle we only need a linear variation for the displacement polynomials since the strain-displacement operator is only of first order, giving a constant strain variation across the element.

$$u = a_1 + a_2\xi + a_3\zeta \qquad 4\text{-}8$$

$$v = a_4 + a_5\xi + a_6\zeta \qquad 4\text{-}9$$

Then only six parameters are required so we will use only u and v at each of the nodes.

Writing equations 4-8 and 4-9 in matrix form yields:

$$\begin{Bmatrix} u \\ v \end{Bmatrix} = \begin{bmatrix} 1 & \xi & \zeta & 0 & 0 & 0 \\ 0 & 0 & 0 & 1 & \xi & \zeta \end{bmatrix} \begin{Bmatrix} a_1 \\ a_2 \\ \cdot \\ \cdot \\ a_6 \end{Bmatrix}$$

Or

$$\{ U \} = [\alpha] \{ \theta \} \qquad 4\text{-}10$$

where $\{ \theta \}$ = vector of prescribed degree of freedom

$[\alpha]$ = matrix of prescribed coefficients

We want to find a relation which relates the u and v displacements directly to the triangle's degree of freedom.

$$\{ U \} = [A] \{ s \} \qquad 4\text{-}11$$

where $\{ U \}$ = assumed displacement field

$\{ s \}$ = actual degree of freedom of element

So assume that $\{ \theta \}$ is related to $\{ s \}$ by $\{ \beta \}$:

$$\{ s \} = [\beta] \{ \theta \} \qquad 4\text{-}12$$

Building the $[\beta]$ matrix :

@ node (1): $\xi = \xi_1 \quad \zeta = \zeta_1$

$$s_1 = a_1 + a_2\xi_1 + a_3\zeta_1$$

$$s_2 = a_4 + a_5\xi_1 + a_6\zeta_1$$

@ node (2) $\xi = \xi_2 \quad \zeta = \zeta_2$

$$s_3 = a_1 + a_2\xi_2 + a_3\zeta_2$$

$$s_4 = a_4 + a_5\xi_2 + a_6\zeta_2$$

@ node (3) : $\xi = \xi_3 \quad \zeta = \zeta_3$

$$s_5 = a_1 + a_2\xi_3 + a_3\zeta_3 \qquad 4\text{-}13$$

$$s_6 = a_4 + a_5\xi_3 + a_6\zeta_3$$

Putting equations 4-13 in matrix form of equation 4-12 results in the following [β] matrix.

$$\underset{6 \times 6}{[\,\beta\,]} = \begin{bmatrix} 1 & \xi_1 & \zeta_1 & 0 & 0 & 0 \\ 0 & 0 & 0 & 1 & \xi_1 & \zeta_1 \\ 1 & \xi_2 & \zeta_2 & 0 & 0 & 0 \\ 0 & 0 & 0 & 1 & \xi_2 & \zeta_2 \\ 1 & \xi_3 & \zeta_3 & 0 & 0 & 0 \\ 0 & 0 & 0 & 1 & \xi_3 & \zeta_3 \end{bmatrix}$$

From equation 4-12, { θ } can be solved for:

$$\{\,\theta\,\} = [\,\beta\,]^{-1} \{\,s\,\} \qquad 4\text{-}14$$

But we want

$$\{\,U\,\} = [\,A\,] \{\,s\,\} \qquad 4\text{-}11$$

and know

$$\{\,U\,\} = [\,\alpha\,] \{\,\theta\,\} \qquad 4\text{-}10$$

then substituting equation 4-14 into equation 4-10 yields

$$\{\,U\,\} = [\,\alpha\,] [\,\beta\,]^{-1} \{\,s\,\} \qquad 4\text{-}15$$

So $[A] = [\alpha][\beta]^{-1}$

Now we can proceed to derive the strain displacement matrix.

Strains are expressed as

$$\{\varepsilon\} = [L]\{U\} \qquad 4\text{-}16$$

where L = strain displacement operator for plane stress $= \begin{bmatrix} \frac{\partial}{\partial \xi} & 0 \\ 0 & \frac{\partial}{\partial \zeta} \\ \frac{\partial}{\partial \zeta} & \frac{\partial}{\partial \xi} \end{bmatrix}$

and

ε = strain matrix $\begin{Bmatrix} \varepsilon x \\ \varepsilon y \\ \gamma xy \end{Bmatrix}$

Substituting equation 4-15 into equation 4-16 yields

$$\{\varepsilon\} = [L][\alpha][\beta]^{-1}\{s\} \qquad 4\text{-}17$$

Then $[B] = [L][\alpha][\beta]^{-1}$ = the strain-displacement matrix.

Once the strains are computed the stresses follow from the equation.

$$\{\sigma\} = [D_p]\{\varepsilon\} \qquad 4\text{-}18$$

where D_p = elasticity matrix for plane stress, defined in section 4.2.1.

σ = stress matrix $\begin{Bmatrix} \sigma x \\ \sigma y \\ Txy \end{Bmatrix}$

4.2.3 Linear Strain Formulation: (L.S.T.)

This element has mid-side nodes as well as the nodes at the vertices, as shown in figure 4.2.

The element is one higher order than the constant strain element (section 4.2.2) because not only can it represent a constant state of strain (and stress), it can also model a linear variation.

Implicit from the title, the strains over the element are to vary linearly, so since the strain-operator for plane stress is first order, the assumed displacement field must vary quadratically. Here area co-ordinates are used since the computation is more direct, and efficient. Noting that complete quadratics in two space require:

$$\left(\begin{matrix}2 \quad 2\\ 2\end{matrix}\right) = \frac{4\ (3)}{2} = 6 \qquad \text{parameters for each displacement}$$

function. Then in total 12 values of displacement must be computed for each element. A logical choice would be to use u and V at the mid-side nodes with the 3 existing nodes (refer to figure 4.2).

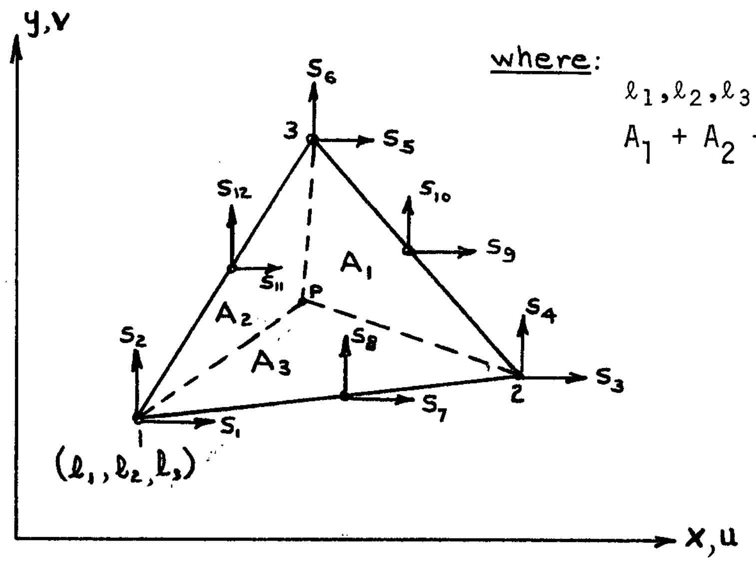

where:

ℓ_1, ℓ_2, ℓ_3 = area co-ordinate

$A_1 + A_2 + A_3 = A_T$

Fig. 4.2 Linear-Strain Triangle

The area co-ordinates are defined as follows:

$$\ell_1 = \frac{A_1}{A_T} \qquad \ell_2 = \frac{A_2}{A_T} \qquad \ell_3 = \frac{A_3}{A_T}$$

(Same as section 3.3)

Noting that each shape function should be unity at one node and zero at all others (since the shape functions are actually interpolation formulae), we obtain the following shape functions:

$$\begin{aligned} N_1 &= \ell_1 (2\ell_1 - 1) \\ N_2 &= \ell_2 (2\ell_2 - 1) \\ N_3 &= \ell_3 (2\ell_3 - 1) \\ N_4 &= 4\ell_1\ell_2 \\ N_5 &= 4\ell_2\ell_3 \\ N_6 &= 4\ell_3\ell_1 \end{aligned} \qquad 4\text{-}19$$

<u>Then</u>

$$U = \sum_{i=1}^{12} N_i \, s_i \qquad 4\text{-}20$$

where

$$\{ U \}^T = \langle u_1 , v_1, u_2, v_2, u_3, \ldots v_6 \rangle$$

<u>Or</u>

$$\{ U \} = [A] \{ s \} \qquad 4\text{-}20a$$

where

$\{ s \}$ = solution vector of displacements where

$$[A]^T_{12 \times 2} = \begin{bmatrix} \ell_1\,(2\ell_1 - 1) & 0 \\ 0 & \ell_1\,(2\ell_1 - 1) \\ \ell_2\,(2\ell_2 - 1) & 0 \\ 0 & \ell_2\,(2\ell_2 - 1) \\ \ell_3\,(2\ell_3 - 1) & 0 \\ 0 & \ell_3\,(2\ell_2 - 1) \\ 4\ell_1\ell_2 & 0 \\ 0 & 4\ell_1\ell_2 \\ 4\ell_2\ell_3 & 0 \\ 0 & 4\ell_2\ell_3 \\ 4\ell_3\ell_1 & 0 \\ 0 & 4\ell_3\ell_1 \end{bmatrix}$$

<u>Area of the Element:</u> Δ

$$\Delta = \frac{1}{2} \det \begin{vmatrix} 1 & 1 & 1 \\ x_1 & x_2 & x_3 \\ y_1 & y_3 & y_3 \end{vmatrix} \qquad \text{4-21}$$

$$= \frac{1}{2} \det \begin{vmatrix} x_1 - x_3 & x_2 - x_3 \\ y_1 - y_3 & y_2 - y_3 \end{vmatrix}$$

<u>let</u>

$a_1 = x_3 - x_2$ $\qquad$ $b_1 = y_2 - y_3$

$a_2 = x_1 - x_3$ $\qquad$ $b_2 = y_3 - y_1$

$a_3 = x_2 - x_1$ $\qquad$ $b_3 = y_1 - y_2$

then

$$\Delta = \frac{1}{2} [a_2 b_1 - b_2 a_1]$$

Relating area co-ordinates to Cartesian Co-ordinates:

$$\begin{Bmatrix} 1 \\ x \\ y \end{Bmatrix} = \begin{bmatrix} 1 & 1 & 1 \\ x_1 & x_2 & x_3 \\ y_1 & y_2 & y_3 \end{bmatrix} \begin{Bmatrix} \ell_1 \\ \ell_2 \\ \ell_3 \end{Bmatrix} \qquad 4\text{-}22$$

Expanding equation 4-22 and making use of the fact that

$$\ell_1 + \ell_2 + \ell_3 = 1$$

Or

$$\ell_3 = 1 - \ell_1 - \ell_2 \qquad 4\text{-}23$$

gives:

$$x = x_1 \ell_1 + x_2 \ell_2 + x_3 (1 - \ell_1 - \ell_2)$$

$$y = y_1 \ell_1 + y_2 \ell_2 + y_3 (1 - \ell_1 - \ell_2) \qquad 4\text{-}24$$

We want $\{ L \} = [J] \{ X \}$ 4-25

where

$\{ L \}$ = first derivative of area co-ordinates (ℓ_i)

$\{ X \}$ = first derivative of Cartesian co-ordinates

$[J]$ = Jacobian matrix

Note : First derivatives are used because the strain operator is first order (contains only first derivatives).

From equation 4-25

$$\begin{Bmatrix} \dfrac{\partial}{\partial \ell_1} \\ \\ \dfrac{\partial}{\partial \ell_2} \end{Bmatrix} = [\,J\,] \begin{Bmatrix} \dfrac{\partial}{\partial x} \\ \\ \dfrac{\partial}{\partial y} \end{Bmatrix} \qquad 4\text{-}26$$

Using the chain rule to relate the two co-ordinates systems:

$$\frac{\partial}{\partial \ell_1} = \frac{\partial x}{\partial \ell_1}\frac{\partial}{\partial x} + \frac{\partial y}{\partial \ell_1}\frac{\partial}{\partial y}$$

$$= a_2 \frac{\partial}{\partial x} - b_2 \frac{\partial}{\partial y} \qquad 4\text{-}27a$$

and:

$$\frac{\partial}{\partial \ell_2} = \frac{\partial x}{\partial \ell_2}\frac{\partial}{\partial x} + \frac{\partial y}{\partial \ell_2}\frac{\partial}{\partial y}$$

$$= -a_1 \frac{\partial}{\partial x} + b_1 \frac{\partial}{\partial y} \qquad 4\text{-}27b$$

then expressing equation 4-27a and 4-27b in the form of equation 4-26, yields the following Jacobian matrix.

$$[\,J\,] = \begin{bmatrix} a_2 & -b_2 \\ -a_1 & b_1 \end{bmatrix}$$

It's inverse is:

$$[\,J\,]^{-1} = \frac{1}{2A} \begin{bmatrix} b_1 & b_2 \\ a_1 & a_2 \end{bmatrix}$$ where A = area of the element

Strain-Displacement Relationship:

We know:

$$\{ \varepsilon \} = \{ X \} \{ U \} \qquad 4\text{-}28$$

where U = displacement (in-plane), $\{\varepsilon\}$ = vector of strains

then from equation 4-25:

$$\{ X \} = [J]^{-1} \{ L \} \qquad 4\text{-}29$$

So

$$\{ \varepsilon \} = [J]^{-1} \{ L \} \{ U \} \qquad 4\text{-}30$$

$$= [J]^{-1} \{ L \} [A] \{ s \} \qquad 4\text{-}30a$$

Therefore

$[B] = \{ L \} [A]$ is the strain-displacement matrix.

where L = strain operator = $\begin{bmatrix} \frac{\partial}{\partial x} & 0 \\ 0 & \frac{\partial}{\partial y} \\ \frac{\partial}{\partial y} & \frac{\partial}{\partial x} \end{bmatrix}$

Evaluating equation 4-30a

$$[J]^{-1} [L] = \frac{1}{2A} \begin{bmatrix} \left(b_1 \frac{\partial}{\partial \ell_1} + b_2 \frac{\partial}{\partial \ell_2}\right) & 0 \\ 0 & \left(a_1 \frac{\partial}{\partial \ell_1} + a_2 \frac{\partial}{\partial \ell_2}\right) \\ \left(a_1 \frac{\partial}{\partial \ell_1} + a_2 \frac{\partial}{\partial \ell_2}\right) & \left(b_1 \frac{\partial}{\partial \ell_1} + b_2 \frac{\partial}{\partial \ell_2}\right) \end{bmatrix}$$

and incorporating the equation $\ell_3 = 1 - \ell_1 - \ell_2$ into $[A]$

yields:

$$
\underset{12 \times 2}{[\,A\,]^T} = \begin{bmatrix}
\ell_1 (2\ell_1 - 1) & 0 \\
0 & \ell_1 (2\ell_1 - 1) \\
\ell_2 (2\ell_2 - 1) & 0 \\
0 & \ell_2 (2\ell_2 - 1) \\
(1 - \ell_2 - \ell_1)\ [2\ (1 - \ell_2 - \ell_1) - 1] & 0 \\
0 & (1 - \ell_2 - \ell_1)\ [\ 2\ (1 - \ell_1 - \ell_2) - 1] \\
4\ell_1\ell_2 & 0 \\
0 & 4\ell_1\ell_2 \\
4\ell_2\ (1 - \ell_2 - \ell_1) & 0 \\
0 & 4\ell_2\ (\ 1 - \ell_2 - \ell_1) \\
4\ (\ 1 - \ell_1 - \ell_2)\ell_1 & 0 \\
0 & 4\ (\ 1 - \ell_1 - \ell_2)\ \ell_1
\end{bmatrix}
$$

The resulting [B] premultiplied by $[\ J\ ]^{-1}$ for use in equation 4 - 30a is shown in table 4.1 on the next page.

TABLE 4.1: STRAIN-DISPLACEMENT MATRIX FOR L.S.T.

$$[B]^T = \frac{1}{2A}\begin{bmatrix}
b_1(4\ell_1 - 1) & 0 & a_1(4\ell_1 - 1) \\
0 & a_1(4\ell_1 - 1) & b_1(4\ell_1 - 1) \\
b_2(4\ell_2 - 1) & 0 & a_2(4\ell_2 - 1) \\
0 & a_2(4\ell_2 - 1) & b_2(4\ell_2 - 1) \\
b_1(4\ell_1 + 4\ell_2 - 3) + b_2(4\ell_2 + 4\ell_1 - 3) & 0 & a_1(4\ell_1 + 4\ell_2 - 3) + a_2(4\ell_2 + 4\ell_1 - 3) \\
0 & a_1(4\ell_1 + 4\ell_2 - 3) + a_2(4\ell_2 + 4\ell_1 - 3) & b_1(4\ell_1 + 4\ell_2 - 3) + b_2(4\ell_2 + 4\ell_1 - 3) \\
4(b_1\ell_2 + b_2\ell_1) & 0 & 4(a_1\ell_2 + a_2\ell_1) \\
0 & 4(a_1\ell_2 + a_2\ell_1) & 4(b_1\ell_2 + b_2\ell_1) \\
b_1(-4\ell_2) + b_2(4 - 4\ell_1 - 8\ell_2) & 0 & a_1(-4\ell_2) + a_2(4 - 4\ell_1 - 8\ell_2) \\
0 & a_1(-4\ell_2) + a_2(4 - 4\ell_1 - 8\ell_2) & b_1(-4\ell_2) + b_2(4 - 4\ell_1 - 8\ell_2) \\
b_1(4 - 8\ell_1 - 4\ell_2) + b_2(-4\ell_1) & 0 & a_1(4 - 8\ell_1 - 4\ell_2) + a_2(-4\ell_1) \\
0 & a_1(4 - 8\ell_1 - 4\ell_2) + a_2(-4\ell_1) & b_1(4 - 8\ell_1 - 4\ell_2) + b_2(-4\ell_1)
\end{bmatrix}$$

Where A = Area of Element

Now the stresses can be computed:

$$\{ \sigma \} = [D] \{ \varepsilon \} \qquad 4\text{-}31$$

Or

$$\{ \sigma \} = [D] [B]^* \{ s \} \qquad 4\text{-}32$$

where $[B]^* = [J]^{-1} [B]$

and $\{ s \}$ = the u and v displacements at the corner and midside nodes.

Mid-Side Node Displacements:

We are not through yet because u and v of the mid-side nodes have not been defined.

From the u and v displacements of the three vertices, we must somehow derive reasonable mid-side displacements.

First resolve the cartesian u and v displacements into tangential and normal displacements at each vertex.

The tangential displacements are shown in figure 4.3.

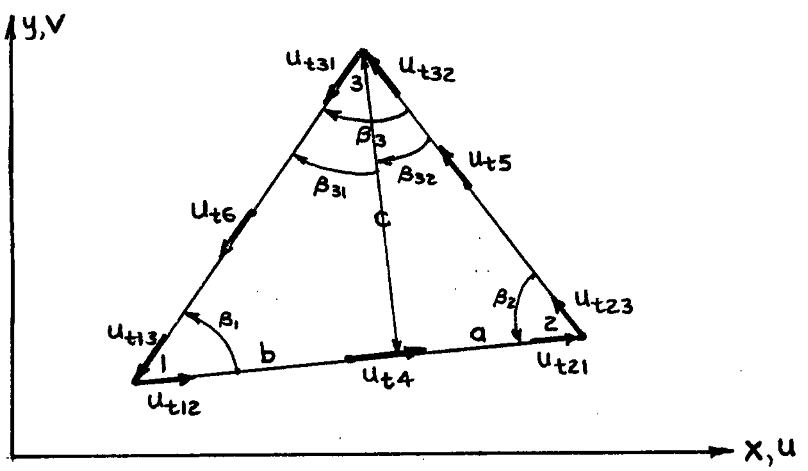

Fig. 4.3 Tangential Displacements

The relations used to resolve the cartesian displacements into tangential components at the vertices are:

@ Node (1):

$$u_{t12} = u_1 \qquad 4\text{-}33$$

$$u_{t13} = - v_1 \sin \beta_1 - u_1 \cos \beta_1 \qquad 4\text{-}34$$

@ Node (2):

$$u_{t21} = u_2 \qquad 4\text{-}35$$

$$u_{t23} = v_2 \sin \beta_2 - u_2 \cos \beta_2 \qquad 4\text{-}36$$

@ Node (3):

$$u_{t32} = v_3 \sin \beta_2 - u_3 \cos \beta_2 \qquad 4\text{-}37$$

$$u_{t31} = - v_3 \sin \beta_1 - u_3 \cos \beta_1 \qquad 4\text{-}37$$

Now define the tangential displacement of a mid-side node to be the average of its end node tangential displacements.

$$u_{t4} = \frac{u_{t12} + u_{t21}}{2} \qquad 4\text{-}39$$

$$u_{t5} = \frac{u_{t23} + u_{t32}}{2} \qquad 4\text{-}40$$

$$u_{t6} = \frac{u_{t31} + u_{t13}}{2} \qquad 4\text{-}41$$

The normal displacements are shown on figure 4.4.

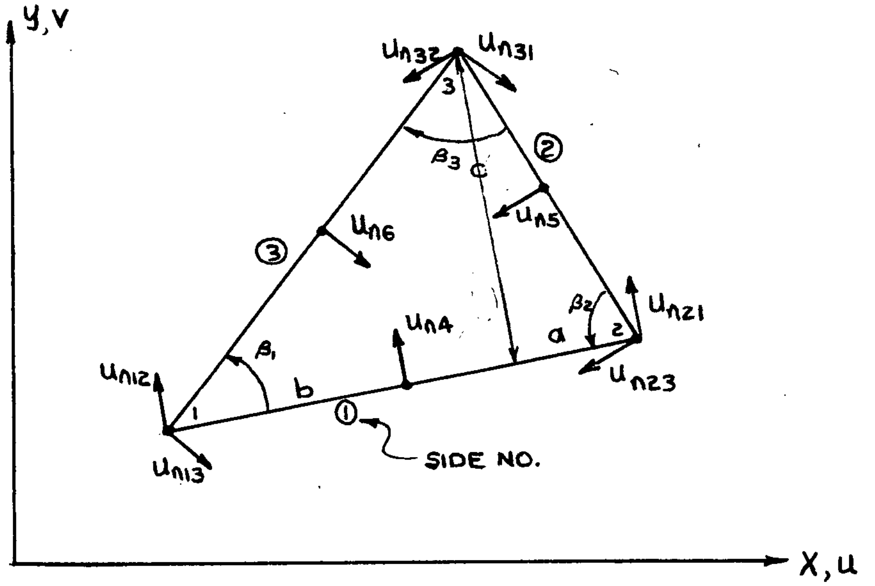

Fig. 4.4 Normal Displacements

The relations used to resolve the cartesian displacements into normal components at the vertices are:

@ Node (1):

$$u_{n12} = v_1 \tag{4-42}$$

$$u_{n13} = u_1 \sin \beta_1 - v_1 \cos \beta_1 \tag{4-43}$$

@ Node (2):

$$u_{n21} = v_2 \tag{4-44}$$

$$u_{n23} = -u_2 \sin \beta_2 - v_2 \cos \beta_2 \tag{4-45}$$

@ Node (3):

$$u_{n31} = u_3 \sin \beta_1 - v_3 \cos \beta_1 \tag{4-46}$$

$$u_{n32} = - u_3 \sin \beta_2 - v_3 \cos \beta_2 \tag{4-47}$$

Define the normal displacement of the mid-side node by an interpol-
-ation of Hermitian cubic (shape) functions.

$$u_{n4} = u_{n12}\ (1 - 3\xi^2 + 2\xi^3) + s_1\omega_1\ (\xi - 2\xi^2 + \xi^3) + u_{n21}\ (3\xi^2 - 2\xi^3) + s_1\omega_2\ (\xi^3 - \xi^2) \qquad 4\text{-}48$$

where:

ω_i = in-plane rotation at node i

s_i = length of side i

ξ = a running dimensionless parameter, varying linearly along an edge from 0 at starting node to 1 at end node. Therefore $= \frac{1}{2}$ of the mid-point of a side.

As can be seen, the Hermitian polynomials are a set of shape functions for an element's side at the ends of which the slopes and values of the normal displacements are used as variables.

Simplifying equation 4-48 yields:

$$u_{n4} = \frac{u_{n\,12}}{2} + \frac{s_1\omega_1}{8} + \frac{u_{n21}}{2} - \frac{s_1\omega_2}{8} \qquad 4\text{-}48$$

Similarly:

$$u_{n5} = \frac{u_{n23}}{2} + \frac{s_2\omega_2}{8} + \frac{u_{n32}}{2} - \frac{s_2\omega_3}{8} \qquad 4\text{-}49$$

$$u_{n6} = \frac{u_{n\,31}}{2} + \frac{s_3\omega_3}{8} + \frac{u_{n13}}{2} - \frac{s_3\omega_1}{8} \qquad 4\text{-}50$$

The final step before these mid-side displacements can be used to compute the strains is to transform them back to the cartesian co-ordinate system. The following equations perform the task:

@ Node (1):

$$uL_1 = u_{t12} \qquad 4\text{-}51$$

$$VL_1 = u_{n12} \qquad 4\text{-}52$$

@ Node (2):

$$uL_2 = u_{t21} \qquad 4\text{-}53$$

$$VL_2 = u_{n21} \qquad 4\text{-}54$$

@ Node (3) :

$$uL_3 = - u_{t32} \cos \beta_2 - u_{t31} \sin \beta_{31} \qquad 4\text{-}55$$

$$VL_3 = u_{t32} \sin \beta_2 - u_{t31} \cos \beta_{31} \qquad 4\text{-}56$$

@ Node (4):

$$uL_4 = u_{t4} \qquad 4\text{-}57$$

$$VL_4 = u_{n4} \qquad 4\text{-}58$$

@ Node (5):

$$uL_5 = - u_{n5} \sin \beta_2 - u_{t5} \cos \beta_2 \qquad 4\text{-}59$$

$$VL_5 = - u_{n5} \cos \beta_2 + u_{t5} \sin \beta_2 \qquad 4\text{-}60$$

@ Node (6):

$$uL_6 = u_{n6} \sin \beta_1 - u_{t6} \cos \beta_1 \qquad 4\text{-}61$$

$$VL_6 = -u_{n6} \cos \beta_1 - u_{t6} \sin \beta_1 \qquad 4\text{-}62$$

4.3 Bending Stresses:

The bending stresses are computed by applying the equation:

$$\{ \sigma_b \} = [D_b] [B_b] \{ \delta_b \}$$

$$\text{where } \{ \sigma_b \} = \begin{Bmatrix} m_x \\ m_y \\ m_{xy} \end{Bmatrix} = \frac{\text{in.- k}_{ip}}{\text{in. of length}}$$

(assumed to be valid over the whole element)

Note

$[D_b]$ is defined by equation 3-56b

$[B_b]$ is defined in Table 3.4

and $\{ \delta_b \}$ = solution vector of displacements. (refer to fig. 3.3)

$$= \begin{Bmatrix} w_1 \\ \theta_{x1} \\ \theta_{y1} \\ w_2 \\ \vdots \\ \theta_{y3} \end{Bmatrix}$$

Again the stresses may be evaluated anywhere within the element but in particular at the nodes as used herein.

CHAPTER 5

BEAM STIFFENER ELEMENT

A beam stiffener element is used in conjunction with a plate. The beam element strengthens the plate, increasing the flexural rigidity of the system. Deformations caused by bending are considered and as in section 3.2 for finite element formulation the assumed displacement fields are substituted into the strain energy and an element stiffness matrix is obtained.

An unsymmetrical section implies that the centroid of the cross section and shear centre do not coincide. Consider an " L " shaped section which acts as a stiffener for the plate shown below

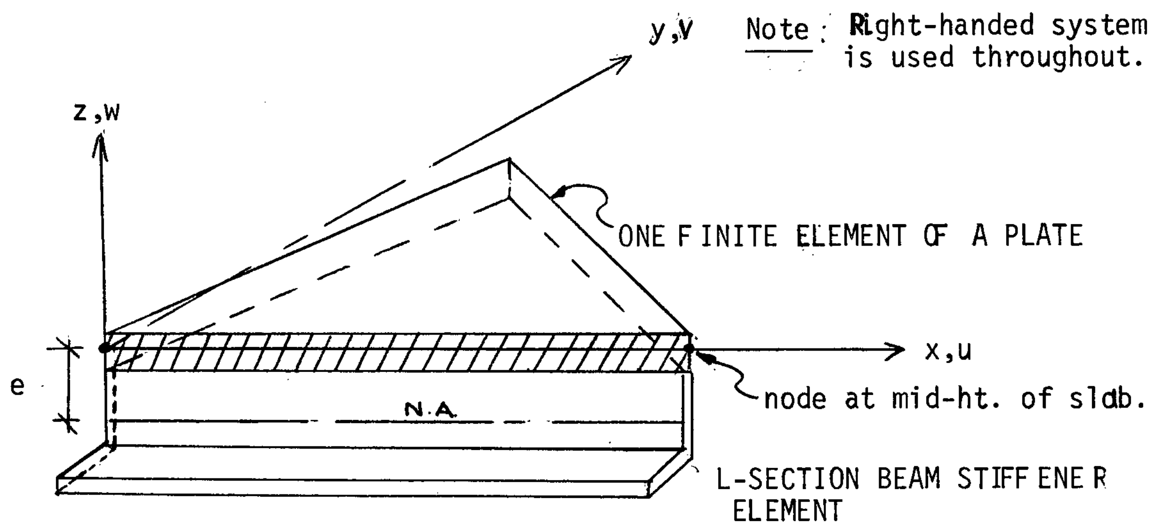

Fig. 5.1 Beam Stiffener Element

Define: - bending about y-axis in the x-z plane to be the <u>strong</u> action of the stiffener.

- bending about the z-axis in the x-y plane to be the <u>weak</u> action of the stiffener.

Let

e = vertical distance from the shear centre of the beam to the neutral plane of the plate section.

If possible we want the beam stiffener element to be compatible with the adjoining plate it is stiffening.

Consider first the bending of a symmetric section. The bending of a doubly unsymmetric section is merely a change in the stiffness matrix of the symmetric bending case.

5.1 Symmetric Bending:

Strong Direction: - consider bending in the vertical (z - x) plane about the y - axis.

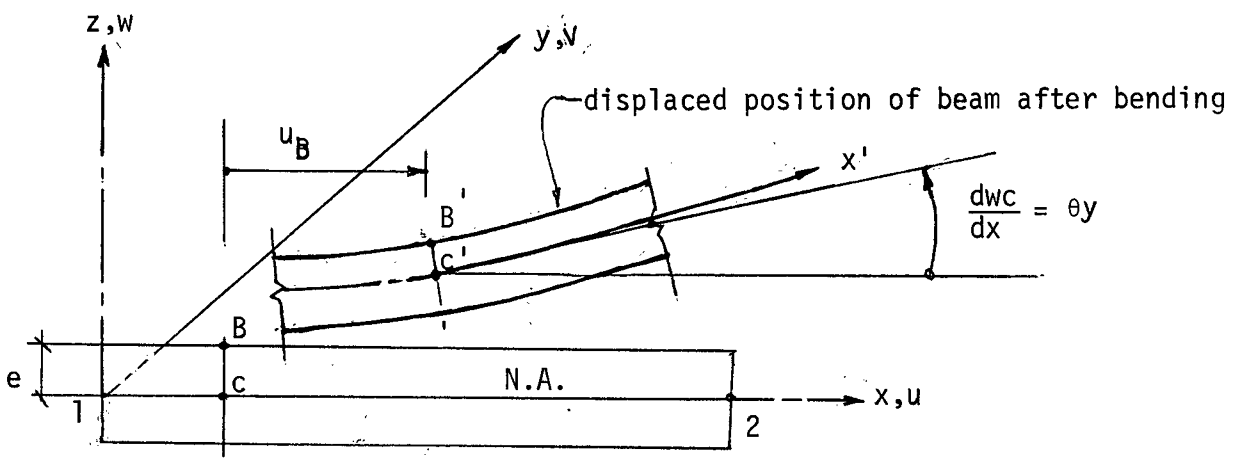

Fig. 5.2 Beam Stiffener Geometry (Strong Direction)

To describe the beam's displaced position u, w and θ_y are used at each end of the element.

From geometry:

$$u_B = u_c - e \frac{dw_c}{dx} \qquad 5\text{-}1$$

$$w_B \simeq w_c \qquad 5\text{-}2$$

For a compatible element, since w of plate is a cubic variation, then w of beam must be cubic.

$$w_c = a_1 + a_2 x + a_3 x^2 + a_4 x^3 \qquad 5\text{-}3$$

let $$u_c = a_5 + a_6 x + a_7 x^2 \qquad 5\text{-}4$$

Then from equation 5-1

$$u_B = a_5 + a_6 x + a_7 x^2 - e\ (a_2 + a_3 2x + a_4 3x^2)$$

$$= (a_5 - ea_2) + (a_6 - e2a_3)\ x + (a_7 - e3a_4)\ x^2 \qquad 5\text{-}5$$

but if u of beam is to be continuous with u of plate, it must have a linear variation.

Then the x^2 term of equation 5-5 must vanish:

$$(a_7 - e3a_4) = 0$$

<u>Or</u>

$$a_7 = 3a_4\, e \qquad 5\text{-}6$$

<u>Relate the Degree of Freedom to the polynomial coefficients:</u>

$$\{ \delta \} = [T] \{ A \} \tag{5-7}$$

$$\text{where } \{ \delta \} = \begin{Bmatrix} u_1 \\ w_1 \\ \theta_{y1} \\ u_2 \\ w_2 \\ \theta_{y2} \end{Bmatrix} \quad \& \quad \{ A \} = \begin{Bmatrix} a_1 \\ a_2 \\ a_3 \\ a_4 \\ a_5 \\ a_6 \end{Bmatrix}$$

and $[T]$ = transformation matrix

Knowing:

$$\theta_y = - \frac{dw_c}{dx} = - a_2 - 2a_3 x - 3a_4 x^2 \tag{5-8}$$

$$u_B = (a_5 - ea_2) + (a_6 - 2ea_3)\, x \tag{5-9}$$

$$w_B = a_1 + a_2 x + a_3 x^2 + a_4 x^3$$

and @ node (1) $x = 0$; @ node (2) $x = \ell$

Then:

$$[T] = \begin{bmatrix} 0 & -e & 0 & 0 & 1 & 0 \\ 1 & 0 & 0 & 0 & 0 & 0 \\ 0 & -1 & 0 & 0 & 0 & 0 \\ 0 & -e & -2e\ell & 0 & 1 & \ell \\ 1 & \ell & \ell^2 & \ell^3 & 0 & 0 \\ 0 & -1 & -2\ell & -3\ell^2 & 0 & 0 \end{bmatrix}$$

Now the stiffness matrix in terms of the polynomial coefficients can be developed from the strain energy (U):

$$U = \frac{EI}{2} \int_0^\ell (w_c'')^2 \, dx + \frac{EA}{2} \int_0^\ell (u_c')^2 \, dx \qquad 5\text{-}11$$

Where the first term of equation 5-11 is the strain enrgy stored in the beam due to pure bending and

the second term is due to axial deformation

Using expression 5-3 and 5-4 and 5-6, equation 5-11 becomes:

$$U = \frac{EI}{2} \left[4a_3^2\ell + 12a_3a_4\ell^2 + 12a_4^2\ell^3 \right] + $$
$$+ \frac{EA}{2} \left[a_6^2\ell + 2a_6^2a_7\ell^2 + \frac{4}{3} a_7^2\ell^3 \right]$$

$$= 2a_3^2\ell\, EI + 6a_3a_4\ell^2\, EI + 6a_4^2\ell^3\, EI + a_6^2\ell \frac{EA}{2} + 3a_6a_4e\ell^2\, EA +$$
$$+ 6a_4^2 e^2\ell^3 \frac{EA}{2}$$

$$= E \left[2a_3^2\ell\, I + 6a_3a_4\ell^2 I + a_4^2 \ell^3 (6I + 6e^2A) + a_6^2\ell \frac{A}{2} + \right.$$
$$\left. + 3ea_6a_4\ell^2 A \right] \qquad 5\text{-}12$$

But we also know that (quadratic form of U)

$$U = \frac{1}{2} \{ A \}^T [K_A] \{ A \} \qquad \text{5-13}$$

So writing equation 5-12 in the form of equation 5-13 and making use of symmetry yields:

$$[K_A] = 2E \begin{bmatrix} & & & & & \\ & & & & & \\ & & 2\ell I & 3\ell^2 I & & \\ & & 3\ell^2 I & \ell^3(6I+6e^2A) & & \frac{3}{2} e\ell^2 A \\ & & & & & \\ & & & \frac{3}{2} e\ell^2 A & & \frac{\ell A}{2} \end{bmatrix}$$

Let $I_o = I + e^2A$, $[K_A]$ becomes:

$$[K_A] = E \begin{bmatrix} & & & & & \\ & & & & & \\ & & 4\ell I & 6\ell^2 I & & \\ & & 6\ell^2 I & 12\ell^3 I_o & & 3e\ell^2 A \\ & & & & & \\ & & & 3e\ell^2 A & & \ell A \end{bmatrix}$$

The stiffness matrix $[\,K_A\,]$ in terms of the polynomial coefficients can be transformed to be expressed in terms of the nodal degree of freedom as follows:

Know

$$\{\,A\,\} = [\,T\,]^{-1}\{\,\delta\,\} \qquad 5\text{-}10$$

and

$$U = \frac{1}{2}\{\,A\,\}^T[\,K_A\,]\{\,A\,\} \qquad 5\text{-}13$$

then substituting equation 5-10 into equation 5-13

$$U = \frac{1}{2}\{\,\delta\,\}^T[\,T\,]^{-1\,T}[\,K_A]\,[\,T\,]^{-1}\{\,\delta\,\}$$

$$= \frac{1}{2}\{\,\delta\,\}^T[\,K_\delta\,]\{\,\delta\,\} \qquad 5\text{-}14$$

where $[\,K_\delta\,] = [\,T\,]^{-1\,T}[\,K_A\,]\,[\,T\,]^{-1}$ is the local stiffness matrix of the beam stiffener element.

The resulting K_δ matrix is:

$$\begin{bmatrix}
L^2 & & & & & \\
0 & 12(r^2+e^2) & & \text{Symmetric} & & \\
-eL^2 & -6L(r^2+e^2) & 4L^2(r^2+e^2) & & & \\
-L^2 & 0 & eL^2 & L^2 & & \\
0 & -12(r^2+e^2) & 6L(r^2+e^2) & 0 & 12(r^2+e^2) & \\
eL^2 & -6L(r^2+e^2) & 2L^2(r^2+e^2) & -eL^2 & 6L(r^2+e^2) & 4L^2(r^2+e^2)
\end{bmatrix}$$

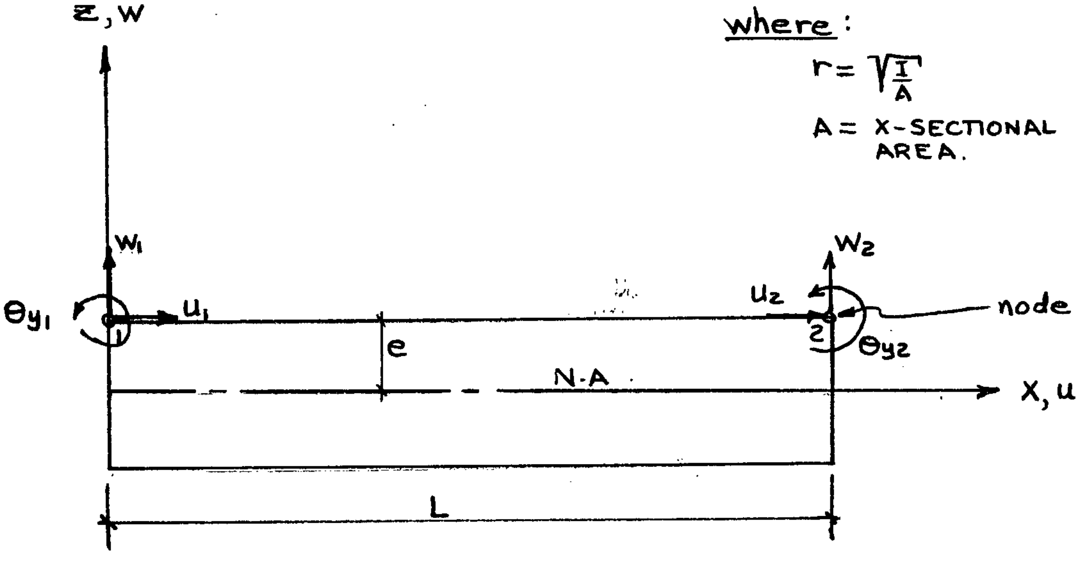

Fig. 5.3 BEAM STIFFENER (DEGREE OF FREEDOM) STRONG DIRECTION

Weak direction bending in the horizontal (x - y) plane about z - axis.

The formulation is analogous to that of the strong direction formulation except the x and y axes are used instead of the x and z axes. The degree of freedom used to describe the deformed position of the beam are u, V and θ_z at each end of the stiffener. Refer to Fig. 5.4 and Fig. 5.5.

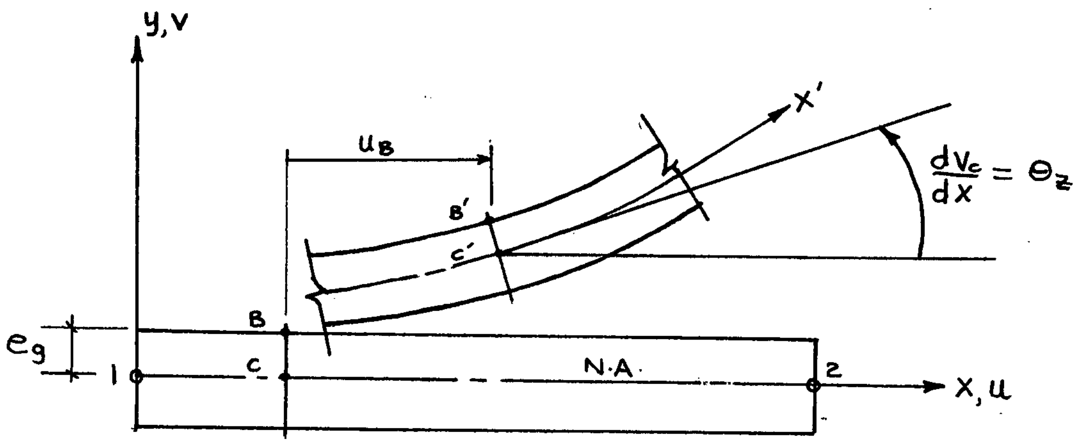

Fig. 5.4 Beam Stiffener Geometry (Weak Direction)

From Geometry:

$$u_B = u_c - e_g \frac{dV_c}{dx} \qquad 5\text{-}15$$

$$V_B \simeq V_c$$

A complete cubic in V is used since the variation along the plate is cubic.

$$V_c = a_1 x + a_2 x + a_3 x^2 + a_4 x^3 \qquad 5\text{-}16$$

and so on; as in the strong direction derivation.

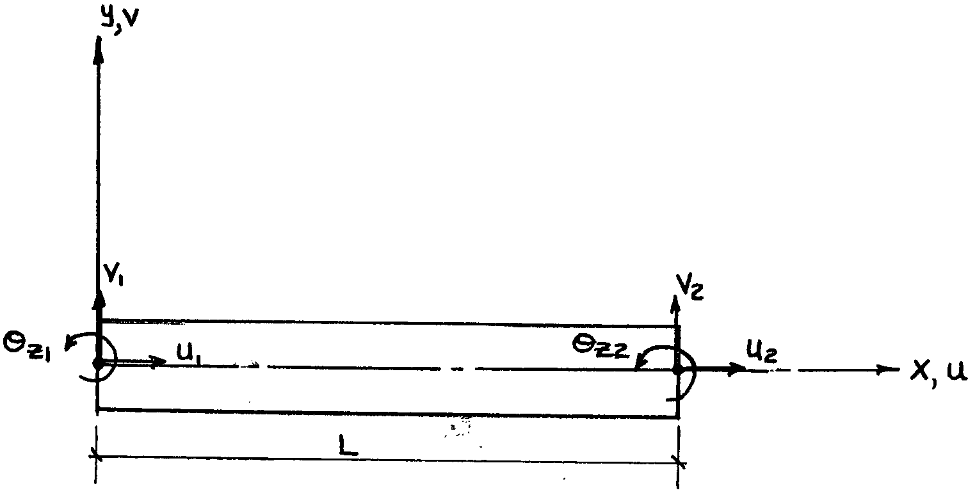

Fig. 5.5 Beam Stiffener (Degree of Freedom Weak Direction)

The same stiffness matrix is obtained as given for the strong direction formulation but relative to the d.o.f. in fig. 5.5.

Torsion: So far we have not considered twisting (rotation) of the section. Refer to figure 5.6.

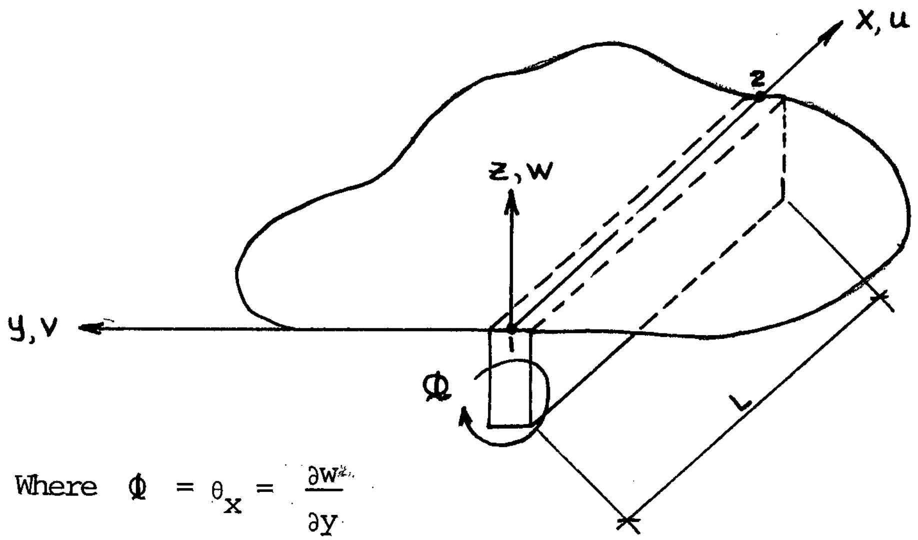

Where $\Phi = \theta_x = \dfrac{\partial w}{\partial y}$

Fig. 5.6 Beam Stiffener (Torsion)

Since we do not have continuity of Θ_x between nodes (1) and (2), there is no point in striving for a compatible element in torsion. But the twist at the nodes will be compatible if we use a linear variation for Φ.

$$\Phi = \Phi_1 \left(1 - \frac{x}{\ell} \right) + \Phi_2 \left(\frac{x}{\ell} \right) \qquad 5\text{-}17$$

Knowing, the strain energy for Torsion (U) is

$$U = \frac{G\, J_{eff}}{2} \int^{\ell} (\Phi')^2 \, dx \qquad 5\text{-}18$$

The stiffness is:

$$[\, K_T \,] = \frac{G\, J_{eff}}{2} \begin{bmatrix} 1 & -1 \\ -1 & 1 \end{bmatrix}$$

Where J = polar moment of inertia

$= \frac{1}{3}hb^3$ for thin sections

Now we can combine the stiffnesses together to form the overall 12 x 12 matrix for one beam element.

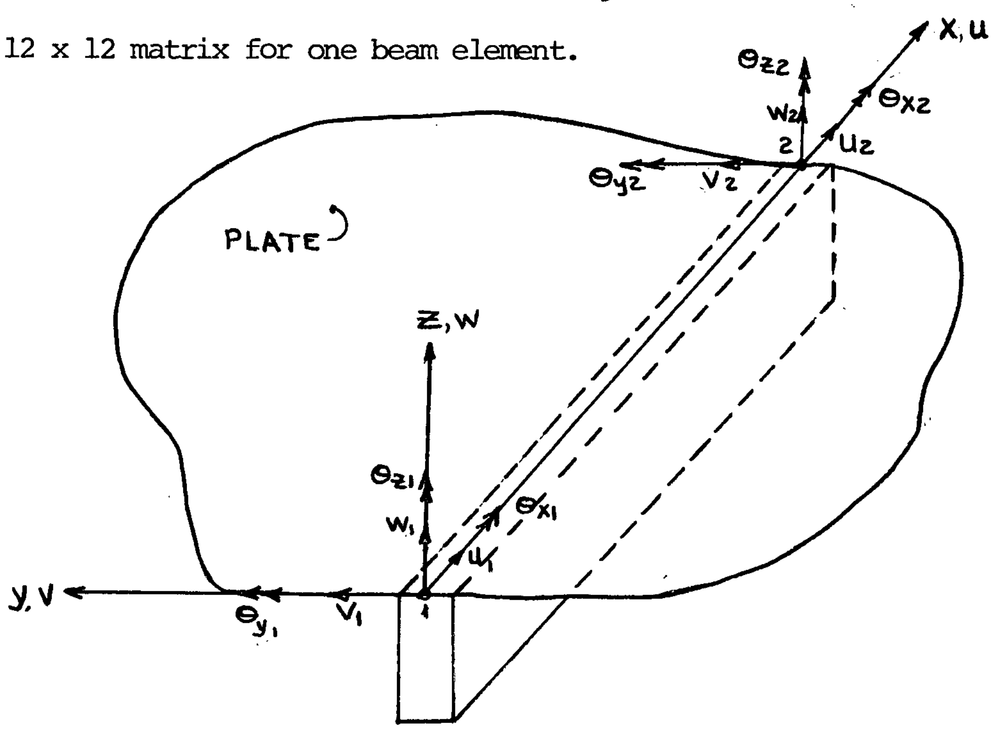

Fig. 5.7 Resultant Beam Stiffener (12 degrees of freedom)

TABLE 5.1: STIFFNESS MATRIX FOR BEAM STIFFENER ELEMENT

$[K_s] = \frac{EA}{L^3}$

L^2											
0	$12\ rE^2$										
0		12 Re					SYMMETRIC				
			$\frac{GJL^2}{EA}$								
$-eL^2$		$-6LRe$		$4L^2Re$							
EL^2	$6L\ rE$				$4L^2rE$						
$-L^2$	0	0		eL^2	$-EL^2$	L^2					
0	$-12Re$				$-6LrE$	0	12 rE				
0		-12 Re		$6LRe$		0		12 rE			
			$-\frac{GJL^2}{EA}$						$\frac{GJL^2}{EA}$		
eL^2		$-6LRe$		$2L^2$ Re		$-eL^2$		$6LRe$		$4L^2Re$	
$-eL^2$	$6LrE$				$2L^2rE$	EL^2	$-6LrE$				$4L^2rE$

Let (R^2+e^2) = Re Strong

(r^2+e^2) = rE weak

E = For weak direction eccentricity

5.2 Unsymmetric Bending: (reference 8)

Consider bending of a beam by couples m_y and m_z acting in two arbitrarily chosen perpendicular axial planes zx and yx. Refer to figure below:

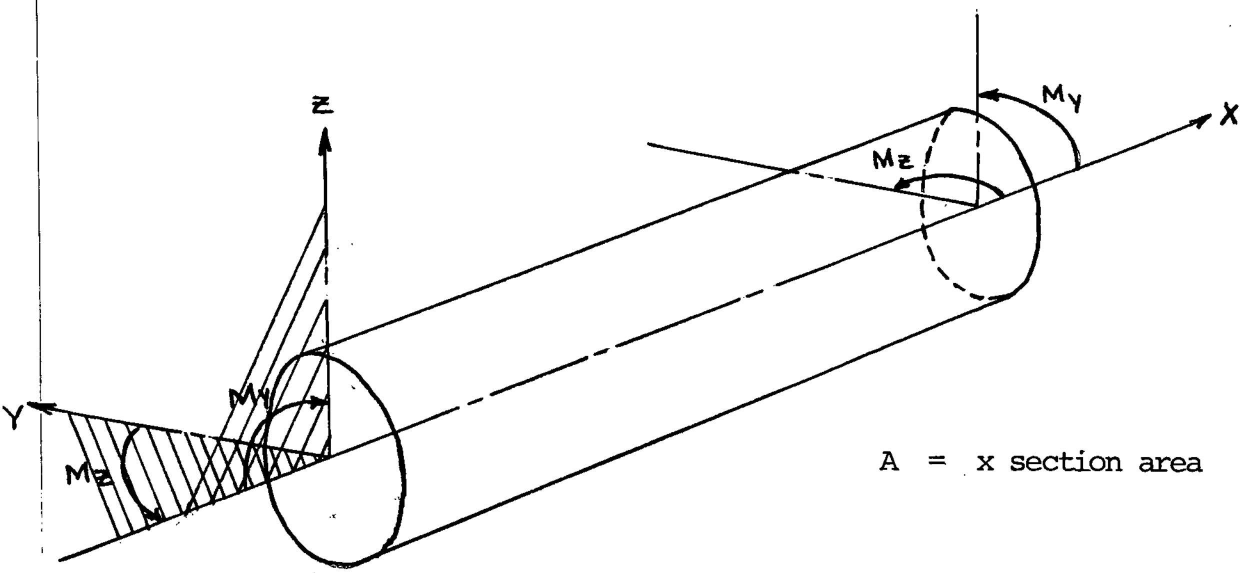

Fig. 5.8 Beam Stiffener Subjected to Couples

Bending in zx plane:

Assume that the magnitudes of the couples are such that bending occurs in the zx plane, so that the neutral axis in each cross section is parallel to the y axis. The radius of curvature due to the bending is r_z, and the bending stresses will be:

$$\sigma_x = E\,\varepsilon \qquad \text{5-19}$$

and $$\varepsilon = \frac{z}{r_z} \qquad \text{5-20}$$

Therefore $$\sigma_x = \frac{Ez}{r_z} \qquad \text{5-21}$$

Then the bending couples can be expressed as:

$$M_y = \int_A z\sigma_x \, dA = \frac{EI_y}{r_z} \quad 5\text{-}22$$

$$M_z = \int_A y\sigma_x \, dA = \frac{EI_{yz}}{r_z} \quad 5\text{-}23$$

Bending in xy plane:

If the magnitudes of the couples cause bending in the xy plane, then you get the analogous equations:

Bending stresses:

$$\sigma_x = E\,\varepsilon \quad \text{and} \quad \varepsilon = \frac{y}{r_y}$$

Therefore

$$\sigma_x = \frac{Ey}{r_y} \quad 5\text{-}24$$

Bending couples:

$$M_z = \int_A y\,\sigma_x \, dA = \frac{EI_z}{r_y} \quad 5\text{-}25$$

$$M_y = \int_A z\sigma_x \, dA = \frac{EI_{yz}}{r_y} \quad 5\text{-}26$$

Note:

$$I_z = \int y^2 \, dA$$

$$I_y = \int z^2 \, dA \quad 5\text{-}28$$

$$I_{yz} = \int_A yz \, dA$$

and

$$r_y = \sqrt{\frac{I_y}{A}}$$

$$r_z = \sqrt{\frac{I_z}{A}} \qquad 5\text{-}28$$

<u>Bending in Both xy and xz plane:</u> (coupled action)

In the general case, the beam deflects in both planes. The relations between the bending moments and curvatures are obtained by combining the equations for the uncoupled cases.

$$M_y = \frac{EI_y}{r_z} + \frac{EI_{yz}}{r_y} \qquad 5\text{-}29$$

$$M_z = \frac{EI_z}{r_y} + \frac{EI_{yz}}{r_z} \qquad 5\text{-}30$$

Since the beam stiffener will always be attached to a plate, then the bending (couples) can always be chosen to act in the xz plane, so $M_z = 0$.

Therefore from equation 5-30

$$\frac{I_z}{r_y} = -\frac{I_{yz}}{r_z}$$

<u>Or</u>

$$r_y = -\frac{I_z}{I_{yz}} r_z \qquad 5\text{-}31$$

then equation 5-29 becomes:

$$M_y = E\left[\frac{I_y}{r_z} + \frac{I_{yz}}{r_y}\right]$$

$$= \frac{E}{r_z}\left[\frac{I_y I_z - I_{yz}^2}{I_z}\right] \qquad 5\text{-}32$$

Strain Energy :

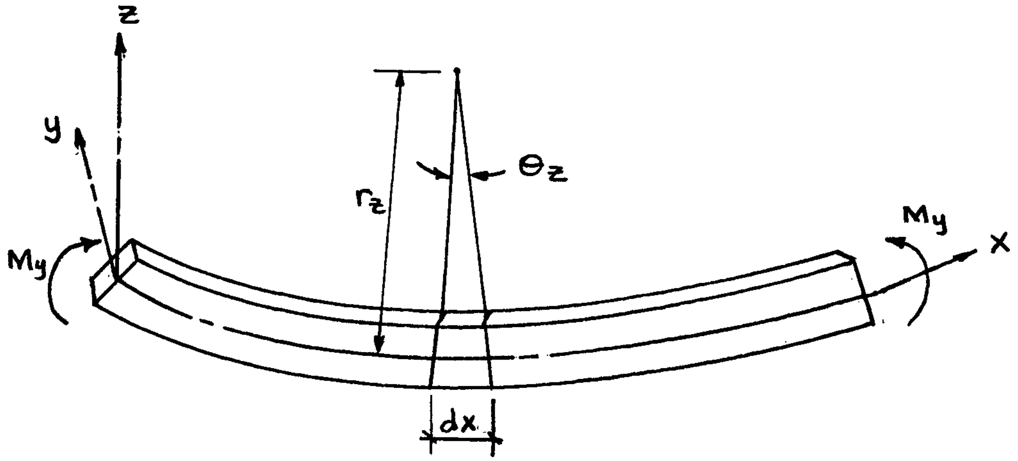

Fig. 5.9 Deflected Beam Under Pure Bending

For pure bending, the total strain energy is:

$$U = \frac{M_y \theta_z}{2} \qquad 5\text{-}33$$

Note:

$$\theta_z = \frac{1}{r_z} \quad ; \qquad d\theta_z = \frac{dx}{r_z} \simeq \frac{d^2z}{dx^2} \simeq w_c'' \, dx \qquad 5\text{-}34$$

Also $$\theta_z = \frac{M_y \ell}{EI_y} \qquad 5\text{-}35$$

Then equation 5-33 can be expressed as:

$$U = \frac{M_y^2 \ell}{2EI_y} \qquad 5\text{-}36$$

If the strain energy due to axial deformations is also considered, the strain energy for an incremental length dx is:

$$U = \frac{1}{2EI_y} \int_0^{\ell} M_y^2 \, dx + \frac{EA}{2} \int_0^{\ell} (u_c')^2 \, dx \qquad 5\text{-}37$$

Incorporating equation 5-32 and 5-34

$$U = \frac{E}{2I_y} \left[\frac{I_y I_z - I_{yz}^2}{I_z} \right]^2 \int_0^{\ell} \frac{1}{r_z^2} \, dx + \frac{EA}{2} \int_0^{\ell} (u_c')^2 \, dx$$

$$= \frac{E}{2I_y} \left[\frac{I_y I_z - I_{yz}^2}{I_z} \right]^2 \int_0^{\ell} (w_c'')^2 \, dx + \frac{EA}{2} \int_0^{\ell} (u_c')^2 \, dx$$

5-38

Note: If a symmetric section is evaluated using equation 5-38, $I_{yz} = 0$, then the equation becomes

$$U = \frac{EI_y}{2I_y} \int_0^{\ell} (w_c'')^2 \, dx + \frac{EA}{2} \int_0^{\ell} (u_c')^2 \, dx$$

which is the same as equation 5-11

note: $(I_z \neq 0)$

We know

$$W_c \simeq w_B = a_1 + a_2 x + a_3 x^2 + a_4 x^3$$

$$u_c = a_5 + a_6 x + a_7 x^2$$

So proceeding as was done for the symmetric case, the stiffness matrix can be developed.

The resulting K_δ matrix is found to be analogous to the one given for a symmetric section in table 5.1

where the values Re and rE become:

$$Re = (e^2 + U^2)$$

$$rE = (E^2 + u^2)$$

and

$$U^2 = \left[\frac{r_y^2 AI_z - I_{yz}^2}{I_z}\right]^2 \frac{1}{r_y^2 A^2}$$

$$u^2 = \left[\frac{r_z^2 AI_z - I_{yz}^2}{I_z}\right]^2 \frac{1}{r_z^2 A^2}$$

E = distance from z axis to shear centre ($e_y \rightarrow$ horizontal distance)

e = distance from center of gravity of slab to shear centre ($e_z \rightarrow$ vertical distance).

CHAPTER 6

NUMERICAL APPLICATIONS

6.1. Constant Stress Applications:

The nine degree of freedom plane stress element developed in section 3.2 is first tested under simple stress conditions. This is to see how much the element's incompleteness hinders its performance. Because of the nodal shear strain constraints, the element will not be able to model the true stress state exactly but perhaps it will be able to make a good or reasonable approximation to it.

A square plate supported as shown in figure 6.1 is subjected to a constant shear stress, a constant normal stress and a linearly varying normal stress (constant moment). The plate is modelled by two finite elements and dimensionless units are used throughout. Rotational degrees of freedom are allowed at all nodes but because the nodal shear strains (rotations) are constrained for each element (section 3.2) there may be some discrepancy here.

The constant shear stress state is simulated by loading the plate as shown in figure 6.1. Table 6.1 presents the resulting deflections and the exact values are also tabulated directly under these values. The u displacements are the same as the exact and the v displacements are only about 7% in error of the exact values. At the free end of the plate, (nodes 3 and 4) the rotational results are reasonable; only about 7% error.

The cantilevered plate using the same grid and boundary conditions as in the constant shear stress loading (figure 6.1) is used to model constant normal stress. The loading is illustrated in figure 6.2. Table 6.2

compares the resulting deflections from the finite element idealization to the exact ones. The u displacements are 16% in error at the free end but the v displacements and the rotations are much greater in error.

A linearly varying normal stress (constant moment) is simulated by the loading shown in figure 6.3. Table 6.3 presents the displacements using the finite elements and also the exact displacements. The u and v displacements are about 26% in error at the free end. The relative error in the rotations at the free ends are 21% (node 3) and 4% (node 4).

In general, the element is unable to model these stress states exactly as was expected due to its incompleteness which is due to constraining the nodal shear strains (rotations). The displacements and rotations in the constant shear stress case were only slightly in error of the exact values. However, in the other two cases with the exception of the u displacements, the predictions from the element were relatively poor.

It is interesting to note the strain energy results from these tests. That is, in the first two constant stress tests, the strain energy error was only 7.5 and 3.1%, respectively, whereas for the last linear stress case, it was much higher at 32%.

In examples to follow, we shall see to what extent the element's incompleteness hinders its performance.

CONSTANT STRESS APPLICATIONS

DIMENSIONLESS UNITS:

$E = 1.0 \quad L = 1.0$

$t = 1.0 \quad \nu = 0.3$

w FREE AT ALL NODES

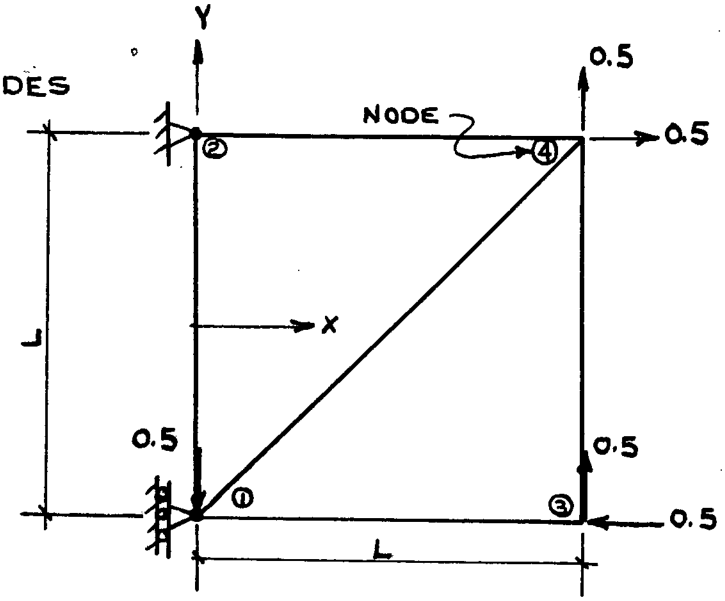

SIMULATING $\tau_{xy} = 1.0$

FIGURE 6.1: CONSTANT SHEAR STRESS

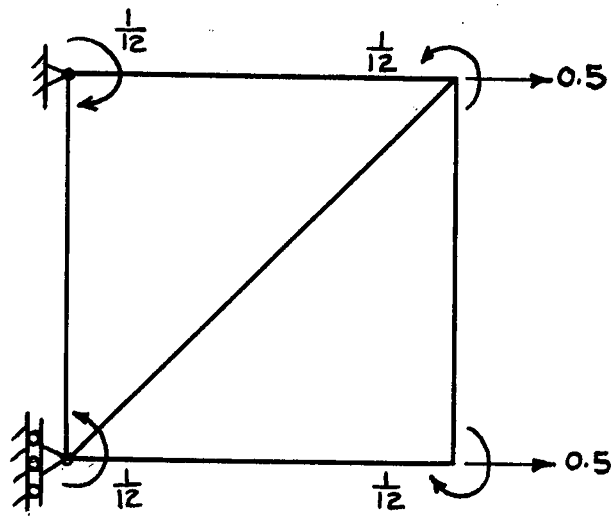

SIMULATING $\sigma_x = 1.0$

FIGURE 6.2: CONSTANT NORMAL STRESS

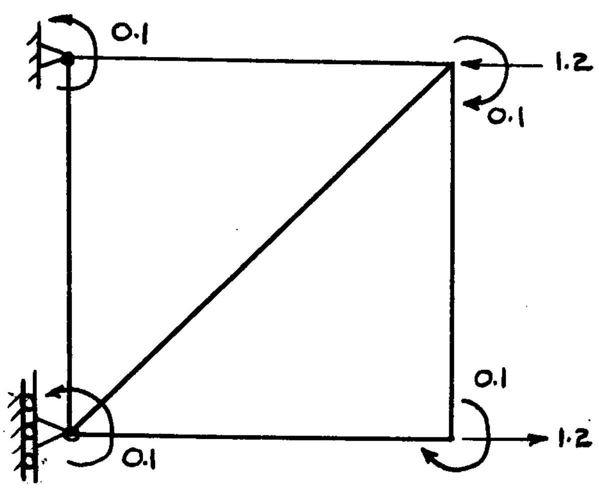

SIMULATING $M = 1.0$ $\left(\sigma_x = -\frac{12Y}{L}\right)$

FIGURE 6.3: CONSTANT BENDING MOMENT

CONSTANT STRESS APPLICATION

TABLE 6.1: DEFLECTIONS FOR CONSTANT SHEAR STRESS

POINT / DISPL.	POINT (1)	POINT (2)	POINT (3)	POINT (4)
u	0.0000	0.0000	0.0000	0.0000
v	0.0000	0.0000	2.4044	2.4044
ω	1.2022	1.2022	1.2022	1.2022
u_{EX}	0.0000	0.0000	0.0000	0.0000
v_{EX}	0.0000	0.0000	2.6000	2.6000
ω_{EX}	1.3000	1.3000	1.3000	1.3000

NOTE: EX = EXACT VALUE
Strain Energy, $U = 1.2022$, $U_{EX} = 1.3000$

TABLE 6.2: DEFLECTIONS FOR CONSTANT NORMAL STRESS

POINT / DISPL.	POINT (1)	POINT (2)	POINT (3)	POINT (4)
u	0.0000	0.0000	0.8353	0.8353
v	0.1353	0.0000	0.1353	0.0000
ω	0.1690	-0.6355	-0.6355	0.1690
u_{EX}	0.0000	0.0000	1.0000	1.0000
v_{EX}	0.3000	0.0000	0.3000	0.0000
ω_{EX}	0.0000	0.0000	0.0000	0.0000

$U = 0.4847$, $U_{EX} = 0.5000$

TABLE 6.3: DEFLECTION FOR CONSTANT MOMENT

POINT / DISPL.	POINT (1)	POINT (2)	POINT (3)	POINT (4)
u	0.0000	0.0000	4.4241	-4.4241
V	-0.1911	0.0000	4.4241	4.2329
ω	-2.6446	-0.6625	9.5108	11.4929
u_{EX}	0.0000	0.0000	6.0000	-6.0000
V_{EX}	0.0000	0.0000	6.0000	6.0000
ω_{EX}	0.0000	0.0000	12.0000	12.0000

$U = 4.0934$, $U_{EX} = 6.0000$

6.2 Cantilever Beam Problem:

Although the element developed in Chapter 3 was meant to model plate and shell type structures, it was felt that it would be beneficial to compare the nine degree of freedom plane stress element (Section 3.2) to other common elements in a familiar plane stress application.

The well known cantilever beam was selected to be modelled. The beam has unit thickness and is loaded by lumping the parabolically varying shear stress at the end nodes as loads. The material properties and the various gridworks used in the analysis are shown in figure 6.4. The boundary conditions at the cantilevered end are fixed entirely. Since the nodal rotation and u-displacement here are fixed, then the u-displacement between the nodes (along the elements' side) is constrained to be zero also.

The results are compared with the constant strain triangle (C.S.T.) and the linear strain triangle (L.S.T.). Table 6.4 presents the tip (end) deflection obtained from the C.S.T., L.S.T., as well as the nine d.o.f. element (section 3.2). From the table, it appears that the C.S.T. has a higher convergence rate but the nine d.o.f. element is more accurate for a given grid of elements. The L.S.T. deflections are superior to both the other two elements. For a grid of four the three element types yield reasonably accurate deflections. The exact deflection is computed from flexural theory. Figure 6.4 illustrates the performance of the three elements as more grid refinements are used. All three types of elements appear to be converging at a reasonable rate to the exact tip deflection. However, for relatively coarse grids, the nine d.o.f. element is far more accurate than the C.S.T. element. Referring back to table 6.4, the stresses obtained from the three types of elements are presented for the various grid sizes. All the stresses appear to be reasonably accurate and are converging it appears to the exact value. The nine d.o.f. element stresses are more accurate than the C.S.T. stresses. The L.S.T. stresses are better than the other two element types, however, it requires far more d.o.f. for a given gridwork than the other two element types.

In general, the nine d.o.f. element performed better than the constant strain element and not quite as good as the linear strain element.

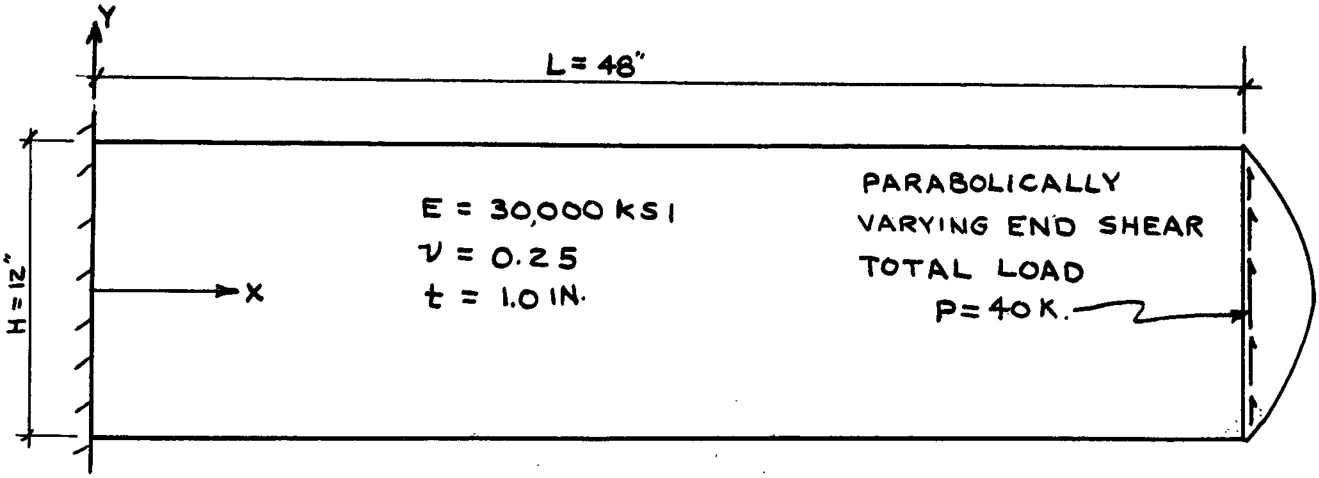

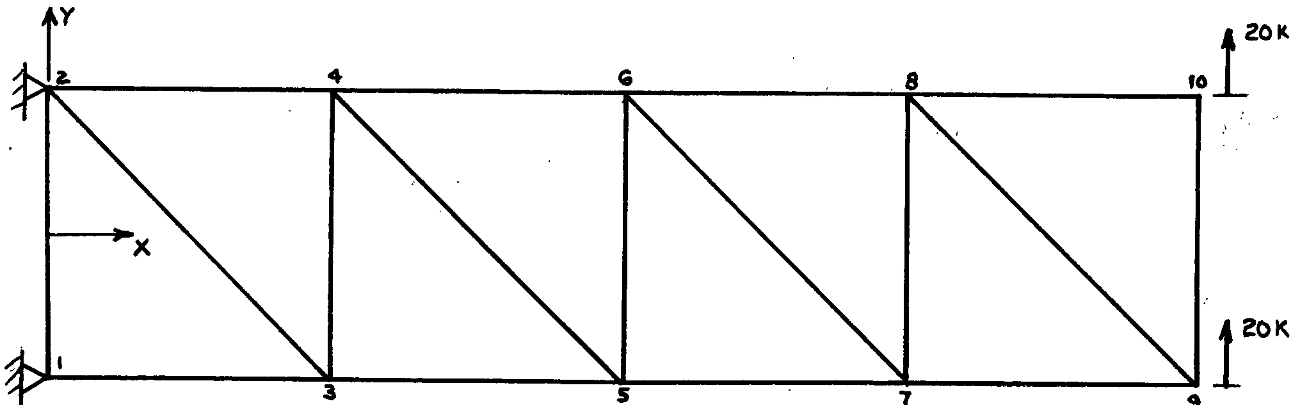

GRID1

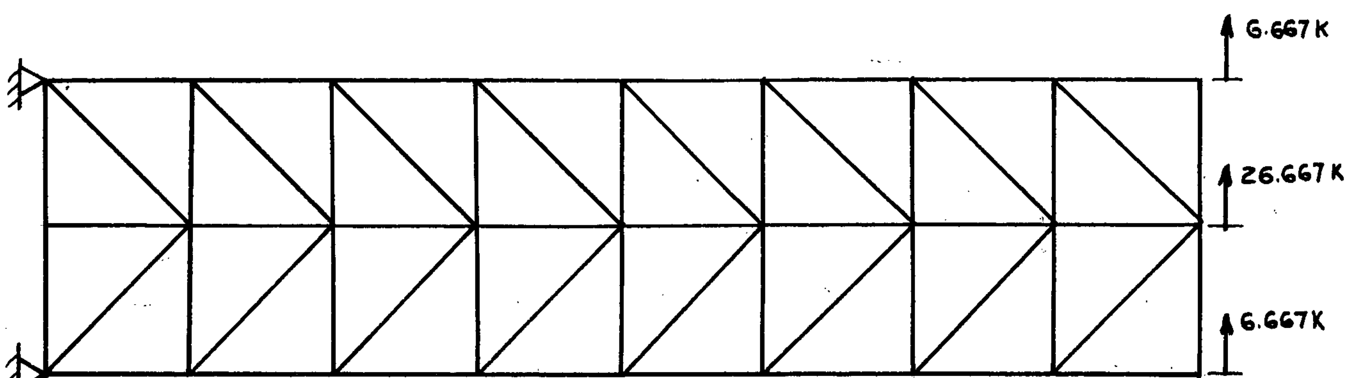

GRID2

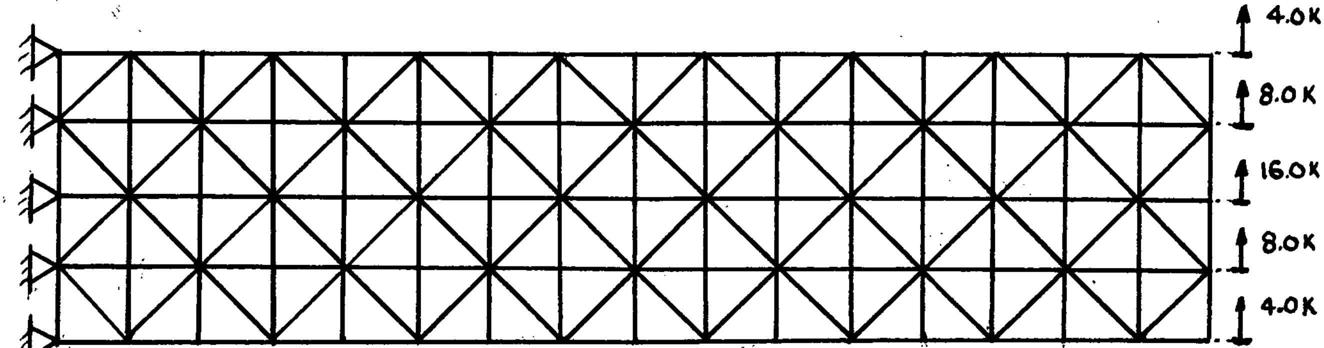

GRID4

FIGURE 6.4: CANTILEVER BEAM (LOADING & GRIDS)

CANTILEVER BEAM

TABLE 6.4: TIP DEFLECTION AND NORMAL STRESS

FINITE ELEMENT GRID	TIP DEFLECTION (IN)			***NORMAL STRESS (K/IN^2)		
	CONSTANT STRAIN TRIANGLE (C.S.T.)	NINE D.O.F. PLANE STRESS ELEMENT*	LINEAR STRAIN TRIANGLE (L.S.T.)	C.S.T.	PRESENT TRIANGLE*	L.S.T.
1	0.0909	0.2302				
2	0.1988	0.2983	0.3550	43.28	47.855	59.145
4	0.3115	0.3291	0.3556	53.51	55.774	60.024
EXACT **		0.3558			60	

ELEMENT TYPE	FINITE ELEMENT GRID	NO. OF DEGREES OF FREEDOM
C.S.T. 9 D.O.F.	1	16 24
C.S.T. 9 D.O.F. L.S.T.	2	50 74 160
C.S.T. 9 D.O.F. L.S.T.	4	162 242 576

NOTE:

* Refers to the 9 D.O.F. plane stress triangle derived in section 3.2 herein (using CST stress calculations).

** Exact solution obtained from flexural theory.

*** Normal stress σ_x

(a) x = 12" and y = 6.0"

CANTILEVER BEAM PROBLEM

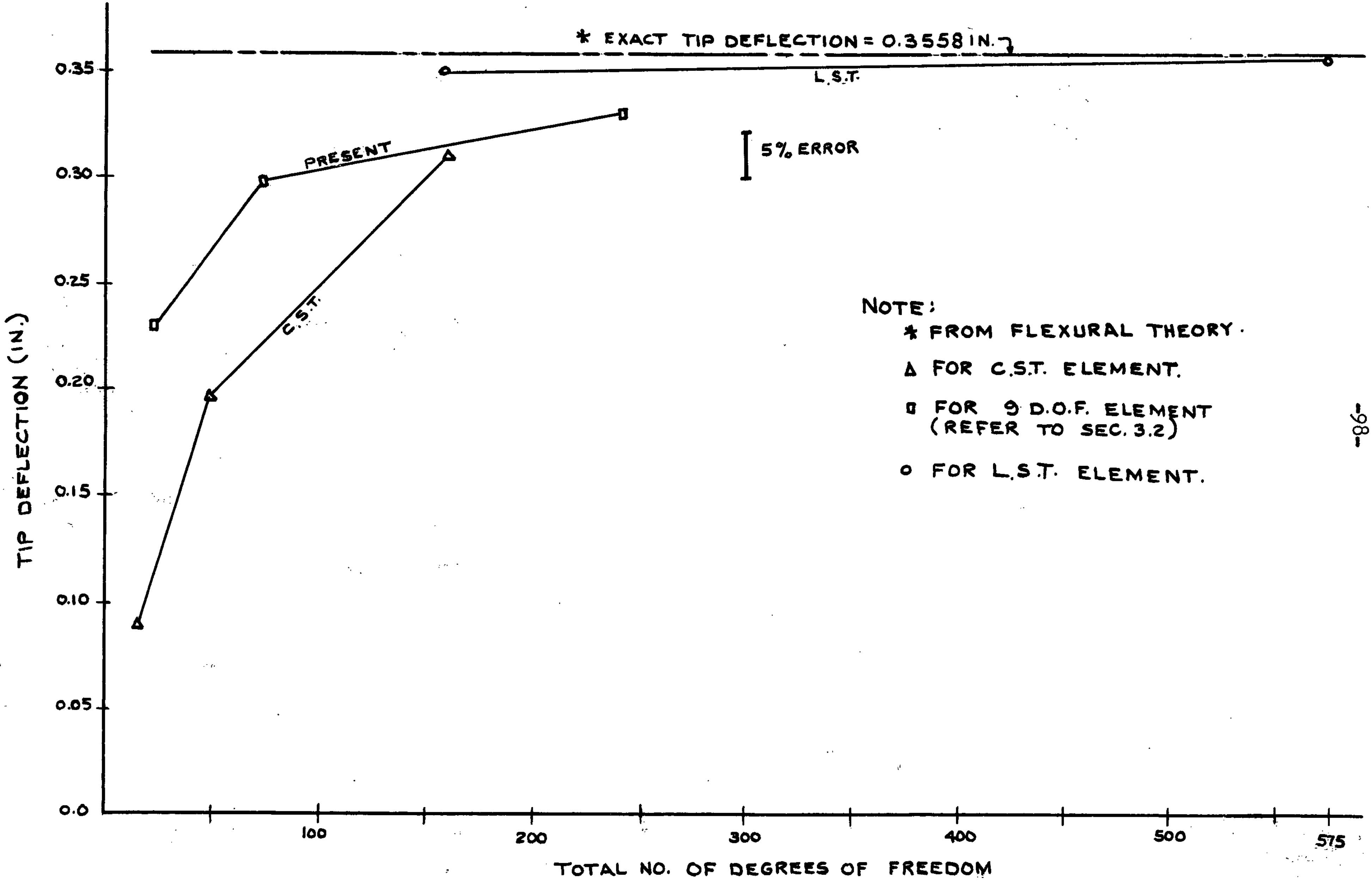

FIGURE 6.5: TIP DEFLECTION VS NO. OF DEGREES OF FREEDOM

6.3 Parabolically Loaded Square Plate:

This example serves to test the new plane stress element derived in section 3.2. Here the elements only act in plane stress because they are loaded in their plane. No bending stresses are induced. The problem is a square plate loaded on two opposite sides by a parabolically distributed normal stress. The other two sides are free. The loading and a typical grid layout are shown in figure 6.6, making use of symmetry only one quarter of the plate is modelled. Various gridworks are used and the results are compared to an exact solution (3). The load vector used is a consistent one based on the virtual work of the parabolic distribution times the cubic distribution for the edge displacement. Table 6.5 illustrates a comparison of the various deflections and strain energy with the exact solution for various gridworks. With each refinement in grid, the deflections u_B, u_C, v_C, v_D appear to be converging monotonically to some values slightly in error of the exact values. The reason for this apparent error is due to the fact that the element is incomplete and the nodal shear strains are constrained, making the element stiffer. The strain energy is also converging in a similar manner, monotonically to a value 13% in error of the exact. Figure 6.7 illustrates the manner in which the strain energy converges with each refined gridwork. Similarly in figure 6.8 the end deflection v_D in the direction of the applied load is converging but to a value roughly 13% in error of the exact.

The resultant stress at a node was computed by calculating the average stress of all the surrounding element contributions. Some characteristic or typical stresses are compared in table 6.6 with the exact for various grid refinements. The linear strain (L.S.T.), constant strain (C.S.T.) and consistent formulation (section 4.2.1) are computed.

As illustrated all three values compare to the exact with only slight error. For all gridworks N_{xB}, N_{yB}, N_{xD} and N_{yD} are exactly the same for the three stress computations. In general the C.S.T. values were better where the three stress values differed. Figure 6.9 shows the rapid convergence of N_{xD} and N_{yB} for refined gridworks to values only slightly in error (2%) of the exact. The reason again is due to the element's incompleteness and the nodal shear strain constraints making the element stiffer, therefore inhibiting it from absorbing as much strain energy as it would if it were complete and no constraints introduced.

The variation of N_{yA} with grid refinements is illustrated in figure 6.10. Here the consistent formulation (section 4.2.1) stresses are very poor and converge slowly to a value approximately 30% in error of the exact. The C.S.T. stresses however converge rapidly and are only slightly in error (for 10 x 10 gridwork 4%). The L.S.T. values on the other hand converge more slowly than the C.S.T. values and for a gridwork of ten are 12% in error with the exact. This is probably due to the displacement field limitations put on the mid-side nodes (section 4.2.3). Figure 6.11 again illustrates the superiority of the C.S.T. stresses for convergence and relatively small error for N_{yc} vs grid size. Here the consistent formulation stresses appear better but they have converged to a value in error of the exact, whereas the C.S.T. are still converging. The variation of N_{yD} with grid size is plotted on figure 6.12 The L.S.T., C.S.T. and consistent formulation yielded identical results for each gridsize. Convergence again is rapid and is only about 3% in error of the exact value.

In general the deflection values compare closely with the exact ones and the stresses (C.S.T.) converge quickly to values only slightly in error of the exact solution. The L.S.T. stresses are not quite as good as the C.S.T. but in some instances are the same. In general the consistent formulation stresses converge slowly and in some instances are in great error with the correct values.

PARABOLICALLY LOADED SQUARE PLATE

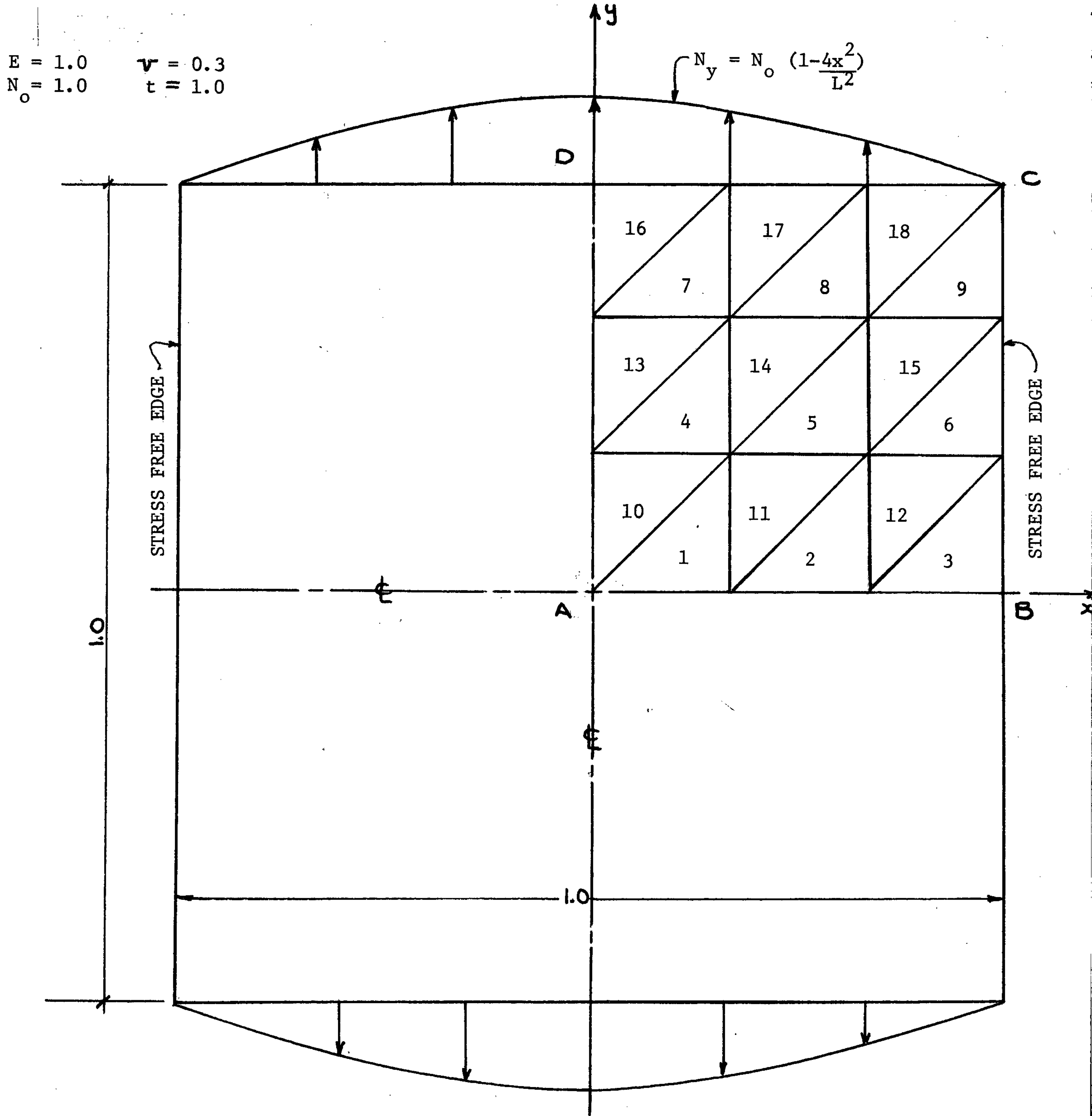

Fig. 6.6: GENERAL LAYOUT & LOADING

(3 X 3 GRID)

TABLE 6.5: DEFLECTIONS AND STRAIN ENERGY

PARABOLICALLY LOADED SQUARE PLATE

FINITE ELEMENT GRID	$\frac{10\ Et}{(1-\nu^2)N_oL}u_B$	$\frac{10^2\ Et}{(1-\nu^2)N_oL}u_C$	$\frac{10E}{(1-\nu^2)N_oL}V_C$	$\frac{10\ Et}{(1-\nu^2)N_oL}V_D$	STRAIN ENERGY U $\frac{10Et^2\ U}{(1-\nu^2)\ L^2N_o^2}$ *
1X1	- 0.9726	2.4235	1.49079	3.90615	2.330552
2X2	- 1.04971	1.57514	1.32862	4.21986	2.374308
3X3	- 1.11621	1.79154	1.25831	4.28982	2.395800
4X4	- 1.15116	2.01203	1.21533	4.32766	2.407972
5X5	- 1.1715	2.15556	1.1889	4.35060	2.415322
6X6	- 1.1844	2.24697	1.17198	4.36557	2.420083
10X10	- 1.2076	2.4023	1.14202	4.39366	2.428882
EXACT	- 1.519928	1.7837	1.27727	5.073478	2.7935695

*NOTE: U FOR WHOLE PLATE.

PARABOLICALLY LOADED SQUARE PLATE

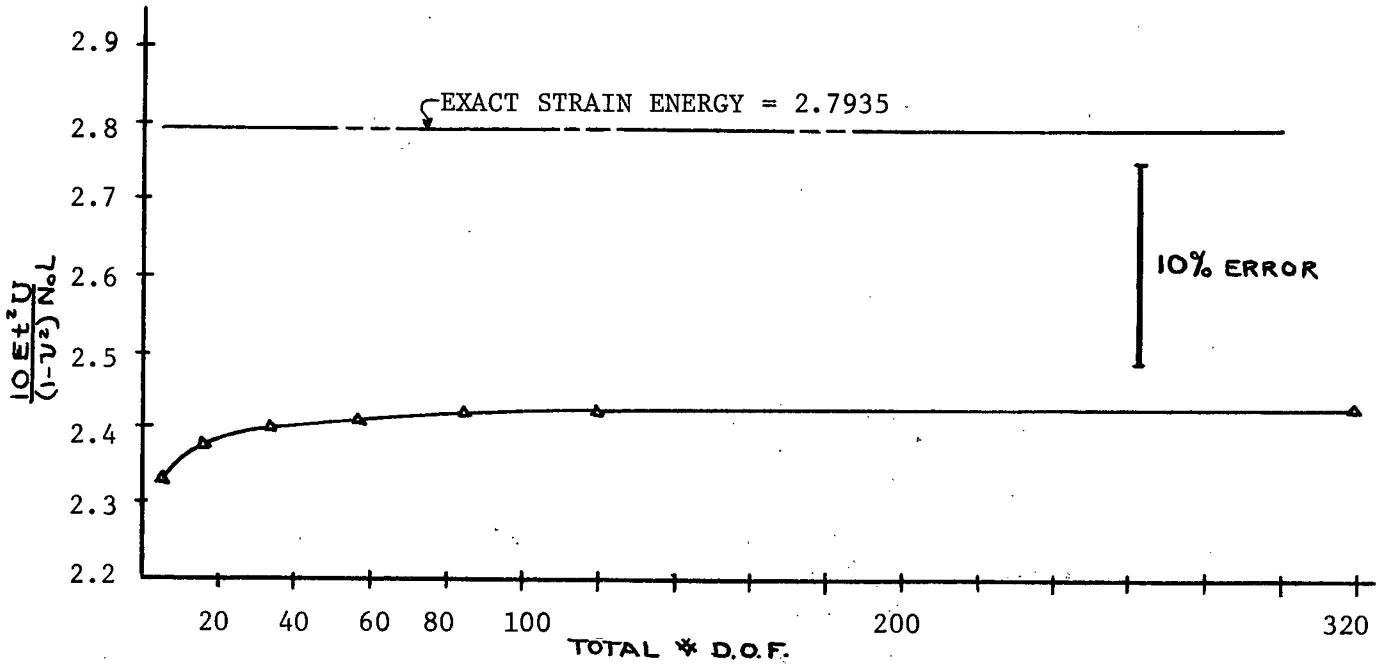

STRAIN ENERGY VS TOTAL NO. OF DEGREES OF FREEDOM

Figure 6.7A

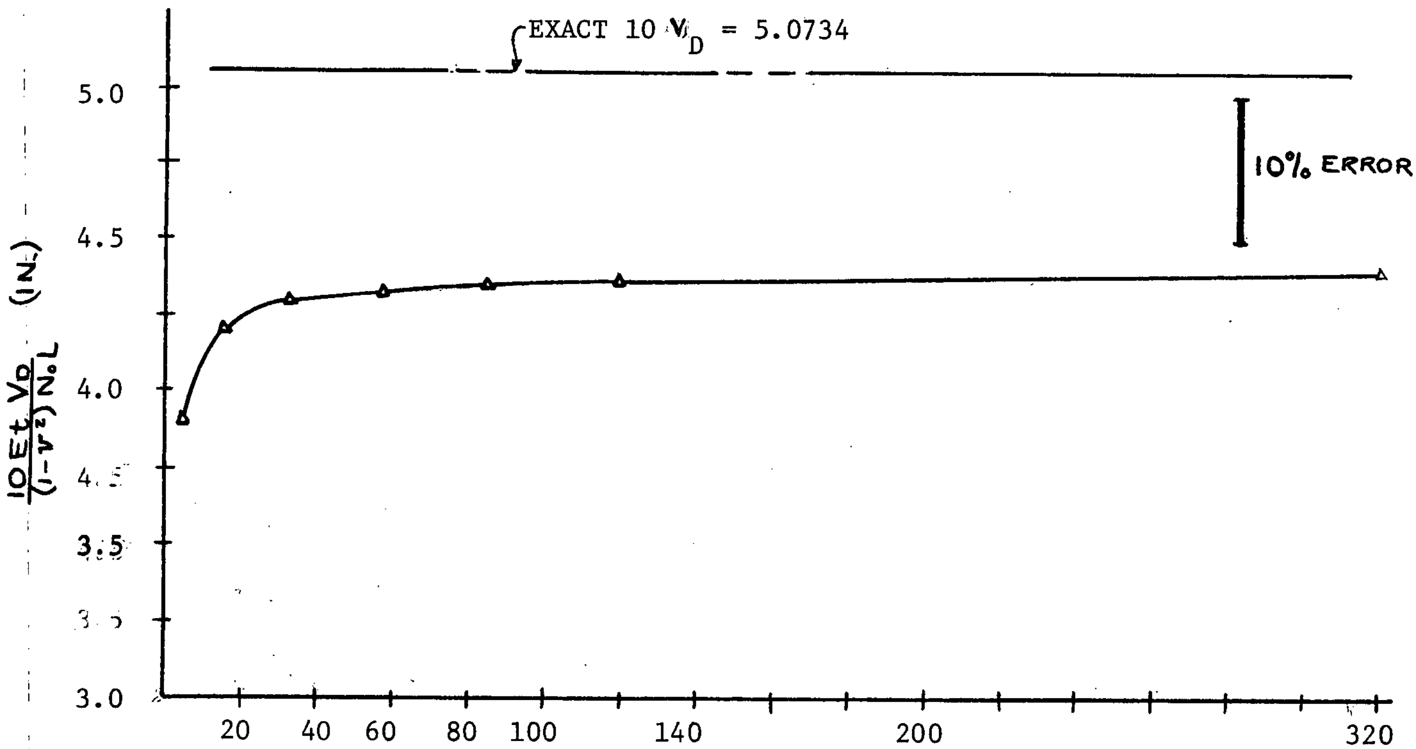

10 V_D VS TOTAL NO. OF DEGREES OF FREEDOM

Figure 6.8

TABLE 6.6: STRESSES

PARABOLICALLY LOADED SQUARE PLATE

FINITE ELEMENT GRID	STRESS (K/IN)	C.S.T. FORMULATION	L.S.T. FORMULATION	CONSISTENT FORMULATION	EACT
1	N_{xA}		0.51201	0.145689	- 0.14095
	N_{yA}		0.98334	0.52098	0.85904
	N_{xB}	- 0.11547	- 0.11547	- 0.115468	0.0
	N_{yB}	0.26352	0.26352	0.263517	0.41067
	N_{xc}		0.097672	0.19957	0.0
	N_{yc}		0.56899	0.295608	0.0
	N_{xD}	0.31081	0.31081	0.31081	0.41067
	N_{yD}	0.87447	0.87447	0.87447	1.0
2	N_{xA}	- 0.047936	- 0.011036	0.12776	- 0.14095
	N_{yA}	0.73788	0.77478	0.56219	0.85904
	N_{xB}	- 0.01905	- 0.019095	- 9.019095	0.0
	N_{yB}	0.37108	0.37108	0.371079	0.41067
	N_{xc}	0.039165	0.12447	0.073391	0.0
	N_{yc}	0.42188	0.62819	0.144118	0.0
	N_{xD}	0.3809	0.3809	0.380904	0.41067
	N_{yD}	0.96216	0.96216	0.96216	1.0
3	N_{xA}	- 0.978739	- 0.10797	0.12403	- 0.14095
	N_{yA}	0.78049	0.75126	0.57773	0.85904
	N_{xB}	- 0.003557	- 0.003557	- 0.003557	0.0
	N_{yB}	0.38307	0.38307	0.383068	0.41067
	N_{xc}	0.02494	0.097614	0.04086	0.0
	N_{yc}	0.3098	0.4980	0.09228	0.0
	N_{xD}	0.39493	0.39493	0.39493	0.41067
	N_{yD}	0.97066	0.97066	0.97066	1.0

TABLE 6.6: STRESSES (CONT'D)

PARABOLICALLY LOADED SQUARE PLATE

FINITE ELEMENT GRID	STRESS (K/IN)	C.S.T. FORMULATION	L.S.T. FORMULATION	CONSISTENT FORMULATION	EXACT
4	N_{xA}	- 0.09141	- 0.14005	0.12215	- 0.14095
	N_{yA}	0.79883	0.75019	0.58526	0.85904
	N_{xB}	0.004855	0.004855	0.004855	0.00
	N_{yB}	0.39143	0.39143	0.39143	0.41067
	N_{xC}	0.017319	0.077801	0.02837	0.0
	N_{yC}	0.24129	0.39898	0.047519	0.0
	N_{xD}	0.40544	0.40544	0.405441	0.41067
	N_{yD}	0.97369	0.97369	0.973689	1.0
5	N_{xA}	- 0.098101	- 0.15529	- 0.12113	- 0.14095
	N_{yA}	0.80855	0.75135	0.589336	0.85904
	N_{xB}	0.0098762	0.009875	0.009876	0.0
	N_{yB}	0.39638	0.39638	0.396379	0.41067
	N_{xC}	0.012509	0.064284	0.02199	0.0
	N_{yC}	0.196605	0.32961	0.05460	0.0
	N_{xD}	0.41144	0.41144	0.41144	0.41067
	N_{yD}	0.97471	0.97471	0.97471	1.0
6	N_{xA}	- 0.102087	- 0.16399	0.12048	- 0.14095
	N_{yA}	0.81430	0.75239	0.59174	0.85904
	N_{xB}	0.013098	0.01309	0.013097	0.0
	N_{yB}	0.39940	0.39940	0.39940	0.41067
	N_{xC}	0.009304	0.05470	0.01816	0.0
	N_{yC}	0.165477	0.27958	0.04574	0.0
	N_{xD}	0.41483	0.41483	0.41483	0.41067
	N_{yD}	0.97489	0.97489	0.97489	1.0

TABLE 6.6 CONT'D: STRESSES

PARABOLICALLY LOADED SQUARE PLATE

FINITE ELEMENT GRID	STRESS (K/IN)	C.S.T. FORMULATION	L.S.T. FORMULATION	CONSISTENT FORMULATION	EXACT
10	N_{XA}	-0.112275	-0.17772	0.11934	-0.14095
	N_{YA}	0.823605	0.7545	0.59566	0.85904
	N_{XB}	0.018819	0.018819	0.018819	0.0
	N_{YB}	0.40412	0.40411	0.40411	0.41067
	N_{XC}	0.003467	0.034398		0.0
	N_{YC}	0.100574	0.17194		0.0
	N_{XD}	0.41922	0.41922		0.41067
	N_{YD}	0.97364	0.97364		1.0

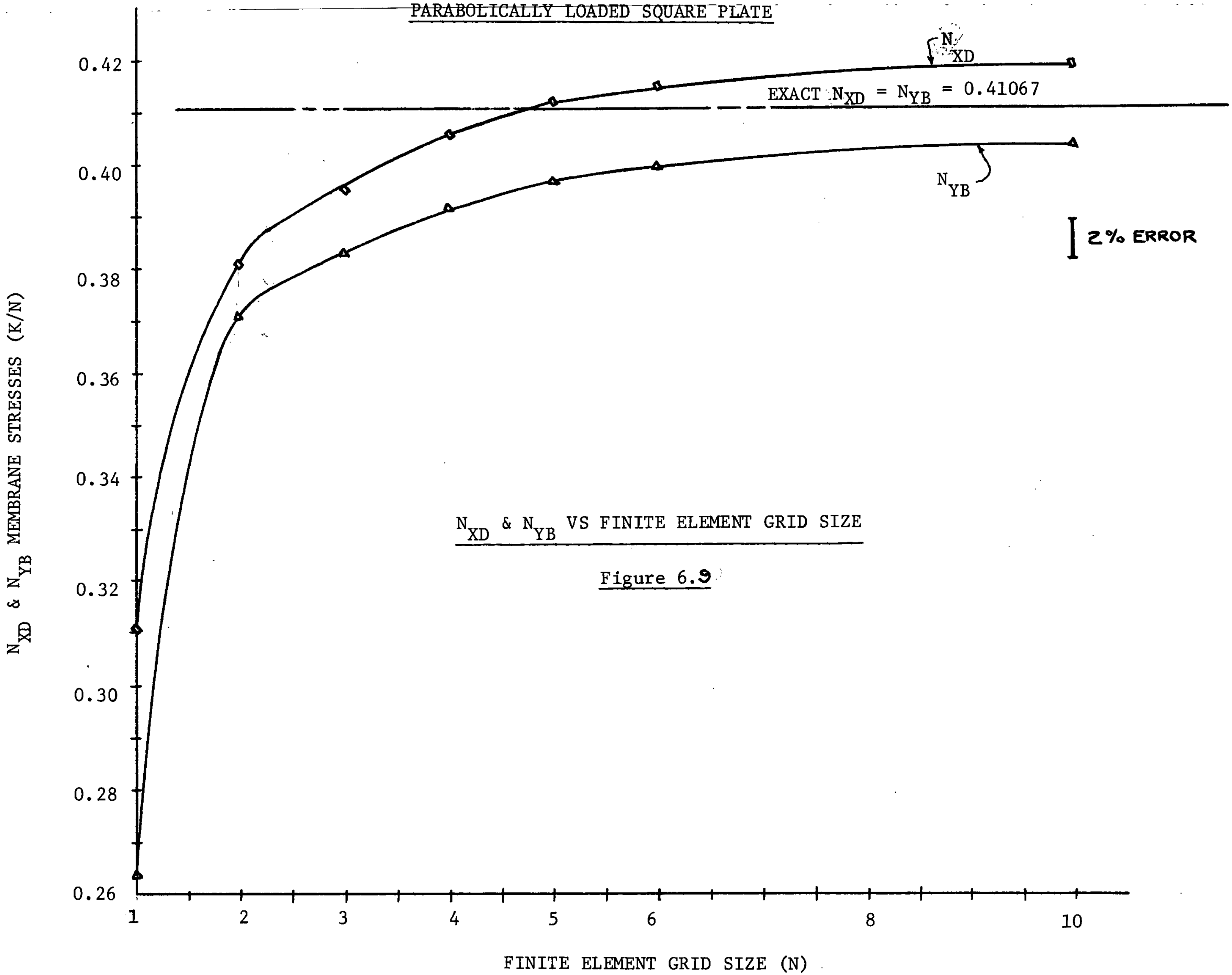

N_{XD} & N_{YB} VS FINITE ELEMENT GRID SIZE

Figure 6.9

PARABOLICALLY LOADED SQUARE PLATE

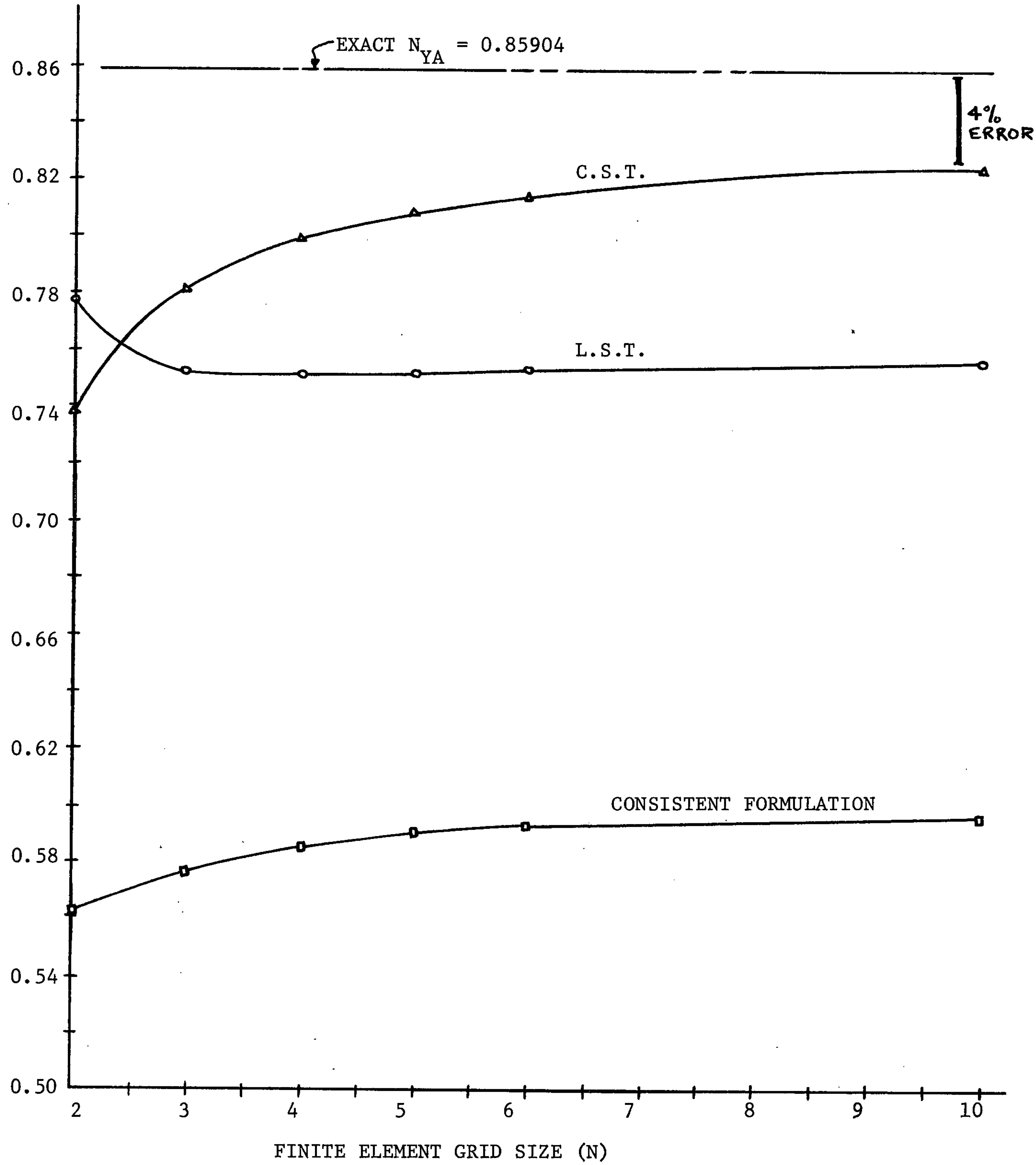

N_{YA} VS FINITE ELEMENT GRID SIZE

FIGURE 6.10

PARABOLICALLY LOADED SQUARE PLATE

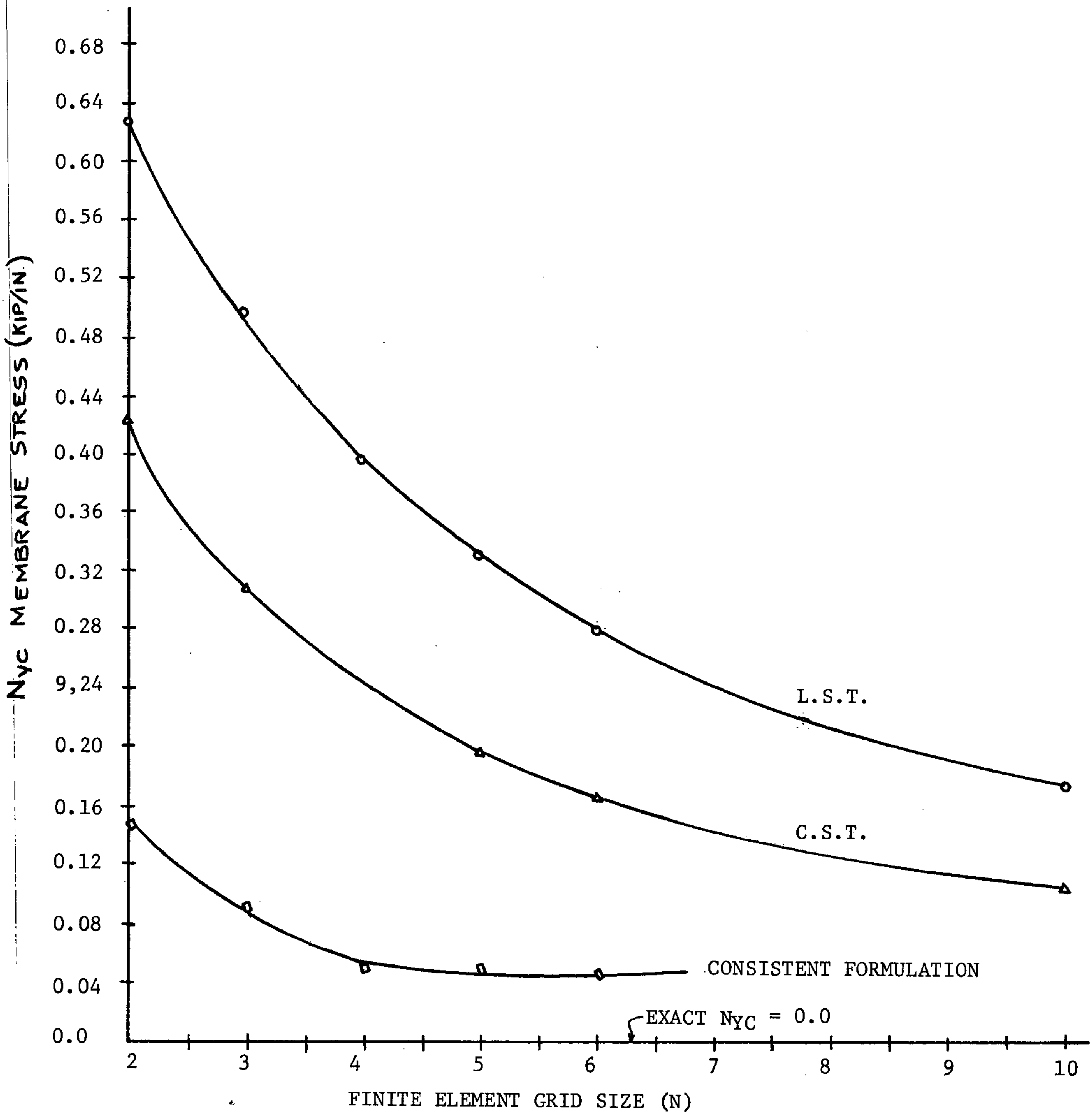

N_{YC} VS FINITE ELEMENT GRID SIZE

FIGURE 6.11

PARABOLICALLY LOADED SQUARE PLATE

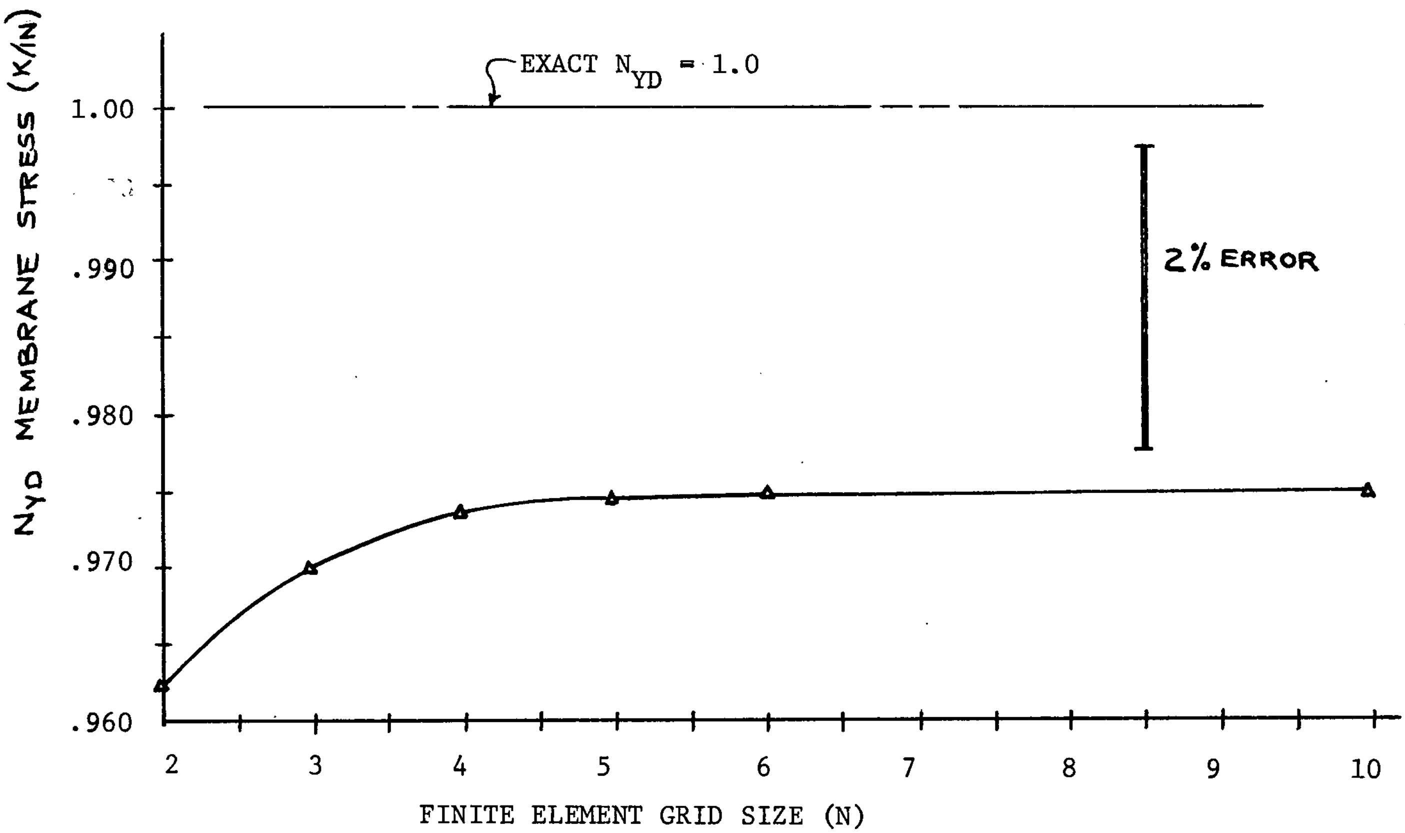

N_{YD} VS FINITE ELEMENT GRID SIZE

FIGURE 6.12

6.4 Cylindrical Shell Roof

A cylindrical shell roof is modelled using the flat triangular element derived in Chapter 3. The shell shown in figure 6.13, because of its configuration is between what is normally termed a shallow shell and what is defined as a deep shell. For this reason, the exact analytical results obtained by shallow shell theory and those obtained from deep shell theory are both presented. The shell is loaded by its own weight, and the loads are lumped at the nodes as vertical forces. The geometry and a typical gridwork is shown in figure 6.13. Only one quarter of the shell is modelled using symmetry.

The deflections are tabulated in table 6.7 and are compared to exact values from reference 3. All deflections converge very rapidly to values only slightly in error of the exact, even for relatively coarse grids. The reason for this convergence to a value slightly in error of the exact is because the element is incomplete and shear strain constraints are imposed at the nodes. Figure 6.14 illustrates graphically the variation of deflection w along edge B - C for various grid refinements. Note the rapid convergence of w_B to a value slightly off the analytical one, even for coarse gridworks. Figure 6.15 plots w_B vs the total number of degrees of freedom. Convergence again is rapid, to a value only 1% in error of the exact for a 10 x 10 grid. Results from a fifteen degree of freedom triangular element which combines the constant strain triangle (six degrees of freedom) for the membrane action and the Zienkiewicz nine parameter plate bending element (Ref. 10) is also presented. Note the larger error for the fifteen d.o.f. element, even when more d.o.f. are used. For very course gridworks, the fifteen d.o.f. element is far too stiff compared to the eighteen d.o.f. element used herein.

The stress at a node is the average of the surrounding element stress contributions. The C.S.T. stresses were the same as the L.S.T. stresses. These values were used instead of the consistent formulation stresses (section 4.2.1.) because of the improved accuracy and convergence characteristics as was illustrated in section 6.1. Table 6.8 compares the various membrane and bending stresses (section 4.3) and the strain energy with the exact values (3) obtained from shallow shell theory. The stresses and strain energy converged to values only slightly in error of the exact. However the bending stress M_{xc} appears to be fluctuating considerably. The variation of N_x along edge A - B is plotted for the different gridworks in figure 6.16. As shown for successively finer grids, the N_{xB} is rapidly approaching a value slightly in error of the exact. In figure 6.17 the distribution of M_y along edge D - c is shown for the various grid sizes. Again it is seen that even for the extremely coarse grid the error is small.

In general the deflections and stresses compare exceptionally well with the exact values but appear to be converging to values slightly in error of the predicted. The reason as was mentioned earlier is due to the fact that the element is incomplete and shear strain constraints are imposed at the elements' nodes.

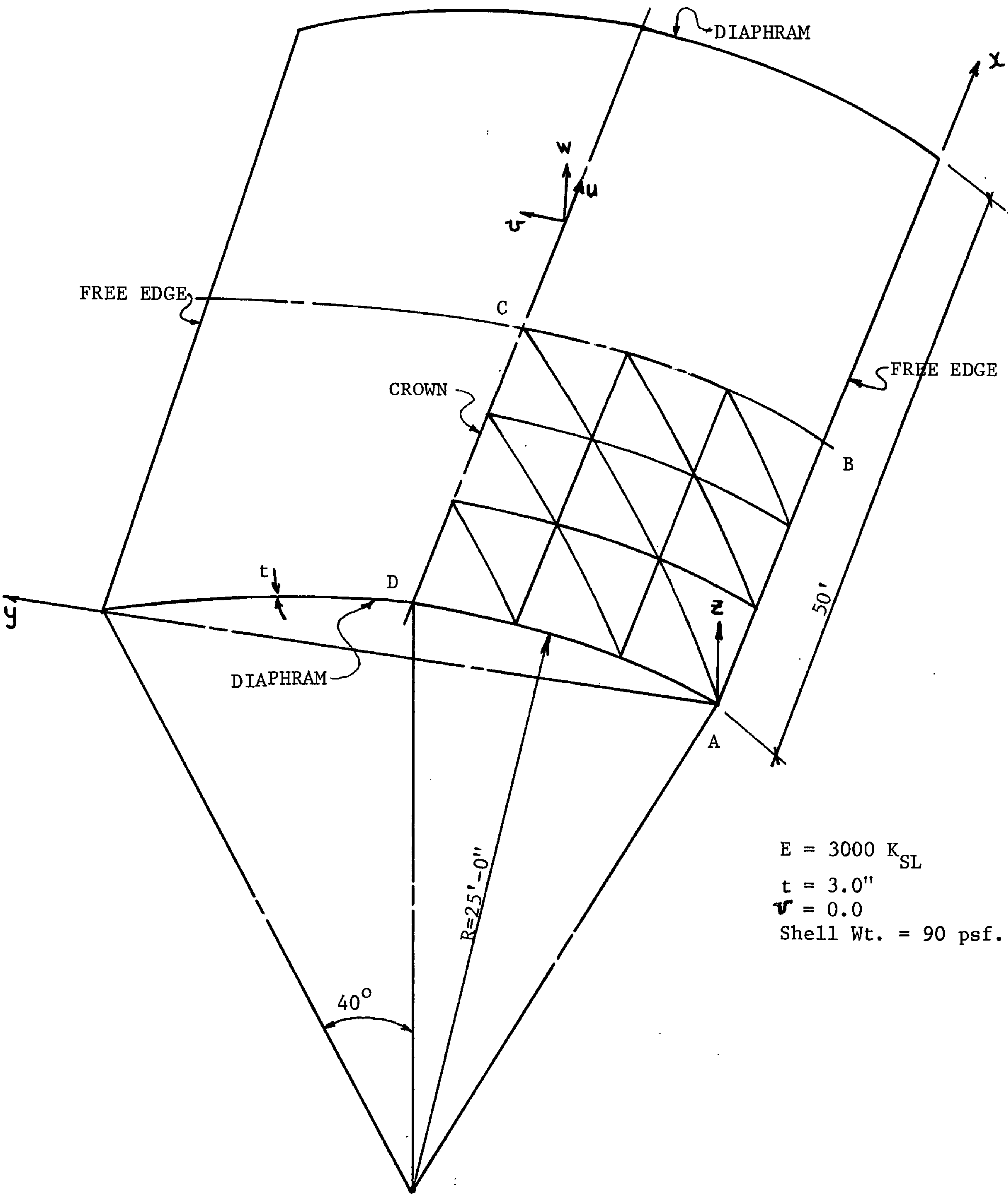

NOTE: MODEL 1/4 OF STRUCTURE DUE TO SYMMETRY CONDITIONS.

Fig. 6.13: CYLINDRICAL SHELL GEOMETRY
(3 X 3 GRID)

TABLE 6.7 : DEFLECTIONS

CYLINDRICAL SHELL

FINITE ELEMENT GRID	NET NO. OF EQUATIONS	$10\,U_A$ (IN)	W_B (IN)	V_B (IN)	$10\,W_C$ (IN)
2 x 2	30	-0.735	-4.571	2.375	6.010
3 x 3	63	-1.049	-3.629	1.912	5.281
4 x 4	108	-1.201	-3.530	1.861	5.234
5 x 5	165	-1.285	-3.527	1.860	5.275
10 x 10	630	-1.417	-3.564	1.881	5.414
EXACT *		?	-3.607	?	?
EXACT **		-1.5133	-3.7033	1.9637	5.2494

NOTE : * FROM DEEP SHELL THEORY

** FROM SHALLOW SHELL THEORY

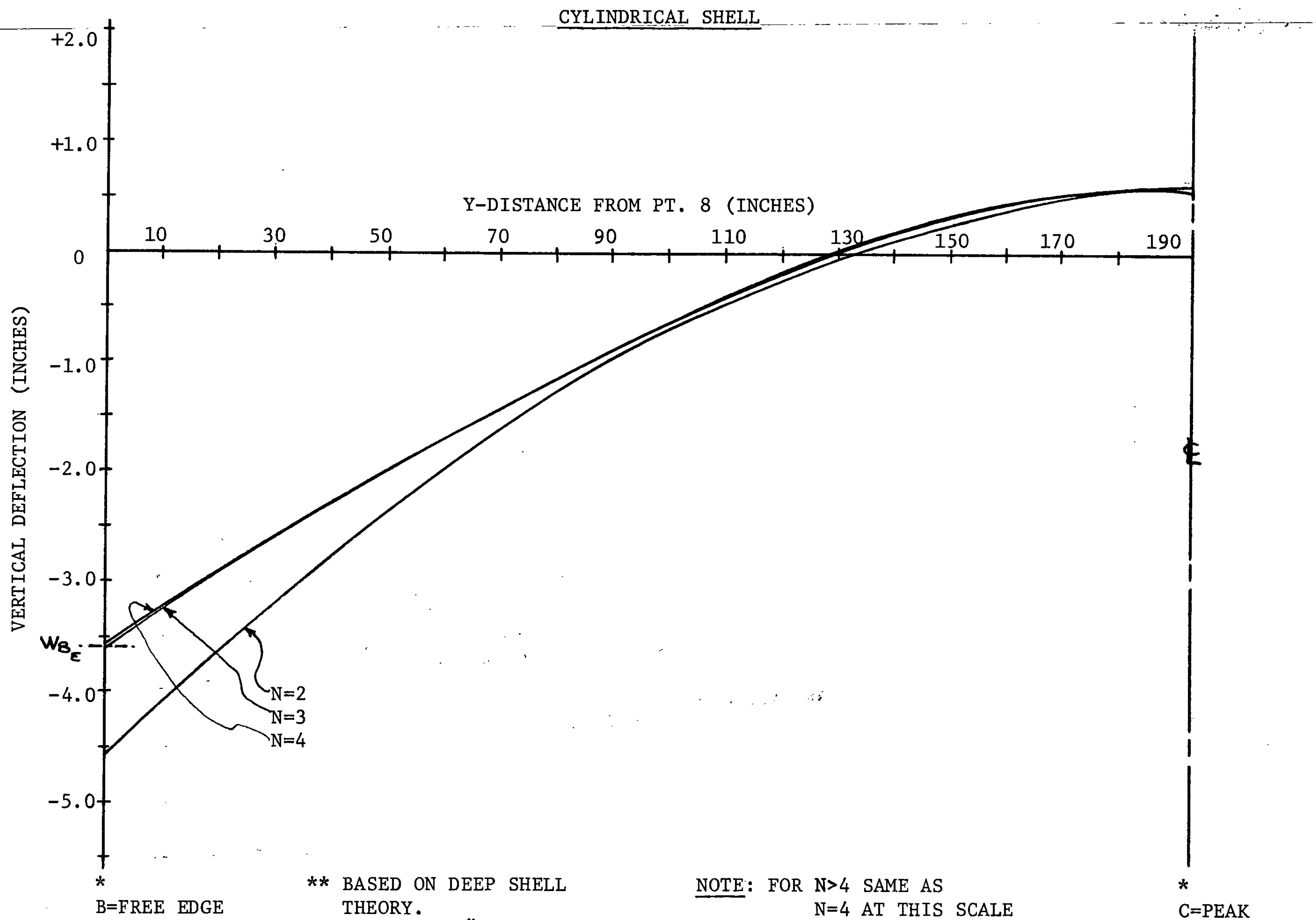

** BASED ON DEEP SHELL THEORY.
$W_{B_E} = 3.607''$ Ref. 2

NOTE: FOR N>4 SAME AS N=4 AT THIS SCALE

W - DEFLECTION ALONG EDGE B-C

FIGURE 6.14

CYLINDRICAL SHELL ROOF

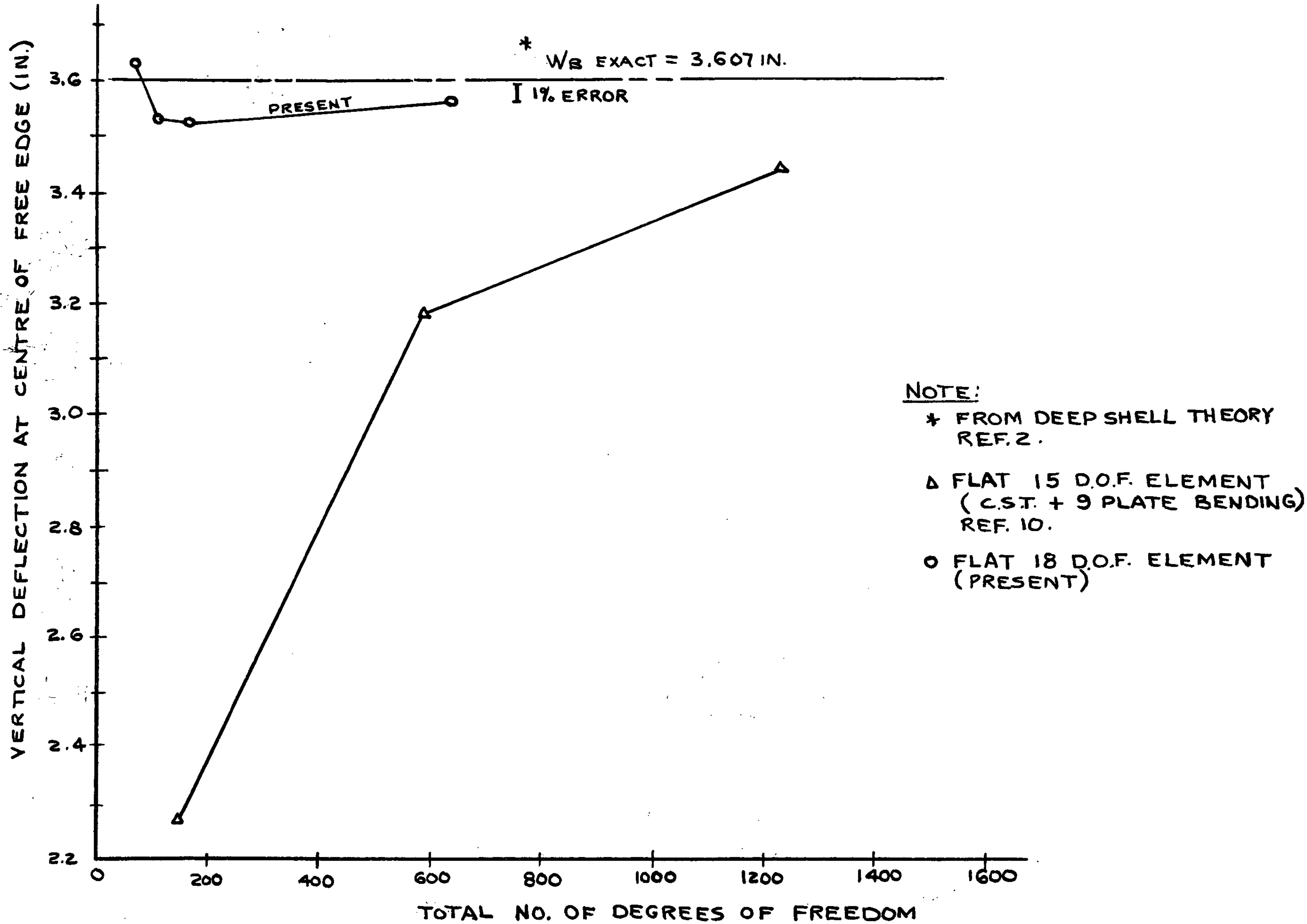

W_B VS TOTAL NO. OF DEGREES OF FREEDOM

FIGURE 6.15

Cylindrical Shell Roof

TABLE 6.8 : STRESSES

(C.S.T.)

GRID SIZE	N_{XB} (K/IN)	M_{XC} (K-IN/IN)	M_{YC} (K-IN/IN)	STRAIN ENERGY (K-IN) #
2 x 2	3.065	-0.099	-2.010	70.93
3 x 3	4.536	-0.075	- 1.822	56.62
4 x 4	5.223	0.005	- 1.788	55.56
5 x 5	5.591	0.085	- 1.744	55.79
10 x 10	6.113	0.254	-1.650	56.78
EXACT *	?	?	?	?
EXACT **	6.4124	0.0927	-2.056	58.828

NOTE : # STRAIN ENERGY FOR TOTAL STRUCTURE
* FROM DEEP SHELL THEORY
** FROM SHALLOW SHELL THEORY

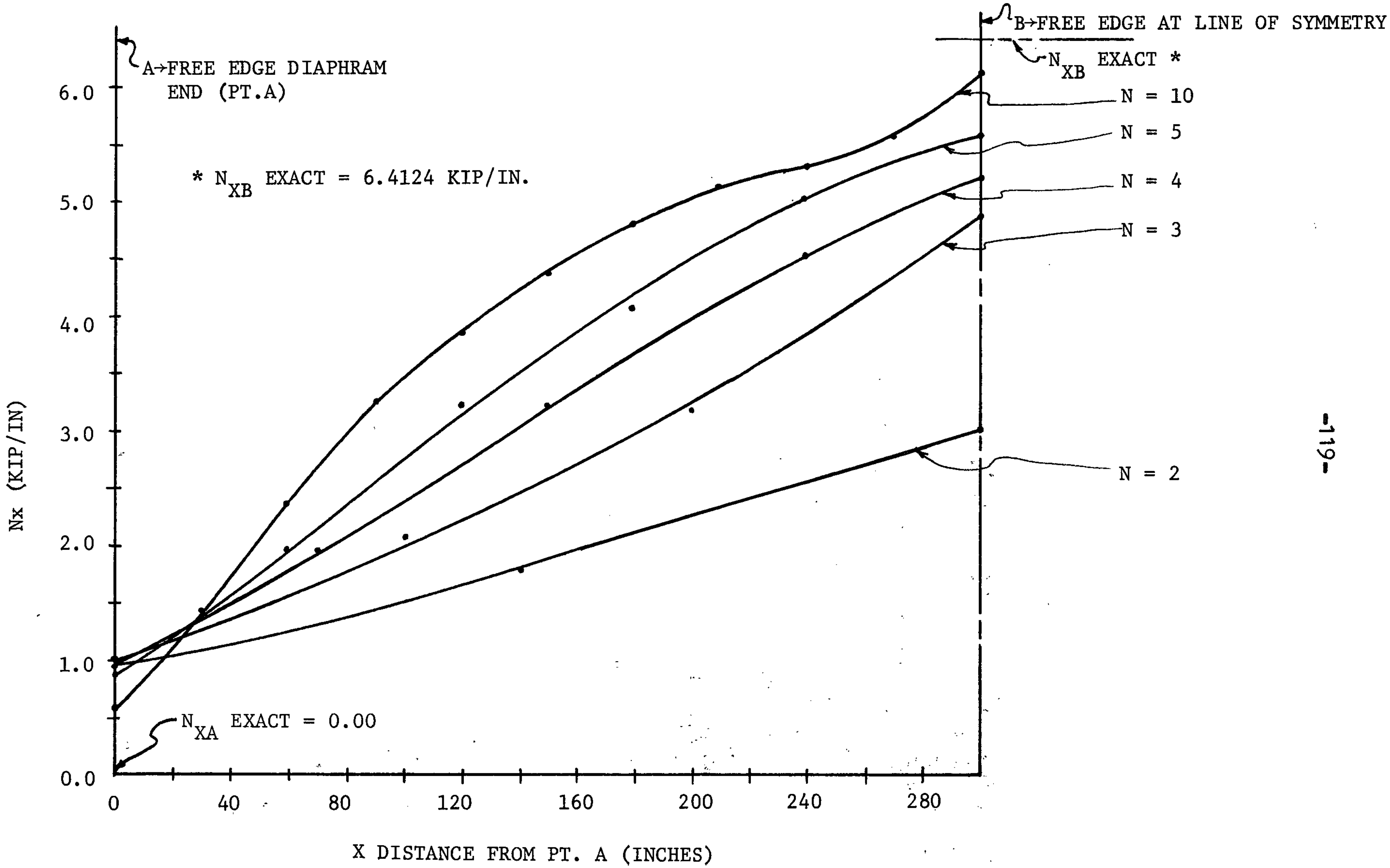

Nx ALONG EDGE A-B

FIGURE 6.16

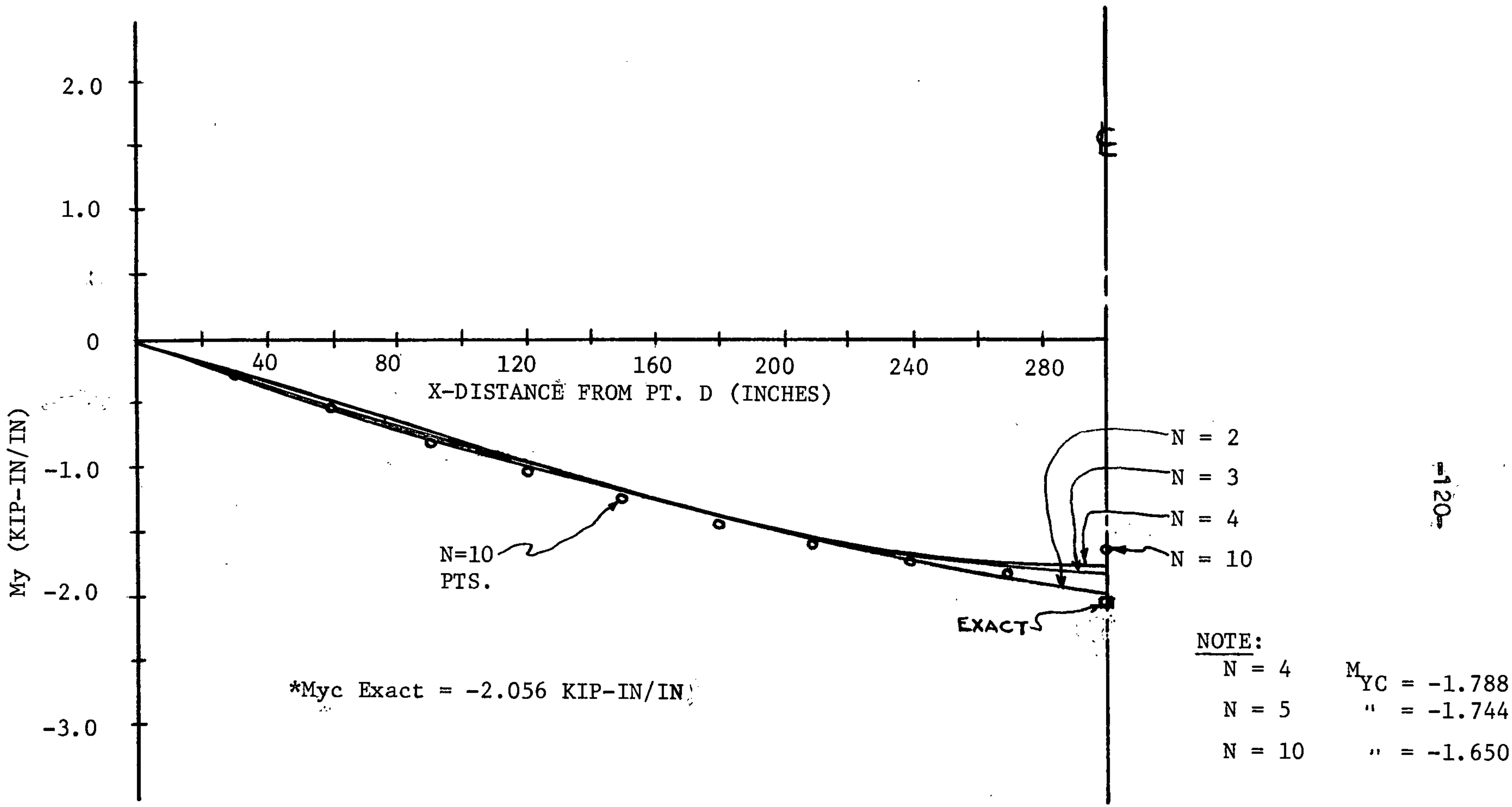

D = DIAPHRAM
END AT LINE OF SYMMETRY.

C=PEAK AT LINES OF SYMMETRY
(I.E. MIDDLE OF ROOF)

My - ALONG EDGE D-C

FIGURE 6.17

6.5 Point Loaded Spherical Shell

A spherical shell is modelled by using the flat eighteen degree of freedom triangular finite element derived in Chapter 3. The spherical shell subjected to a point load creates regions of large bending stresses, a region where there are mainly membrane stresses and a region of high stress concentration. Because the problem is axisymmetric and rectangular co-ordinates are used throughout the analysis, one quarter of half the sphere is modelled. A non-uniform grid spacing is used where the ratios of successive elements are taken as 1 : 2 : 3 : 4, ...N, to provide a better representation of results in the region of high stress gradients near the pole. Figure 6.18 illustrates the general layout and the loading.

The deflections resulting from the point loading at the pole are tabulated in table 6.9. The exact values obtained analytically reference 6 are also given. Convergence is rapid and for a relatively coarse grid, the deflections at the pole and equator compare extremely well. Figure 6.19 illustrates graphically the rapid convergence to a value slightly in error of the exact of the z displacement at the pole with the number of elements used. The normal displacement near the pole vs the colatitude direction along the sphere is shown in figure 6.20 with the exact values. The displacements compare very well with the exact ones.

The stresses based on the C.S.T. and L.S.T. formulation are presented in table 6.11 with the exact ones. The L.S.T. stresses appear to be better where they differ radically from the C.S.T. values. In many instances the C.S.T. and L.S.T. stresses are almost the same. In general the stresses are only slightly in error of the exact values. Table 6.10 compares the stresses N_θ, N_Φ, M_θ and M_Φ at the pole and equator with the exact ones based on shallow shell theory. These stresses are from the L.S.T. formulation and are reasonably close to the exact values for the finer grids. The distribution of the membrane stresses near the pole in the colatitude direction are shown in figure 6.21. Again both N_θ and N_Φ are close to the exact solution (FLÜGGE - reference 6). More remote from the pole at colatitude angles of twenty to ninety degrees, the membrane stresses are compared to the exact ones in figure 6.22. The stresses based on the finite element solution follow very closely the distribution of the stresses based on the analytical results.

In general the displacements away from the pole region compare very closely with the exact solution. Away from the pole the bending stresses die out and the membrane stresses dominate. These membrane stresses remote from the pole follow the analytical values very closely. Again it is seen (figure 6.19) as in the previous examples that the displacements appear to be converging rapidly but to values only slightly in error of the exact. This is due to the fact that the element is incomplete and also because of the nodal shear constraints introduced.

POINT LOADED SPHERE

4x4 ELEMENT GRID:

E = 1.0 p = 1.0
ν = 0.3 t = 0.02
R/t=50

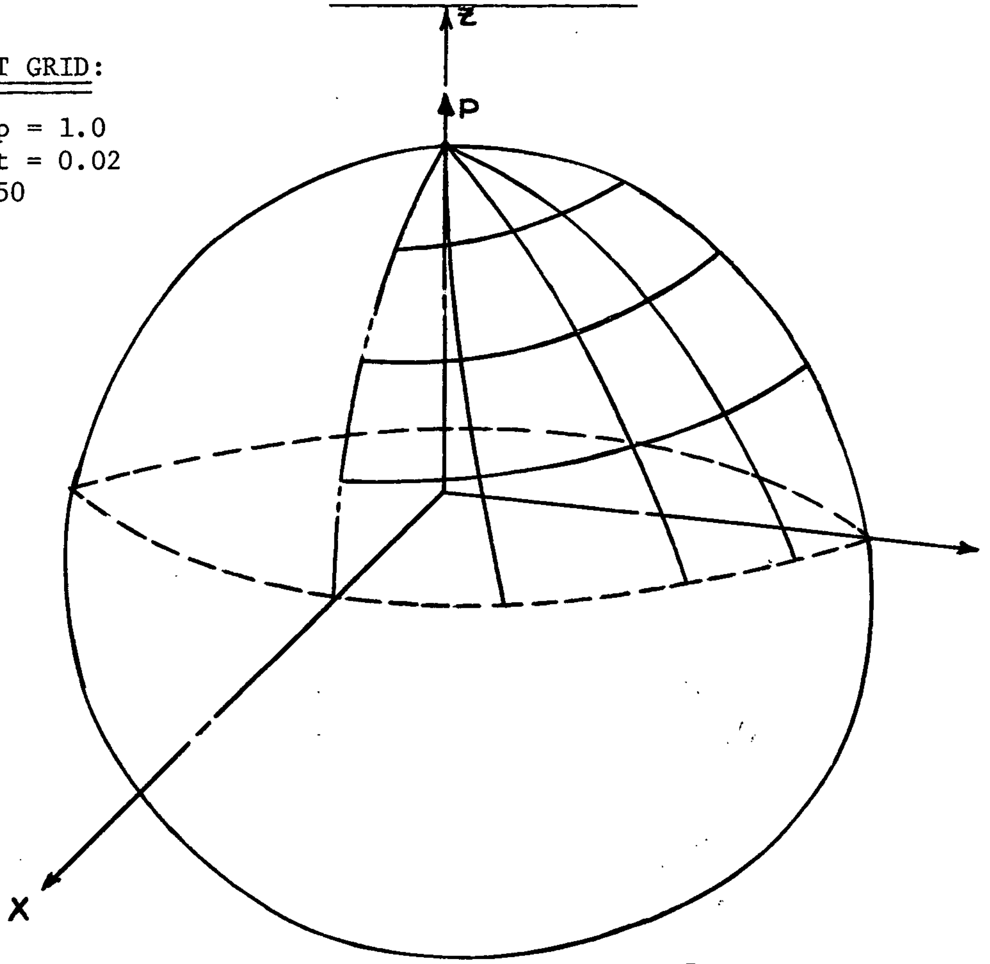

NOTE:

- 1/4 OF SPHERE IS MODELLED USING A NONUNIFORM GRID FOR COLATITUDE DIRECTION.
- RATIO OF SIDES IS 1:2:3...N
  N = No. OF ELEMENTS HIGH.
- N = 4 IS SHOWN.

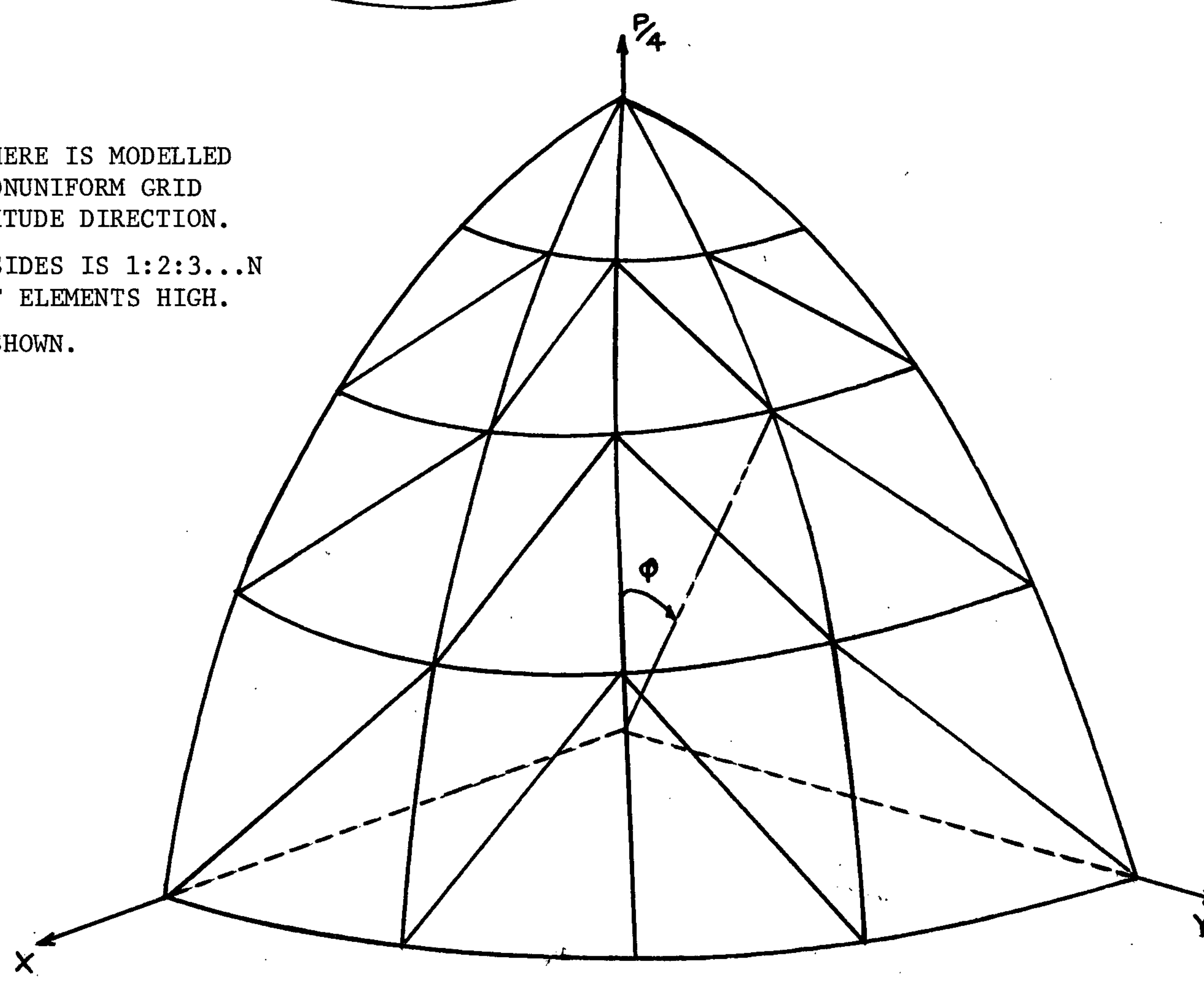

FIG. 6.18: SPHERICAL SHELL

TABLE 6.9: DEFLECTIONS

POINT LOADED SPHERE

FINITE ELEMENT GRID	DEFLECTION @ POLE (IN.) (Et W/P)	DEFLECTION @ EQUATOR (IN.) (Et W/P)
2	6.1054	- 0.2908
4	8.0346	- 0.2235
8	20.1638	- 0.1993
10	21.8660	- 0.19901
12	22.3918	- 0.1984
14	22.4478	- 0.1979
EXACT *	21.200	?
EXACT **	21.093	- 0.2069

NOTE:

* Value for deep shell Theory.

** Value for Shallow Shell Theory.

STRESS UNITS:

$N = K_{ip} / IN.$

$M = K_{ip} - IN/ IN.$

TABLE 6.10: STRESSES (L.S.T.)

FINITE ELEMENT GRID	AT POLE				AT EQUATOR			
	N_θ	N_ϕ	$M_\theta \times 10^{-1}$	$M_\phi \times 10^{-1}$	N_θ	N_ϕ	$M_\theta \times 10^{-3}$	$M_\phi \times 10^{-3}$
2	- 0.9589	2.0684	- 0.0788	- 0.069	0.4996	0.3043	0.5376	0.2162
4.	4.7133	5.099	0.501	0.287	-0.1861	0.1329	- 6.319	- 5.987
8	12.388	12.331	1.307	- 0.601	-0.1334	0.1473	0.0267	0.00310
10	12.660	12.637	2.210	- 0.913	-0.1318	0.1462	0.0279	0.00347
12	12.465	12.455	3.012	- 1.209	-0.1301	0.1458	0.0264	0.00217
14	12.180	12.177	3.685	- 1.470	-0.1287	0.1458	0.0278	0.00134
EXACT**	10.313	10.313	∞	∞	-0.1592	+ 0.1592	≃ 0	≃ 0

POINT LOADED SPHERE

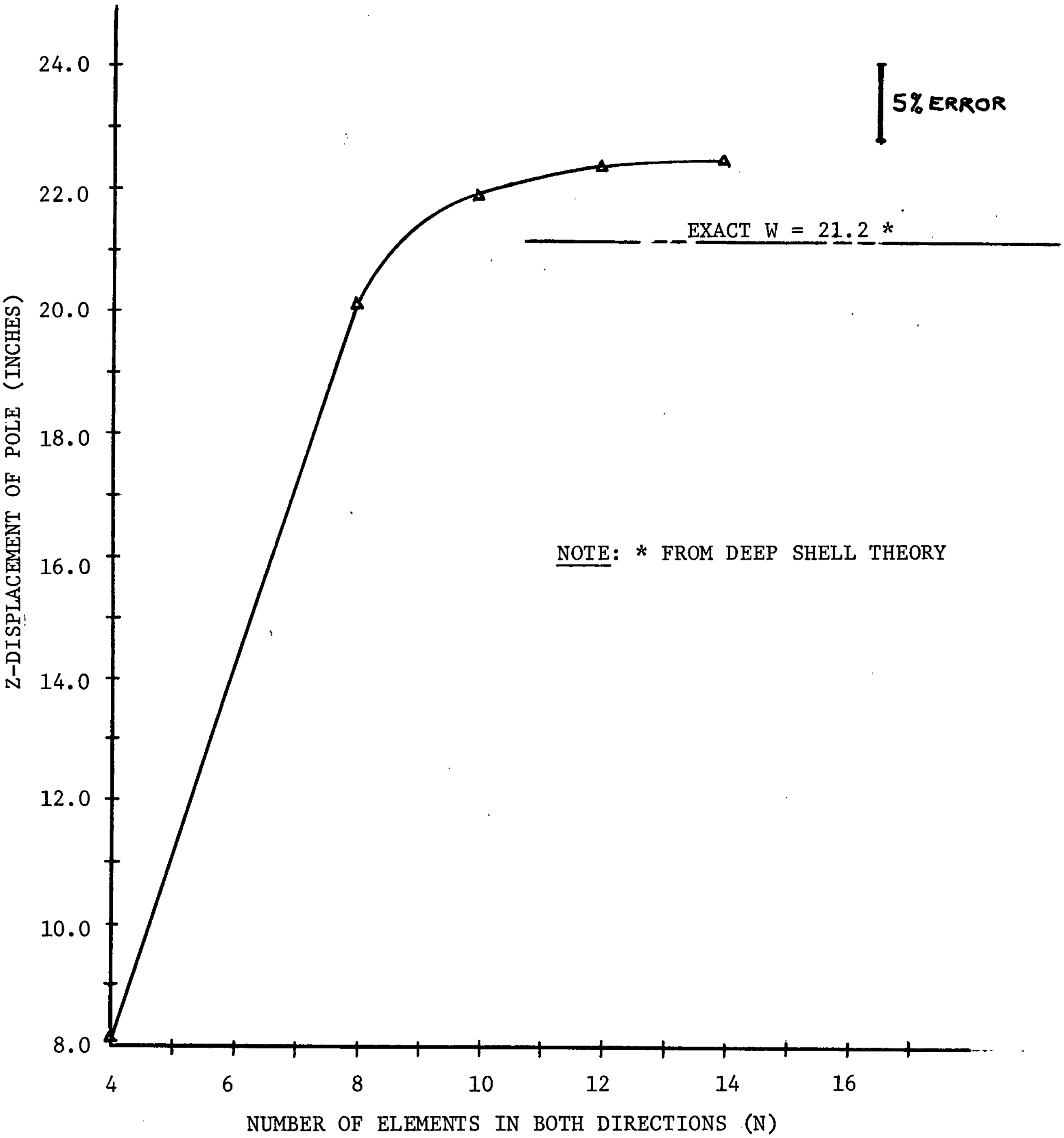

DEFLECTION AT POLE VS FINITE ELEMENT GRID

FIGURE 6.19

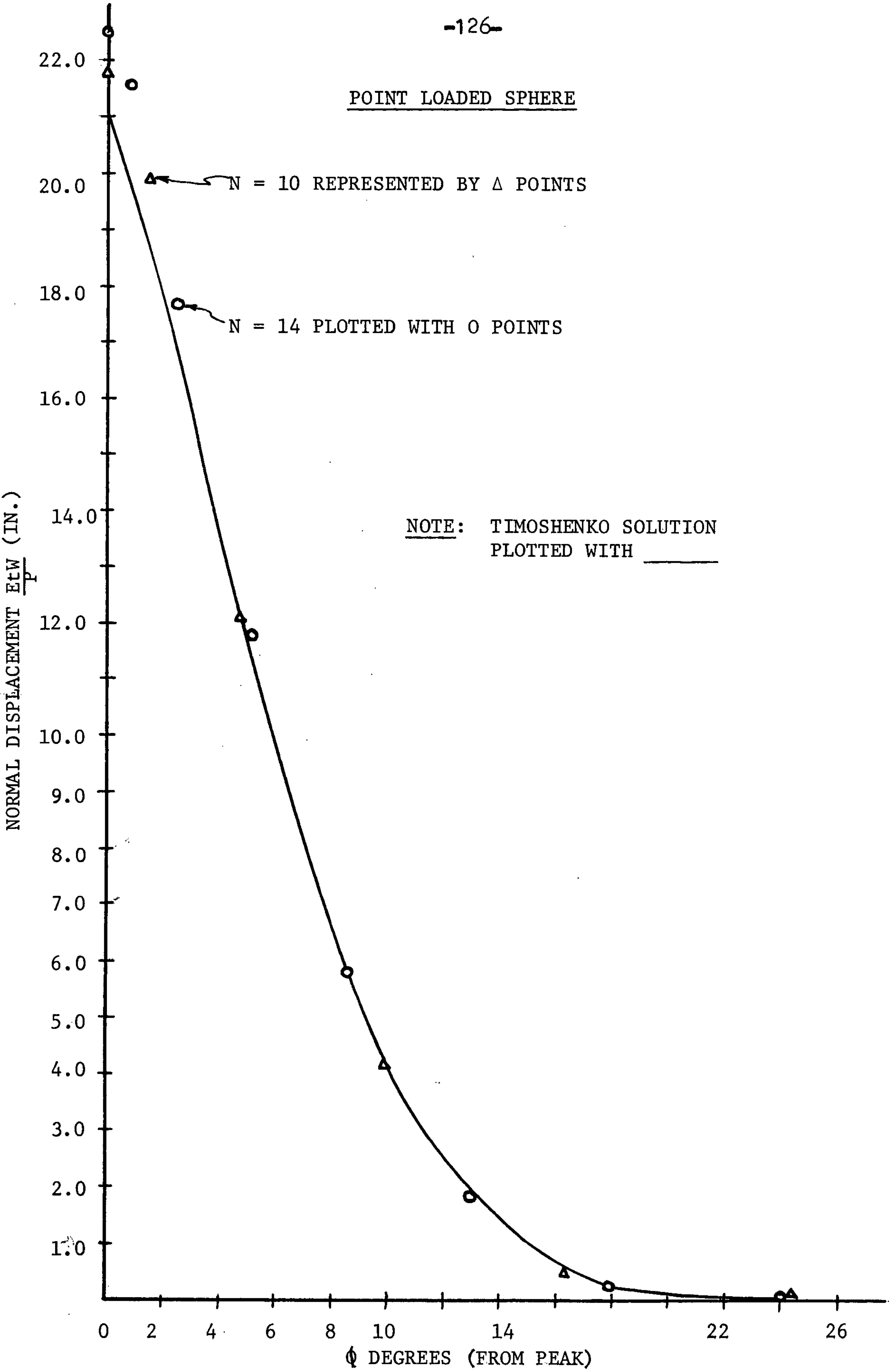

NORMAL DISPLACEMENT VS ANGLE Q NEAR POLE

FIGURE 6.20

TABLE 6.11 STRESSES

POINT LOADED SPHERE

FINITE ELEMENT GRID	STRESSES (K/IN)	C.S.T. FORMULATION	L.S.T. FORMULATION	EXACT
2	$N_{\Theta P}$ N_{QP} $N_{\Theta E}$ N_{QE}	-0.5974 2.1221 -0.6921 0.0746	-0.9589 2.0684 0.4996 0.3043	10.313 10.313 -0.1592 0.1592
4	$N_{\Theta P}$ N_{QP} $N_{\Theta E}$ N_{QE}	3.3125 4.7298 -0.18113 0.15643	4.7133 5.099 -0.1861 0.1329	10.313 10.313 -0.1592 0.1592
8	$N_{\Theta P}$ N_{QP} $N_{\Theta E}$ N_{QE}	10.546 11.7947 -0.1603 0.1498	12.388 12.331 -0.1334 0.1473	10.313 10.313 -0.1592 0.1592
10	$N_{\Theta P}$ N_{QP} $N_{\Theta E}$ N_{QE}	11.5366 12.305 -0.1564 0.14658	12.660 12.637 -0.1318 0.1462	10.313 10.313 -0.1592 0.1592
12	$N_{\Theta P}$ N_{QP} $N_{\Theta E}$ N_{QE}	11.7286 12.2365 0.1542 0.1457	12.465 12.455 0.1301 0.1458	10.313 10.313 -0.1592 0.1592

NOTE: - SUBSCRIPT P $\leftrightarrows$ POLE

- SUBSCRIPT E $\leftrightarrows$ EQUATOR

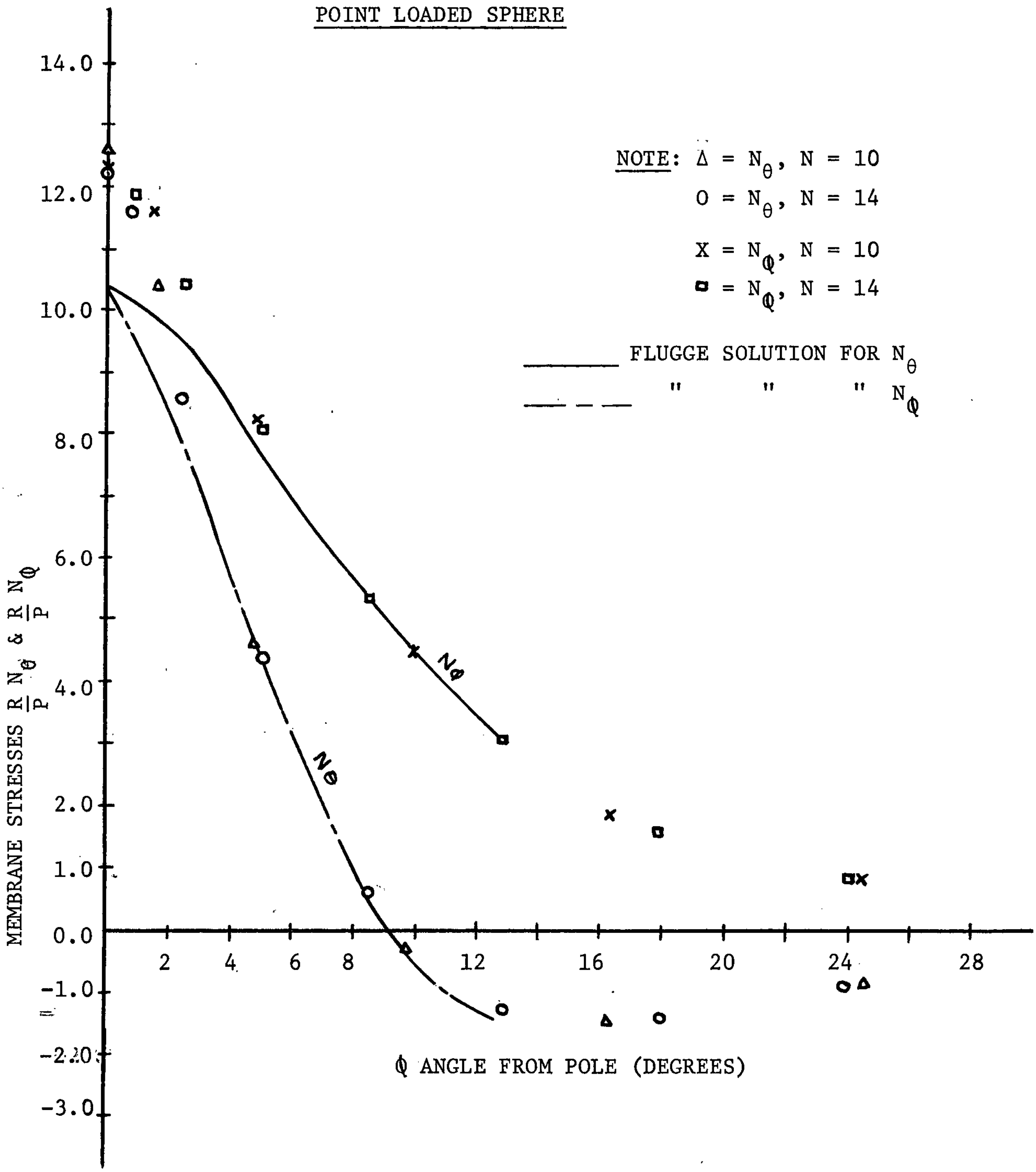

MEMBRANE STRESSES VS ANGLE ϕ NEAR POLE

FIGURE 6.21

POINT LOADED SPHERE

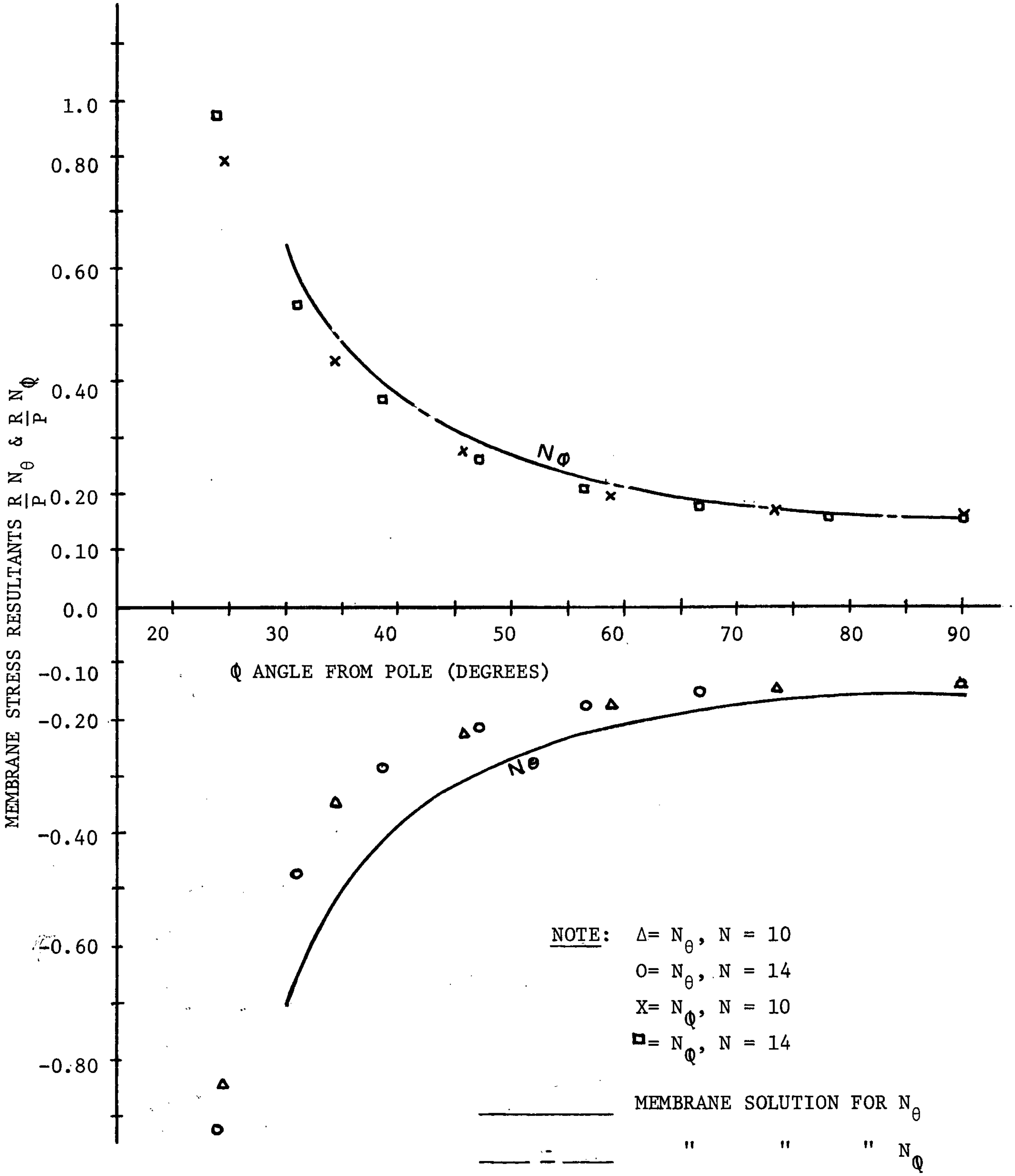

MEMBRANE STRESSES VS ϕ ANGLE REMOTE FROM POLE

FIGURE 6.22

6.6 Non-prismatic Folded Plate Structure

The next application is to a non-prismatic folded plate structure. This structure will deform in an unsymmetrical manner when subjected to loads. The structure's geometry and loading are shown in figure 6.23. A uniform line loading is applied at top fold lines as indicated. The basic plate units which make up the structure are trapezoidal in shape (shown in figure 6.24). The eighteen degree of freedom finite element developed in Chapter 3 is used. The various gridworks employed are shown in figure 6.25. The results are compared with:

(1) Experimental (reference 5) - Tests performed on a scale model.

(2) Analytical (reference 5) - A theory for long non-prismatic folded plates is presented and applied.

(3) High Order Finite Element (Beavers - reference 1) - A finite element representation using a high order finite element is presented. A complete quintic polynomials is used for bending and complete cubics are utilized for the two in-plane displacements. An eighteen degree of freedom in-plane element is combined with an eighteen degree of freedom plate bending element, resulting in a thirty-six degree of freedom triangular element. Sprecial constraint equations are also introduced for the skewed boundaries.

The stresses are computed by averaging the stresses of the surrounding element contributions that are all coplanar to each other. The stresses presented include the membrane stresses which are constant over the thickness of the element and the small bending stresses that are assumed to be constant across the width of the element but are extremely small. The stresses from the L.S.T. formulation (section 4.2.3) are presented for the membrane portion and the bending stresses based on section 4.3 are presented.

Table 6.12 presents the vertical deflection along fold lines c and E for the various finite element grids. The deflections obtained from the element derived in Chapter 3 herein, compare reasonably well with the Beavers (1), experimental (5) and analytical (5) results. This is shown graphically on figure 6.26 the vertical deflection along fold line c is plotted for each of the gridworks used. Notice the steady convergence toward the analytical result for each subsequent grid refinement.

The longitudinal stresses along fold line c and E are tabulated in table 6.13 for each gridwork. Again the values appear to be steadily converging to the experimental and analytical results with each grid refinement. The stresses presented are based on the C.S.T. and L.S.T. stresses (section 4.2.2 and 4.2.3). Figures 6.27 and 6.28 illustrate graphically the variation of longitudinal stresses along fold lines C and E respectively for the different gridworks. In both figures one can see the rapid convergence toward the analytical values.

The transverse moment at midspan is illustrated in figure 6.29 for the gridwork N = 128. The moments are compared with Beaver's high order finite element results. The results are not too far apart and in some instances differ only slightly.

In general the finite element representation of the non-prismatic folded plate structure yielded reasonably good results.

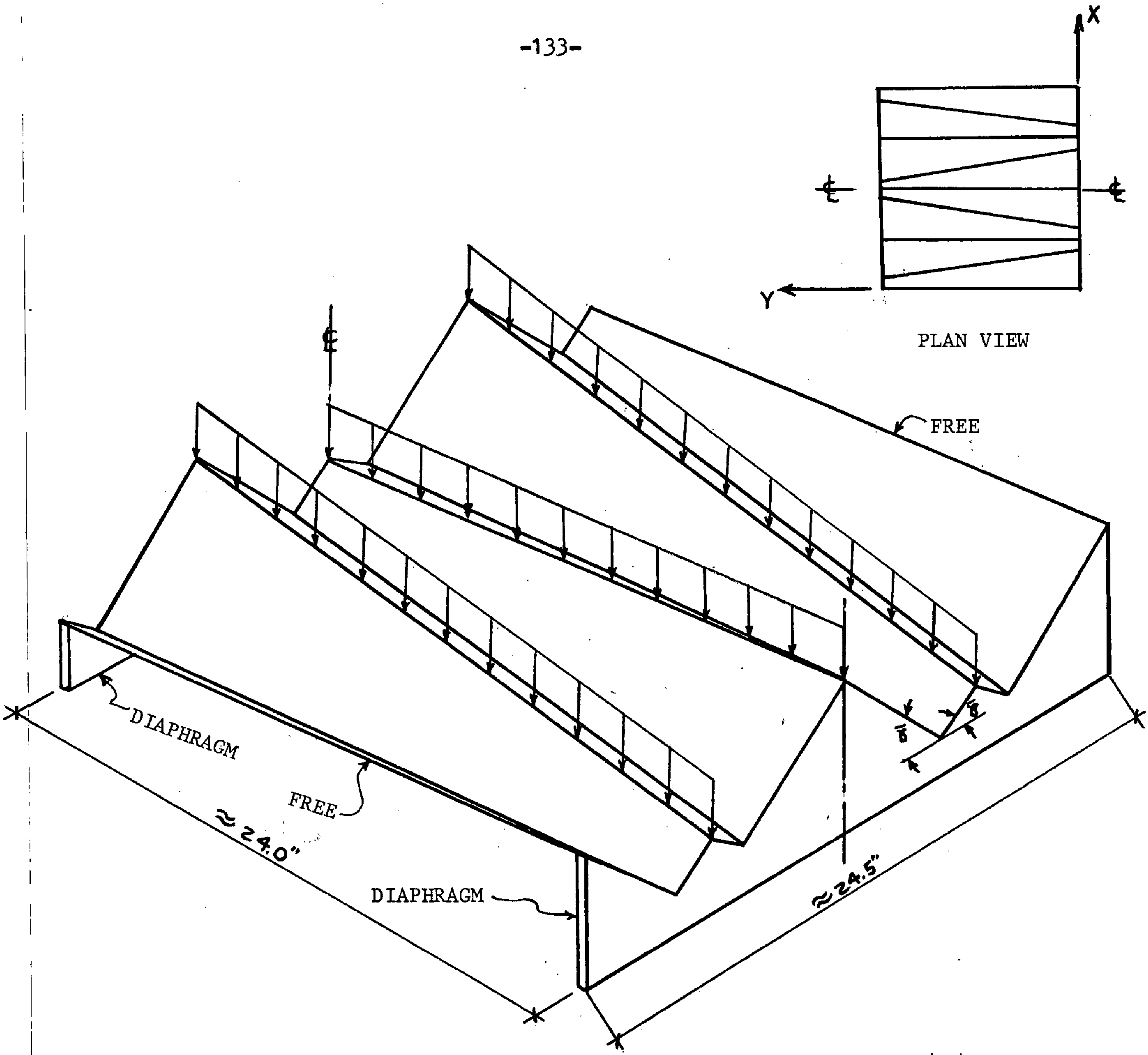

NOTE: ALL ANGLES $\bar{\gamma} = 40^{\circ}$
LOAD = 2.334 #/IN. OF HORIZONTAL PROJECTION
ALUMINUM MATERIAL
E = 10.4 x 10^3 KSL
t = 0.063
ν = 0.33
8 PLATES IN ALL

NONPRISMATIC FOLDED PLATE

FIGURE 6.23

NONPRISMATIC FOLDED PLATE

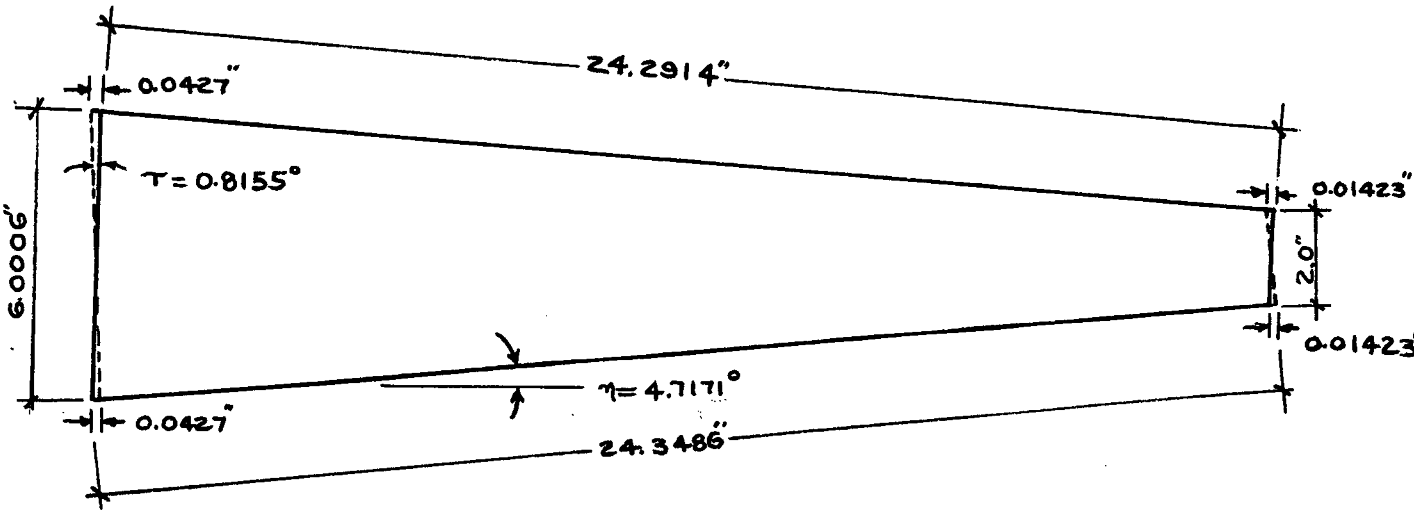

ACTUAL PLATE DIMENSIONS

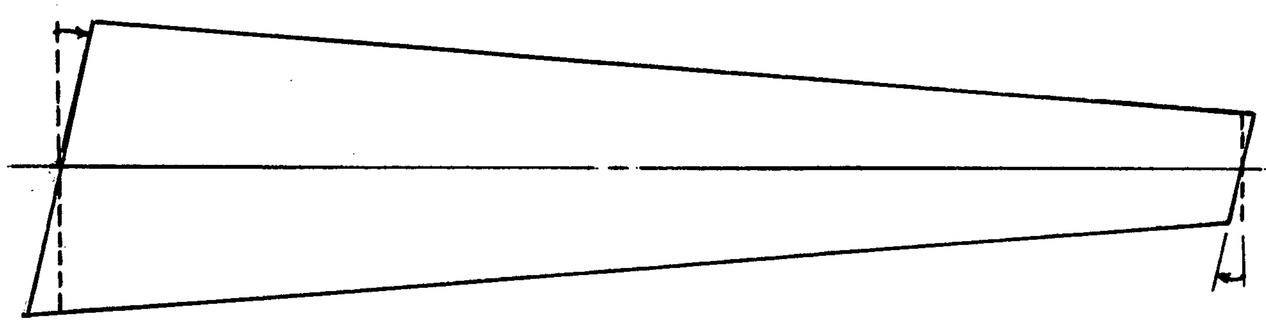

EXAGGERATED PLATE GEOMETRY

PLATE GEOMETRY

FIGURE 6.24

NONPRISMATIC FOLDED PLATE

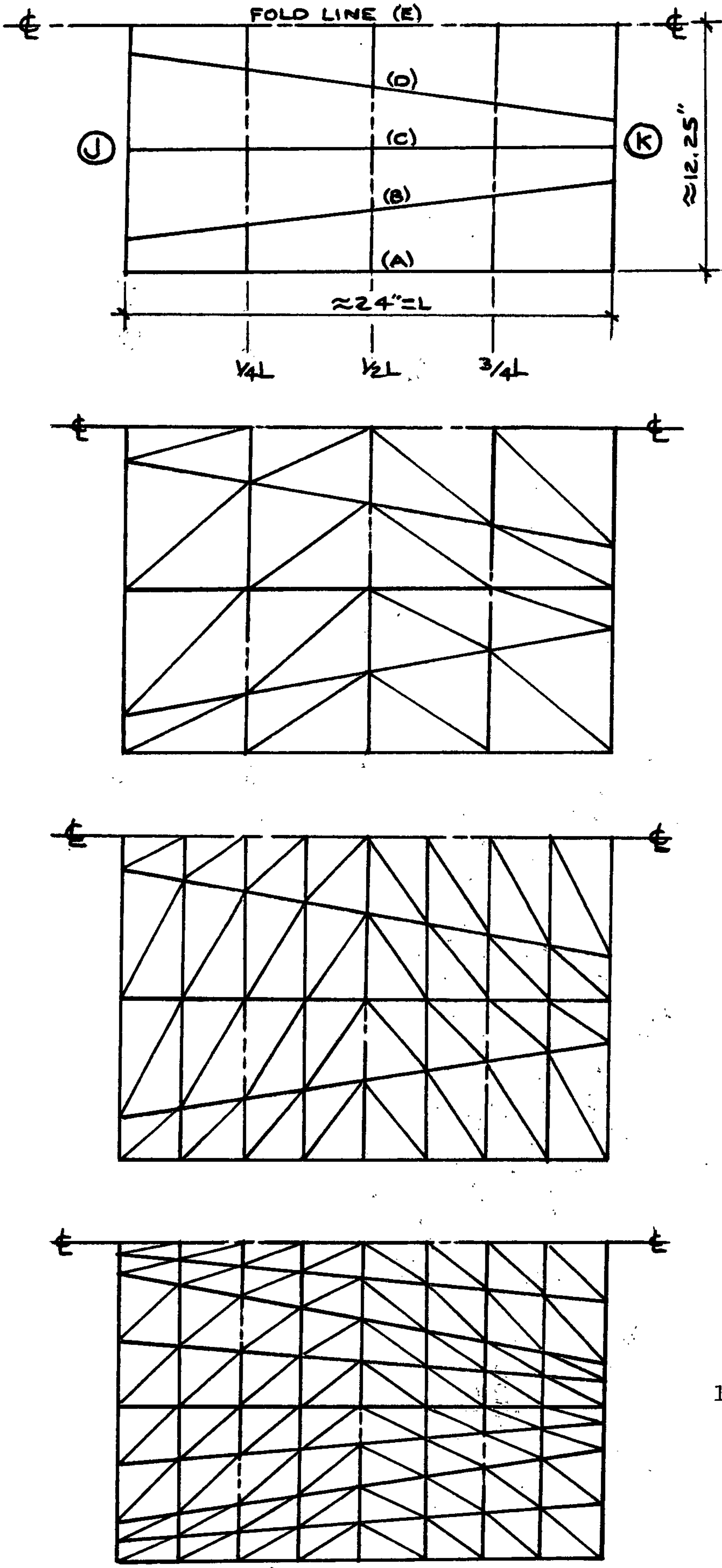

MODEL PLAN VIEW

32 ELEMENT MESH

64 ELEMENT MESH

128 ELEMENT MESH

FIGURE 6.25: MODEL & MESH PATTERNS

TABLE 6.12: DEFLECTIONS

NONPRISMATIC FOLDED PLATE

FINITE ELEMENT GRID	DISTANCE ALONG FOLD LINE OF L	VERTICAL DEFLECTION ALONG FOLD LINE C $X_{10}3$ IN				VERTICAL DEFLECTION* ALONG FOLD LINE E $X_{10}-3$		
		F.E.	BEAVERS	EXPT.	ANALYTIC	F.E.	EXPT.	ANALYTIC
32	1/4 L	1.402	2.2	2.3	2.1	2.027	3.1	3.1
	1/2 L	2.168	3.5	3.1	3.2	2.502	3.9	3.8
	3/4 L	1.800	2.9	2.6	2.7	1.652	2.4	2.5
64	1/4 L	1.532	2.2	2.3	2.1	2.264	3.1	3.1
	1/2 L	2.384	3.5	3.1	3.2	2.755	3.9	3.8
	3/4 L	2.003	2.9	2.6	2.7	1.814	2.4	2.5
128	1/4 L	1.816	2.2	2.3	2.1	2.693	3.1	3.1
	1/2 L	2.832	3.5	3.1	3.2	3.304	3.9	3.8
	3/4 L	2.365	2.9	2.6	2.7	2.165	2.4	2.5

NOTE:
F.E. = RESULTS FROM FINITE ELEMENT DERIVED IN CHAPTER 3

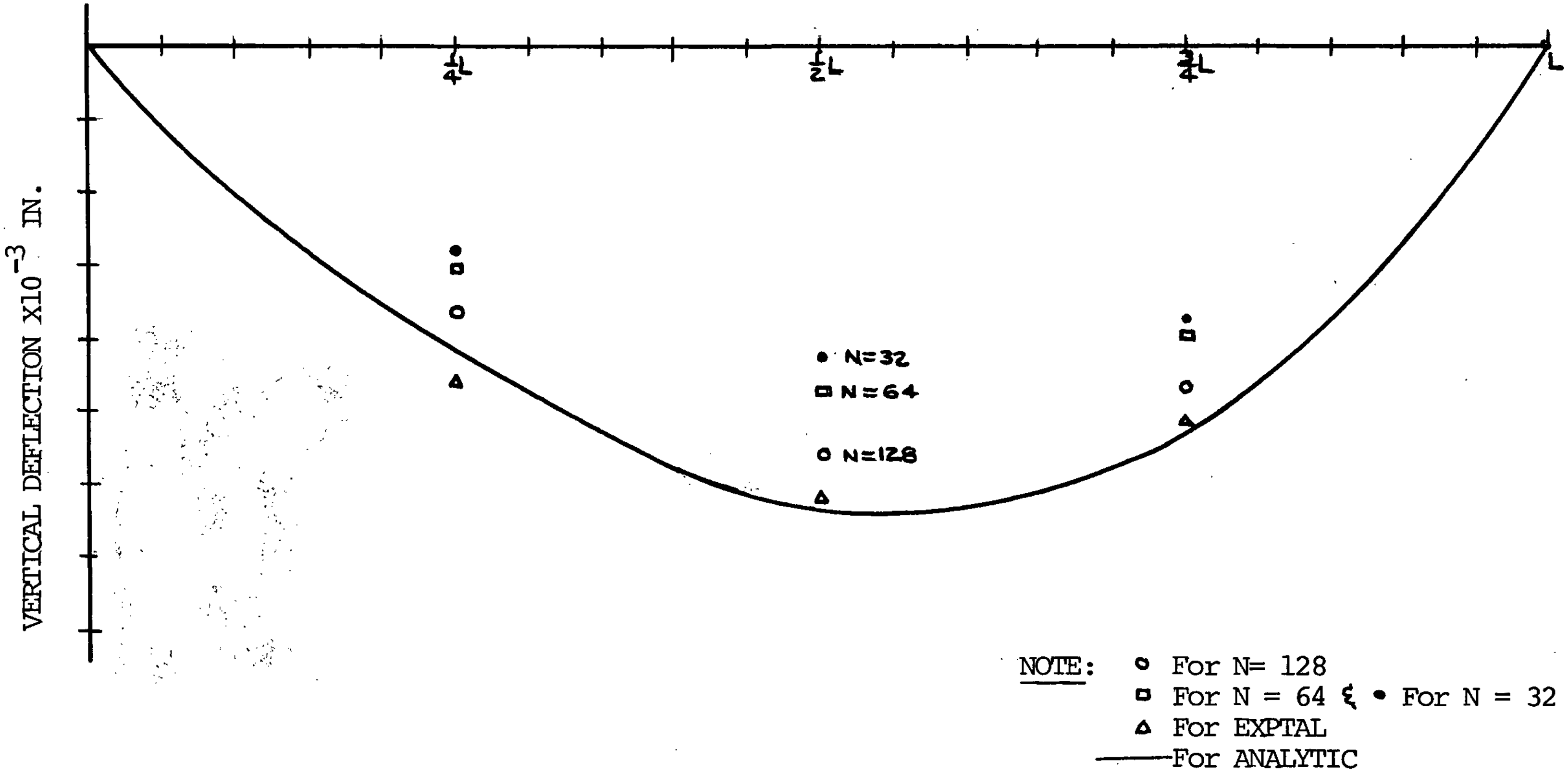

FIGURE 6.26: VERTICAL DEFLECTION ALONG FOLD LINE C

TABLE 6.13 LONGITUDINAL STRESSES (PSI)

NONPRISMATIC FOLDED PLATE

FINITE ELEMENT GRID	DISTANCE ALONG FOLD LINE C				DISTANCE ALONG FOLD LINE E (C.L.)			
	1/4 L	1/2 L	3/4 L	L	1/4 L	1/2 L	3/4 L	L
32	-94.14 * -178.90	-271.69 -386.66	-190.95 -324.32	-237.79 -350.47	-196.44 -334.67	-245.49 -396.11	-87.00 -201.09	-85.60 -162.48
64	-94.95 -203.70	-303.97 -438.39	-259.71 -415.70	-187.64 -270.51	-264.30 -427.83	-271.63 -455.02	-84.73 -240.86	-41.48 -135.80
128	-226.47 -279.25	-466.69 -533.34	-465.92 -546.30	-245.90 -294.44	-488.65 -574.35	-488.20 -575.68	-260.57 -331.90	-77.55 -99.71
EXPTAL. ANALYTIC	-356. -344.	-586 -573	-666. -635.		-710. -676.	-702 -655	-418 -428	

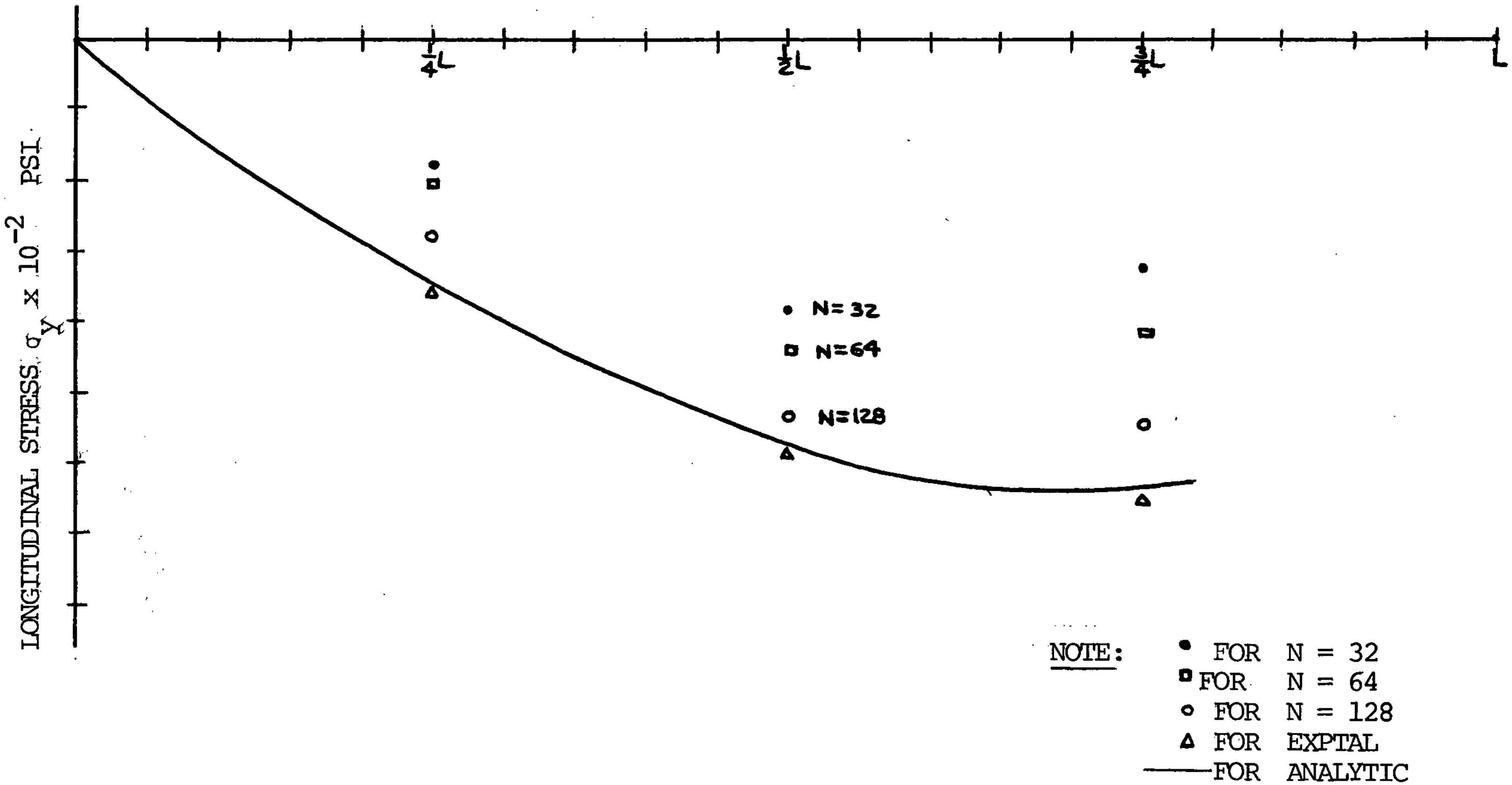

FIGURE 6.27: LONGITUDINAL STRESS ALONG FOLD LINE C

(L.S.T. STRESSES)

NON-PRISMATIC FOLDED PLATE

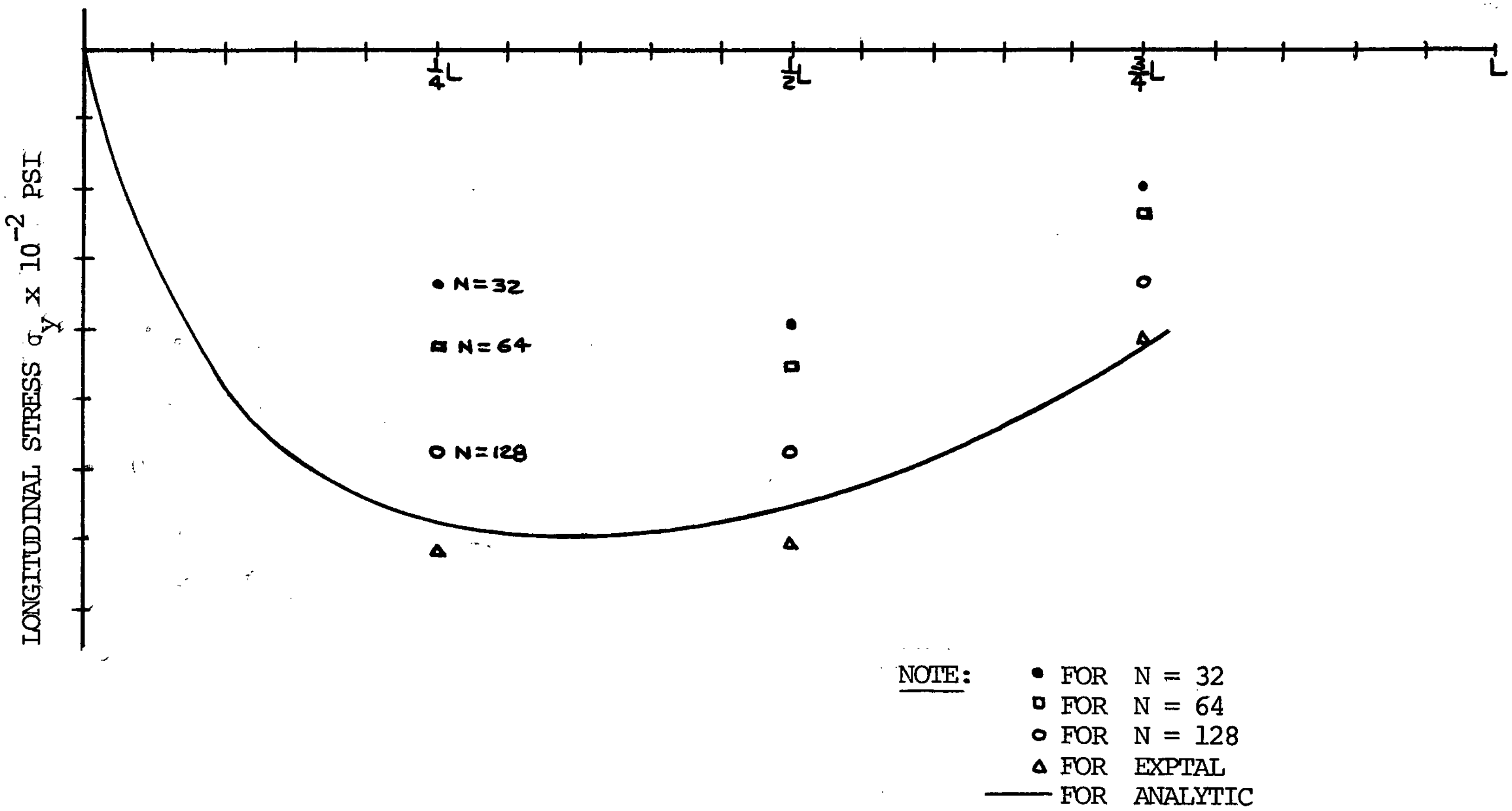

FIGURE 6.28: LONGITUDINAL STRESS ALONG FOLD LINE E CL.

(L.S.T. STRESSES)

NONPRISMATIC FOLDED PLATE

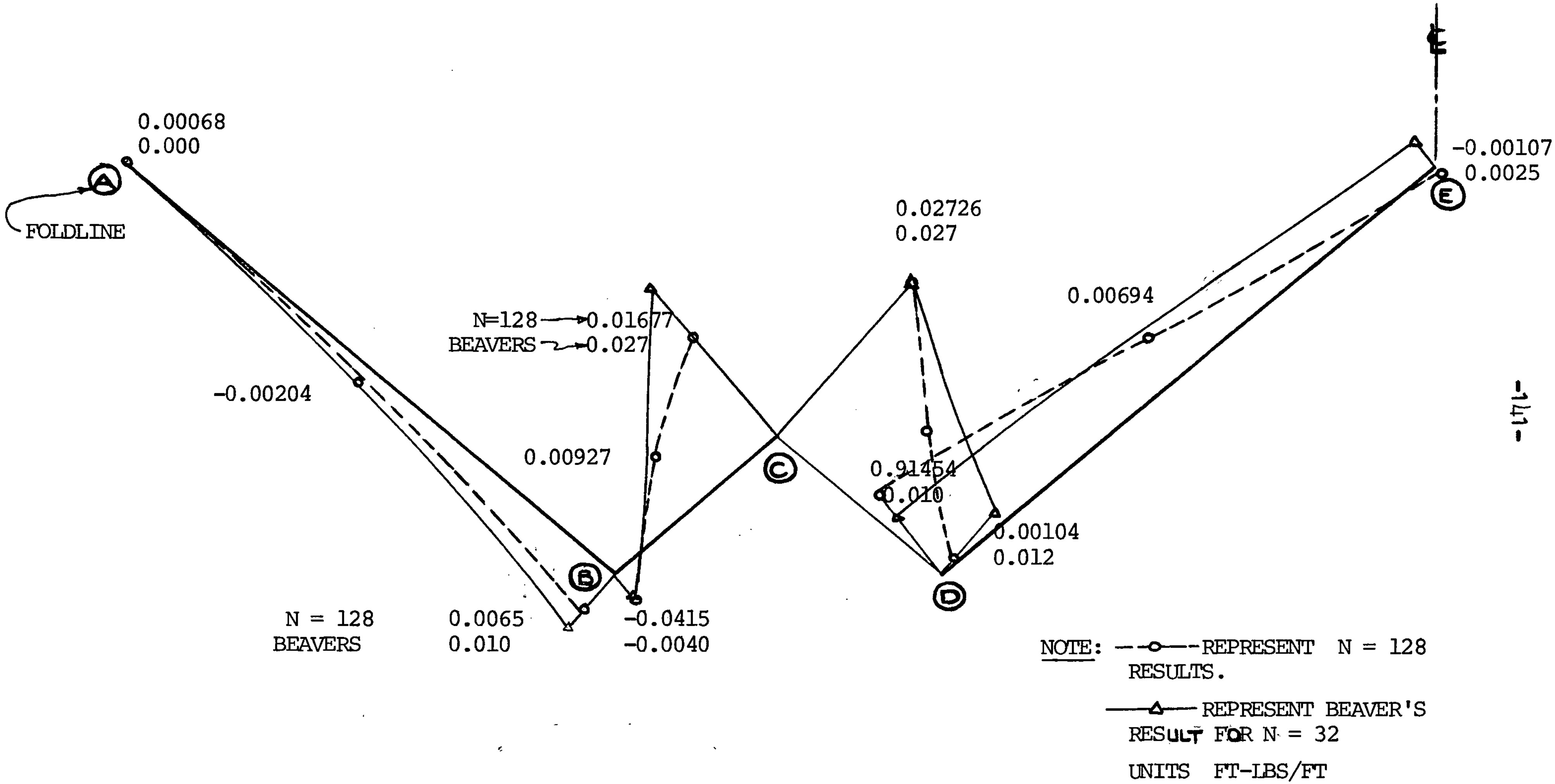

FIGURE 6.29: TRANSVERSE MOMENT AT MIDSPAN

For N = 128

6.7 Beam Stiffener Application:

The twelve degree of freedom beam stiffener element developed in section 5.1 is tested using two different load cases. The section in each case is symmetric. The general layout is shown in figure 6.30. The beam elements support a thin flexurally weak plate which is modelled with the finite element developed in Chapter 3.

For load case one, the beam is simply supported and a vertical load is applied at midspan. From flexural theory, the maximum deflection is computed as a check. The beam elements yielded an answer less than two per cent in error.

Load case two is a moment applied at 30 degrees to the major principal plane of the section (refer to figure 6.31) at each end of the simply supported beam. The deflection was again computed from reference 8 as a check. The result using the beam elements was less than one per cent in error.

It appears that the stiffness matrix derived in section 5.1 for the beam element, using the strain energy approach is an accurate representation.

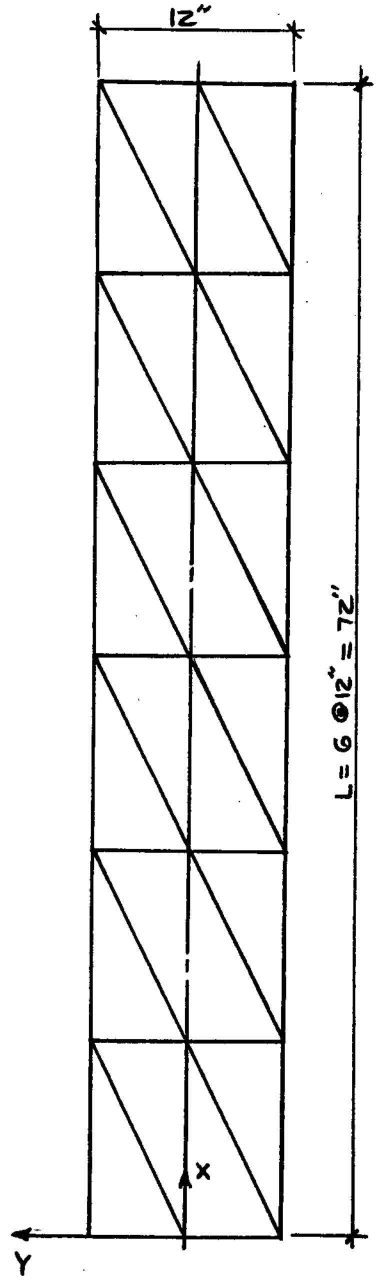

BEAM PROPERTIES:

$A = 2.94$

$I_y = 12.3$

$R_y = 2.05$

$I_x = 1.22$

$R_x = 0.64$

$E_G = 2.5$

$E_s = 0.0$

$I_{yz} = 0.0$

$J = 13.52$

BOUNDARY CONDITIONS

SIMPLY SUPPORTED.

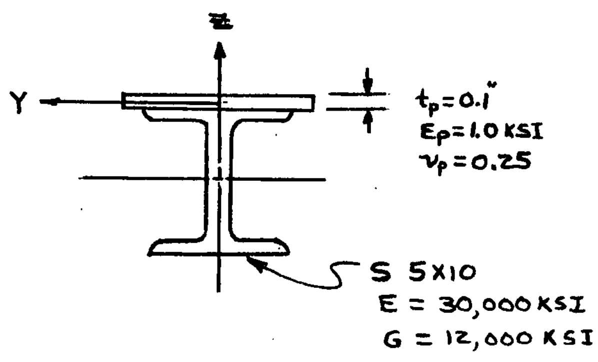

FIGURE 6.30: BEAM STIFFENER PROBLEM

BEAM STIFFENER PROBLEM

LOAD CASE (1):

VERTICAL LOAD APPLIED AT MIDSPAN. $P = -1.0K$

RESULTS:

FROM FLEXURAL THEORY $\Delta C.L._{MAX} = \frac{PL^3}{48EI} = -0.021''$

PROGRAM YIELDED $\Delta C.L._{MAX.} = -0.0206''$

% ERROR IN Δ = 1.9%

LOAD CASE (2):

Please refer to figure 6.31

$M = 50''K$

ONE SUPPORT: S.S.

$M_Y = 43.301''K$

$M_Z = -25.00''K$

OTHER SUPPORT S.S.

$M_Y = -43.301''K$

$M_Z = 25.00''K$

$A=5.34$, $I_Y=56.9$, $I_Z=3.8$

$J = 60.7$, $L = 144''$

$R_Z = 0.844$ $R_Y = 3.264$

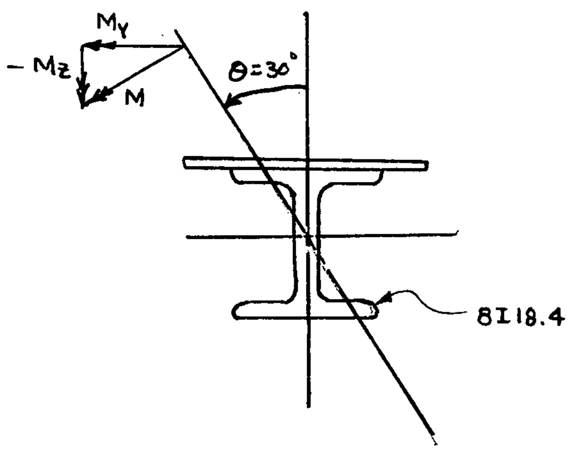

Figure 6.31

RESULTS:

PREDICTED Δ MAX = 0.5722"

FROM TIMOSHENKO STR. OF MAT'LS. PG. 232

$$\Delta\, MAX^2 = \left(\frac{ML^2 \cos\theta}{8EI_Y}\right)^2 + \left(\frac{ML^2 \sin\theta}{8EI_Z}\right)^2$$

PROGRAM RESULTS:

$$\Delta\, MAX = \sqrt{\Delta_X^2 + \Delta_Y^2 + \Delta_Z^2} = 0.5677''$$

% ERROR IN Δ = 0.786%

CONCLUSIONS

Presented herein has been a shallow shell element of arbitrary triangular shape. The element was developed by combining a nine degree of freedom plate bending element with a nine degree of freedom in-plane element. An incomplete cubic polynomial was used to describe the normal out of plane displacement and cubic polynomials were used to describe the two in-plane displacements. Constraints and static condensation were used to reduce the number of generalized co-ordinates for the in-plane displacements.

The eighteen degree of freedom triangular finite element was developed with the intent of modelling plate and shell structures. It is assumed that the behavior of a continuously curved surface can be adequately represented by the behavior of a surface built up of small flat elements. The stresses are computed three different ways. The consistent formulation (strain-displacement matrix, etc.) is compared with the constant strain triangle stresses. A technique is developed to compute the midside node displacements from the vertex nodes and the element configuration. Then the linear strain triangle stresses are computed and compared to the other two stress results.

To assess the new nine parameter plane stress element, a parabolically loaded square plate was modelled. The plate, due to its in-plane loading, had only membrane stresses. The deflections and strain energy converged rapidly to values only marginally in error of the exact solution. The consistent stresses were very poor but the constant strain triangle and linear strain triangle stresses converged rapidly to values that compared closely with the exact values.

A cylindrical shell roof was represented next. Loaded only by its own weight, the load was lumped at the various nodes as vertical forces. In general the deflections and stresses (C.S.T. and L.S.T.) converged rapidly to values only slightly off the analytical results. Even for relatively coarse grids, the results obtained were reasonable.

We wanted to investigate how the element might perform in regions of large bending stresses, regions of large membrane stresses and finally in regions of high stress concentration. So a point loaded spherical shell was modelled. The results again indicated relatively rapid convergence and reasonable accuracy with the analytical values for both deflections and stresses.

In each case the deflections, stresses and strain energy appeared to converge fairly rapidly toward values slightly in error of the analytically predicted ones. This characteristic is attributed to the fact that shear strain constraints were used at the nodes and the finite element is incomplete.

A non-prismatic folded plate structure was studied next. We were not sure how the element would act for this type of unsymmetrical bending and whether the fold lines might introduce errors. However, the results were quite encouraging. The deflections and stresses were compared to experimental, analytical and a finite element analysis using a high order element.

A twelve degree of freedom beam stiffener element was formulated using the strain energy expression, with the intent of combining it with the finite element. At first the formulation was performed for a symmetric crossection. Then two numerical examples were tested. The deflections were only marginally in error with those predicted from flexural theory even when the beam stiffeners were loaded unsymmetrically. Later the formulation was generalized to include beam stiffeners with unsymmetrical crossections.

APPENDIX A.1

DISCUSSION OF PROGRAM

A computer program using Fortran IV language was developed for the analysis of folded plate and shell structures. The program utilizes the eighteen degree of freedom finite element and the twelve degree of freedom beam stiffener element based on the theory discussed earlier. A general flow chart of the program is given in Appendix A.3.

Given a structure, a geometrical model is constructed from it. The model is divided up into a suitable gridwork of elements. These triangular elements should have relatively low aspect ratios although it is not essential. Next the apexes of these elements are numbered but care should be taken so as to minimize the band width of the master stiffness matrix. With the nodal points numbered, the degrees of freedom are determined next by summing the constraint numbers. For each node it must be determined if some nodal movements are inhibited from motion or not. This vector of nodal movements (constraints) represents the boundary and symmetry conditions of the structure. The appropriate node numbers are then associated with each element. The beam stiffeners are treated the same way. Note that each beam stiffener element only extends over the region of one finite element. This way the band width from the finite elements is not destroyed.

The main features of the program can be considered to be divided into the following procedure:

1) Number nodal degrees of freedom, establish band width, check problem size, and read in Finite Element data.

2) If beam stiffeners are used read in the pertinent data.

3) Compute the bending element stiffness matrix.

4) Compute the in-plane element stiffness matrix.

5) Combine the bending and in-plane stiffness matrices and build the structure (master) stiffness matrix.

6) If beam stiffeners are used compute each beam stiffener's stiffness matrix and add to the structure stiffness matrix.

7) Build the master load vector.

8) Solve for the unknown degrees of freedom (nodal displacements).

9) Compute the membrane stresses and bending stresses for each element then find the resultant values at each node by averaging all surrounding element contributions.

Of course co-ordinate transformations and other steps have been omitted but these represent the core to the whole procedure.

The program is set up to handle 2,000,000 bytes. One million of these are set aside for the master stiffness matrix. This means that the

Master stiffness matrix can handle 125,000 double precision words (or two full words). The other 1,000,000 bytes are used by the remainder of the program. The examples presented herein did not utilize all of this available core area.

Note: All units are expressed in kips and inches.

All real numbers are double precision and all integers are single full words.

APPENDIX A.2

INPUT DATA

A description of input items is discussed, following Table A.2.1.

TABLE A.2.1: FORMAT OF INPUT DATA CARDS

CARD/ ITEM #	IDENTIFIER	DESCRIPTION	FORTRAN FORMAT	CARD COLUMNS
1	NLC	TOTAL NO. OF LOAD CASES	I5	1 - 5
	NSTRT	STRUCTURE IDENTIFICATION NO.	I5	6- 10
	NDOF	CONTROL FOR DUPLICATING DEGREE OF FREEDOM NO. (NO. = NUMBER)	I5	11-15
2	ν	POISSON'S RATIO FOR F.E. (FINITE ELEMENT)	F5.3	1 - 5
	T	THICKNESS OF F.E.	F5.3	6- 10
	E	YOUNGE'S MODULUS OF ELASTICITY FOR F.E.	F15.2	11-25
	NBEAM	TOTAL NO. OF BEAM STIFFENERS USED	I5	26-30
	NOELEM	CONTROL FOR WHETHER PROBLEM IS TO BE SOLVED WITH OR WITHOUT F.E.	I5	31-35
	ITER	NUMBER OF ITERATIONS REQUESTED FOR VARIABLE BANDWIDTH MATRIX DECOMPOSITION ROUTINE	I5	36-40
3	NE	TOTAL NO. OF FINITE ELEMENTS IN PROBLEM	I5	1 - 5
	NNODES	TOTAL NO. OF NODES IN PROBLEM	I5	6-10
	NVAR	NO. OF VARIABLES (DEGREE OF FREEDOM) PER NODE	I5	11-15

TABLE A.2.1 (CONT'D)

CARD/ ITEM #	IDENTIFIER	DESCRIPTION	FORTRAN FORMAT	CARD COLUMNS
	NNODEL	NO. OF NODES PER ELEMENT	I5	16-20
	ICOFW	FIELD WIDTH USED FOR READING IN EACH ELEMENT'S NODE NUMBERS. (EXPLAINED FOLLOWING TABLE)	I5	21-25
	NODAL DATA (FOR EACH NODE)			
4	X, Y, AND Z COORDINATES AND		3F10.0	1 -30
	NODAL CONSTRAINTS (IX VECTOR) : IF NDOF = 0		6I2	31-42
		OR IF NDOF = 1	6I4	31-54
		OR IF NDOF = 2	6I5	31-60
	FINITE ELEMENT DATA (FOR EACH ELEMENT)			
5	ICO (I, J), J NODE NO.'S FOR THE I'TH ELEMENT :			
		IF ICOFW = 2	3I2	1 - 6
		OR IF ICOFW = 3	3I3	1 - 9
	BEAM STIFFENER DATA (FOR EACH STIFFENER)			
6	JNL	(LOWER NODE NO.)	I5	1 - 5
	JNG	(GREATER NODE NO.)	I5	6- 11
	JNP	(ORIENTATION NODE USED TO DEFINE ORIENTATION OF STIFFENER'S WEAK PLANE)	I5	11-15
7	X (JNP)	GLOBAL COORDINATES OF JNP	F10.1	1- 10
	Y (JNP)	NOT DEFINED IF JNP IS NOT	F10.1	11-20
	Z (JNP)	SPECIFIED - EXPLAINED FOLLOWING THIS TABLE.	F10.1	21-30

TABLE A.2.1 (CONT'D)

CARD/ ITEM #	IDENTIFIER	DESCRIPTION	FORTRAN FORMAT	CARD COLUMNS
	FOR EACH BEAM STIFFENER**			
8	RG	RY RADIUS OF GYRATION (GREATER)	F7.3	1 - 7
	RS	RZ RADIUS OF GYRATION (SMALLER)	F7.3	8- 14
	A	TOTAL XSECT. AREA OF STIFFENER	F7.3	15-21
	ECG	EY ECCENTRICITY (GREATER)	F7.3	22-28
	ECS	EZ ECCENTRICITY (SMALLER)	F7.3	29-35
	PJ	POLAR MOMENT OF INERTIA	F7.3	36-42
	E	YOUNGE'S MODULUS OF ELASTICITY FOR BEAM STIFFENER MATERIAL	F7.3	43-49
	G	SHEAR MODULUS OF ELASTICITY	F7.3	50-56
	IZ*	MOMENT OF INERTIA W.R.T. Z AXIS	F7.3	57-63
	IYZ	PRODUCT OF MOMENT OF INERTIA W.R.T. Y AND Z AXES.	F7.3	64-70

Note:

* If the beam stiffener is symmetric then the value of IZ can be any value other than zero, but it must be entered. (Stiffener will bend with only R_Y)

** If all beam stiffeners are the same shape, enter a 0.0 for RG on subsequent cards and the values on the previous card are assumed.

** If all beam stiffeners are of the same material, enter a 0.0 for E on subsequent cards and the values on the previous card are assumed.

Refer to Figure A.1.1.

TABLE A.2.1 (CONT'D)

CARD/ ITEM #	IDENTIFIER	DESCRIPTION	FORTRAN FORMAT	CARD COLUMNS
	LOAD INFORMATION			
9	JNODES	TOTAL NO. OF LOADED NODES	I5	1 - 5
	IVERT	CONTROL USED TO INDICATE IF LOADS NEED TO BE TRANSFORMED TO THE GLOBAL SYSTEM.	I5	6- 10
	FOR EACH LOADED NODE (K AND INCHES)			
10	KNODE	LOADED NODE NO.	I5	1 - 5
	FX	LOAD APPLIED IN X-DIRECTION	F10.2	6- 15
	FY	LOAD APPLIED IN Y-DIRECTION	F10.2	16-25
	FZ	LOAD APPLIED IN Z-DIRECTION	F10.2	26-35
	MX	MOMENT APPLIED ABOUT X-AXIS	F10.2	36-45
	MY	MOMENT APPLIED ABOUT Y-AXIS	F10.2	46-55
	MZ	MOMENT APPLIED ABOUT Z-AXIS	F10.2	56-65
11	IEL	IF LOADS ARE TO BE TRANSFORMED TO THE GLOBAL SYSTEM, THIS IS THE ELEMENT WHICH IS NORMAL TO FZ AND PARALLEL TO FX AND FY. (EXPLAINED FOLLOWING THIS TABLE)	I5	1 - 5

Detailed Description:

The first card of the program allows the user to assign the structure an identification number so that he may easily refer to it at some future date.

If more than one load case is to be applied to the structure, then the solution routine saves the decomposed structure stiffness matrix and the subsequent displacements and stresses are computed very quickly without having to decompose the structure stiffness matrix each time. The NDOF is used to facilitate where one wants to assign duplicate degree of freedom numbers to various nodes. Here is how it is used:

- If no duplicate degree of freedom numbering is desired, leave NDOF blank.
- If you wish to use duplicate degree of freedom numbering, then
  - for reading in actual degree of freedom number in fields of 4, enter 1 for NDOF
  - for reading in actual degree of freedom number in fields of 5, enter 2 for NDOF

Example

Want node 13's degree of freedom to be same as node 4's degree of freedom, then enter - 4 - 4 - 4 - 4 - 4 - 4 for constraints of node 13.

Example

Want w of node 16 to be same as u of node 5, then enter 0 1 19 0 1 1 for constraints of node 16, where the actual d.o.f. no. 19 ↔ the actual d.o.f. no. for u displ. of node 5.

The second card defines the material properties of the finite elements. All finite elements are assumed to have the same thickness T. If beam stiffeners are used, then enter the total number (NBEAM). If no beam stiffeners are used, then leave NBEAM blank. Note: Each beam stiffener element extends over the length of one finite element only. It may be desired to run a structure that is composed of beam stiffeners only or you may wish to neglect the strength of the adjoining slab of finite elements. If the user enters a 1 for NOELEM, then only the stiffness of the beam stiffeners is considered and the deflections due to the applied loads are computed. Normally one would wish to include the effect of the plate of finite elements so NOELEM is left blank. ITER is the number of iterations used by the solution routine for decomposing the variable bandwidth master stiffness matrix. For no iterations, this value is left blank.

The third card is used to indicate the total number of nodes and elements in a problem. For the element used, NVAR, the number of degree of freedom per node is six. The number of nodes per element, NNODEL is three. The variable ICOFW is used to indicate the width of the fields for reading the node numbers of each element.

- If the total number of nodes is less than or equal to 99 then set ICOFW = 2 and the nodes are read in fields of 2.
- If the total number of nodes is greater than 99 then set ICOFW =3 and the nodes will be read in fields of 3.

The fourth item regards specifying the global x, y, and z co-ordinates and the six constraint values for each node. The six constraints correspond to u, v, w, θ_x, θ_y, θ_z movements. Either a 1 (free) or a 0 (fixed) is entered for each of the constraints. Note: all 1's do not need to be entered since a blank here represents a 1 (free ie. unconstrained motion).

The fifth item entails denoting the three node numbers which correspond to each element. These values are entered three per card (each element) and are in field widths according to the value of ICOFW.

If beam stiffeners are not used in a particular problem, then items six and seven can be disregarded.

Item six regards inputting the lower node number (JNL), the greater node number (JNG) and a third node number (JNP) of the beam stiffener. The JNP node number's co-ordinates are used to define the orientation of the weak plane of the stiffener. There are three cases which could exist:

(1) The weak axis of the stiffener is in the x - y plane (horizontal) i.e. the stiffener is vertical. Then JNP does not need to be entered. The X (JNP), Y (JNP) and Z (JNP) does not need to be entered either.

(2) The weak plane of the stiffener is not in the horizontal plane but its orientation can be defined by using the co-ordinates of a known node. Then the node number is entered for JNP. On the following card enter only - 0.0 for X (JNP) and leave Y (JNP) and Z (JNP) blank.

(3) The weak plane of the stiffener is not in the horizontal plane and its orientation has to be described by introducing the co-ordinates of a new constrained node. Give JNP a number in the range [NNODES + 200 $\leq$ NNODES + 400] and on the next card, enter the values of X (JNP), Y (JNP), Z (JNP).

Item six is done for each beam stiffener.

Item seven is also done for each beam stiffener. On each card, one per stiffener, the section and material properties are entered (noted in Table A.2.1).

Item eight the total number of loaded nodes (JNODES) is entered. If the loads are acting in the Z - direction (vertical), then there is no need to transform them, so a blank or 0 is entered for IVERT. If they are acting in a different direction, then they should be transformed to the global system before the master load vector is built, so a 1 is entered for IVERT.

Item nine; for each loaded node, its number is entered and then its magnitude (F_x, F_y, F_z, M_x, M_y, M_z). If the load has to be transformed (IVERT = 1), then the next card should indicate the number of the element (IEL) for which F_z is normal and F_x and F_y are acting in the same plane (w.r.t. local axes of the element). If IVERT = 0 then IEL is not entered.

<u>Note:</u> It is impossible to load in a direction which is constrained from motion.

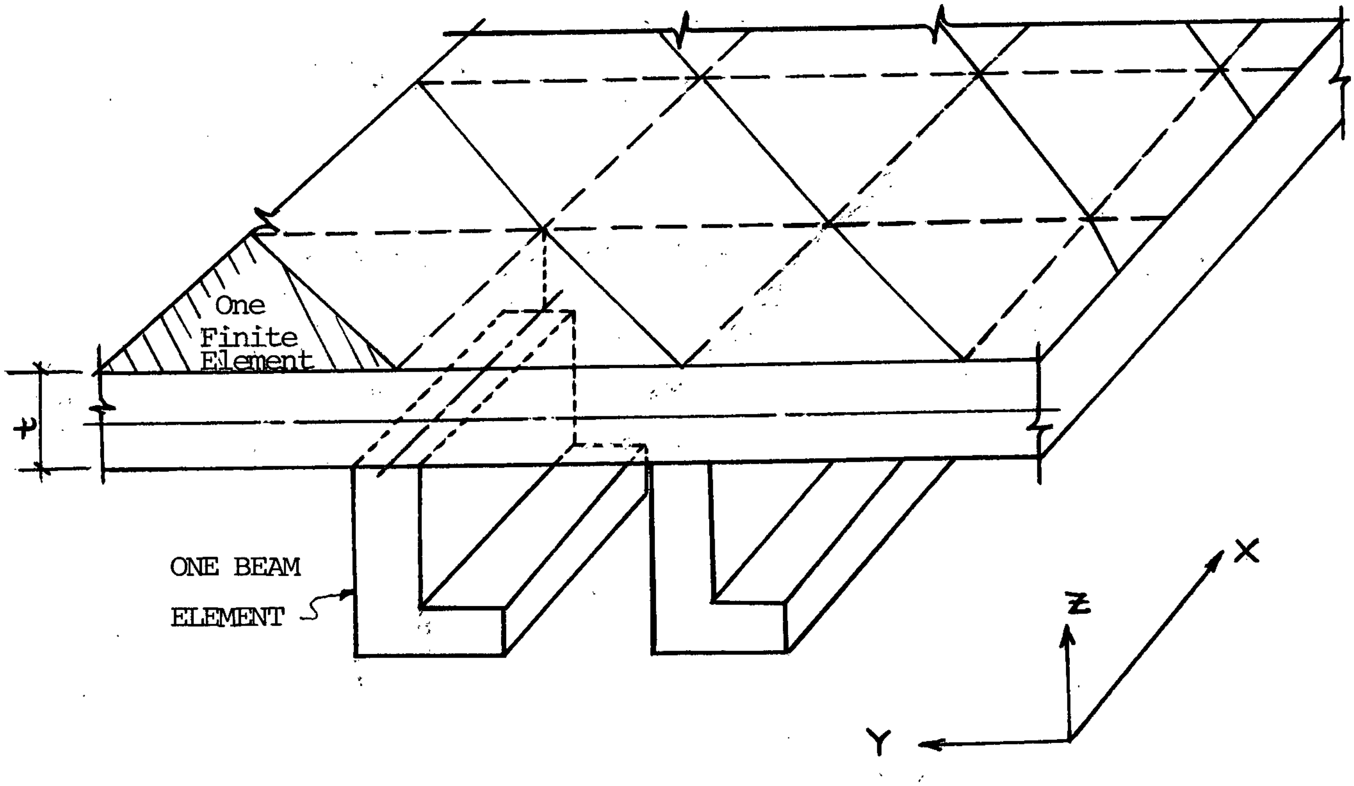

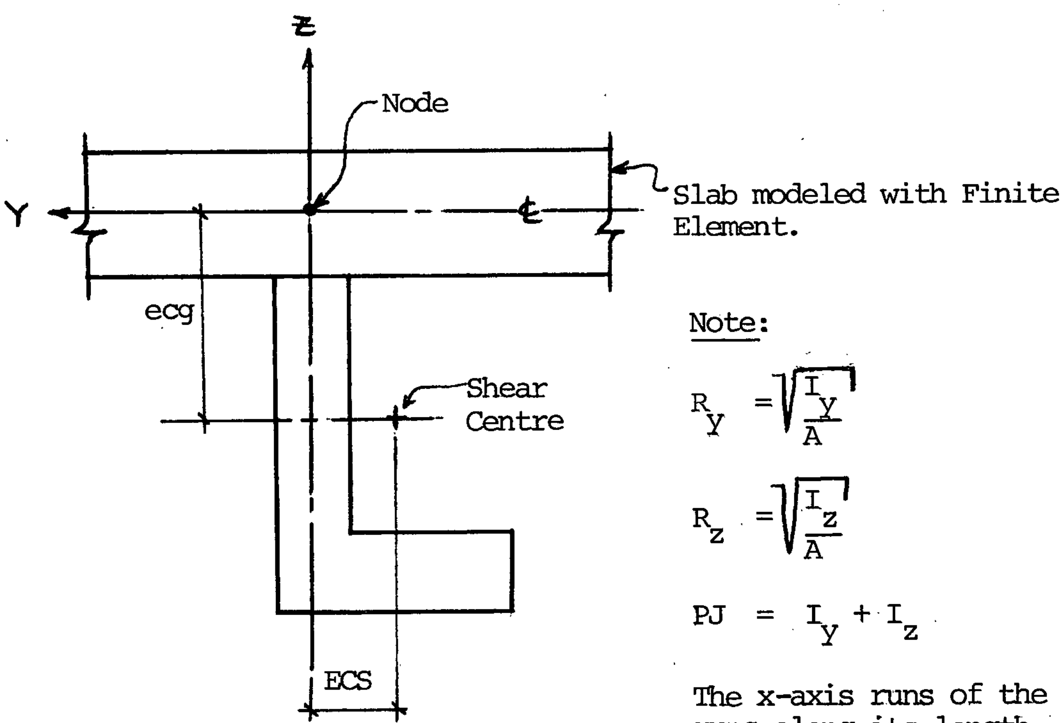

ONE BEAM ELEMENT

<u>Note:</u>

$R_y = \sqrt{\frac{I_y}{A}}$

$R_z = \sqrt{\frac{I_z}{A}}$

$PJ = I_y + I_z$

The x-axis runs of the stiffener runs along its length

FIGURE A.1.1 BEAM STIFFENER SECTION PROPERTIES

APPENDIX A.3

FLOW CHART FOR COMPUTER PROGRAM

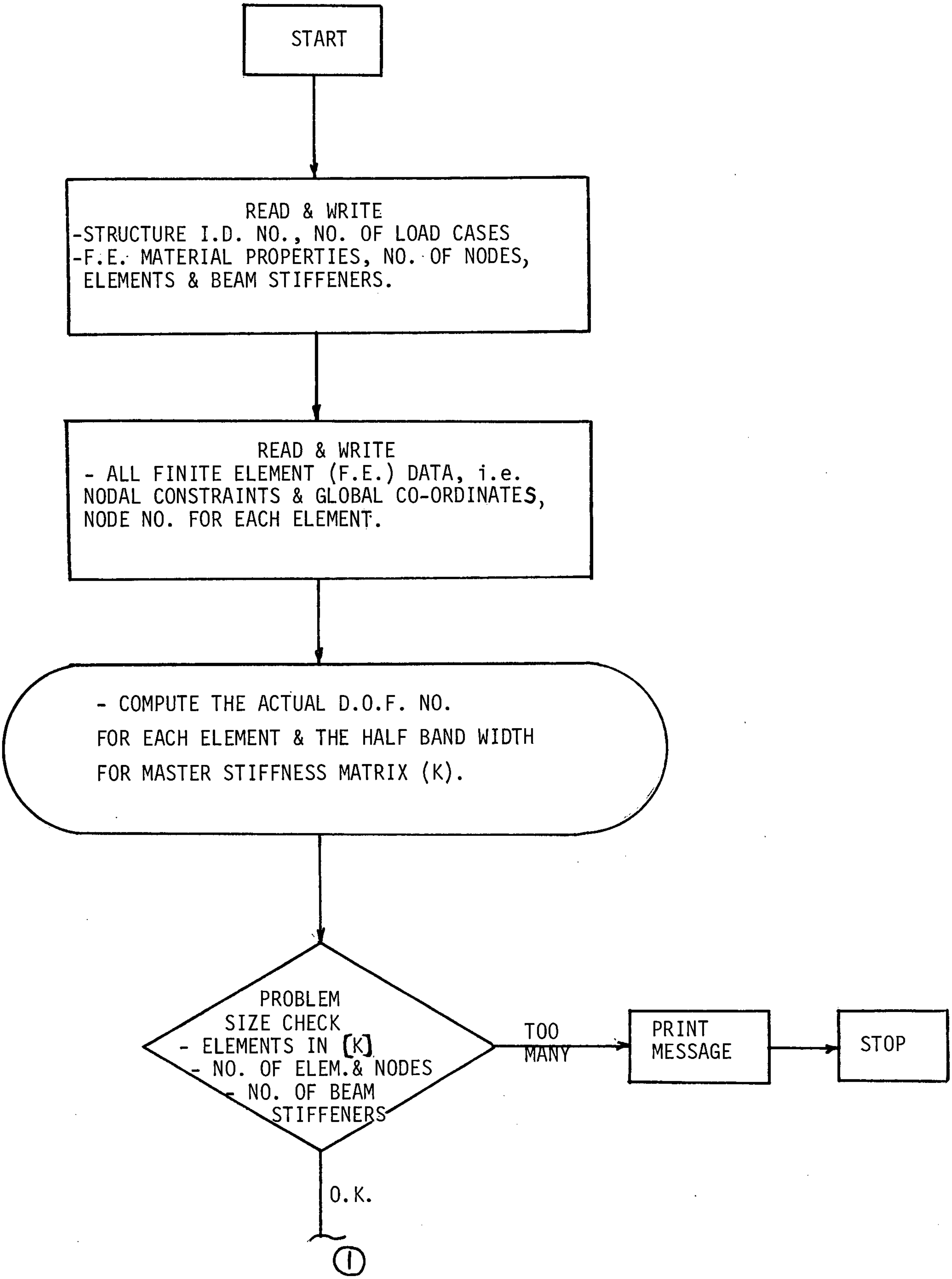

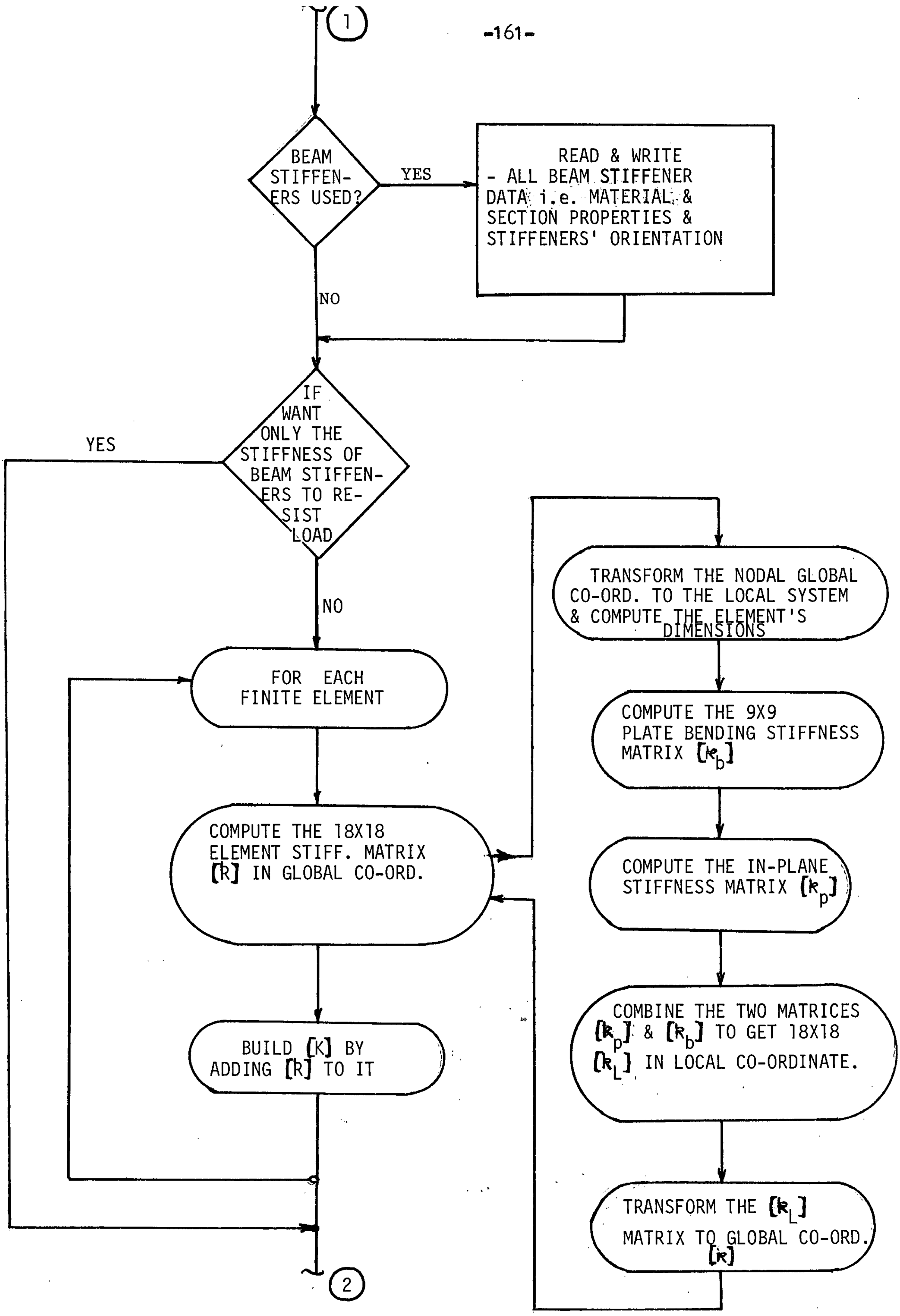
1
BEAM STIFFENERS USED?
YES
READ & WRITE - ALL BEAM STIFFENER DATA i.e. MATERIAL & SECTION PROPERTIES & STIFFENERS' ORIENTATION
NO
IF WANT ONLY THE STIFFNESS OF BEAM STIFFENERS TO RESIST LOAD
YES
NO
FOR EACH FINITE ELEMENT
COMPUTE THE 18X18 ELEMENT STIFF. MATRIX [k] IN GLOBAL CO-ORD.
BUILD [K] BY ADDING [k] TO IT
TRANSFORM THE NODAL GLOBAL CO-ORD. TO THE LOCAL SYSTEM & COMPUTE THE ELEMENT'S DIMENSIONS
COMPUTE THE 9X9 PLATE BENDING STIFFNESS MATRIX [k_b]
COMPUTE THE IN-PLANE STIFFNESS MATRIX [k_p]
COMBINE THE TWO MATRICES [k_p] & [k_b] TO GET 18X18 [k_L] IN LOCAL CO-ORDINATE.
TRANSFORM THE [k_L] MATRIX TO GLOBAL CO-ORD. [k]
2

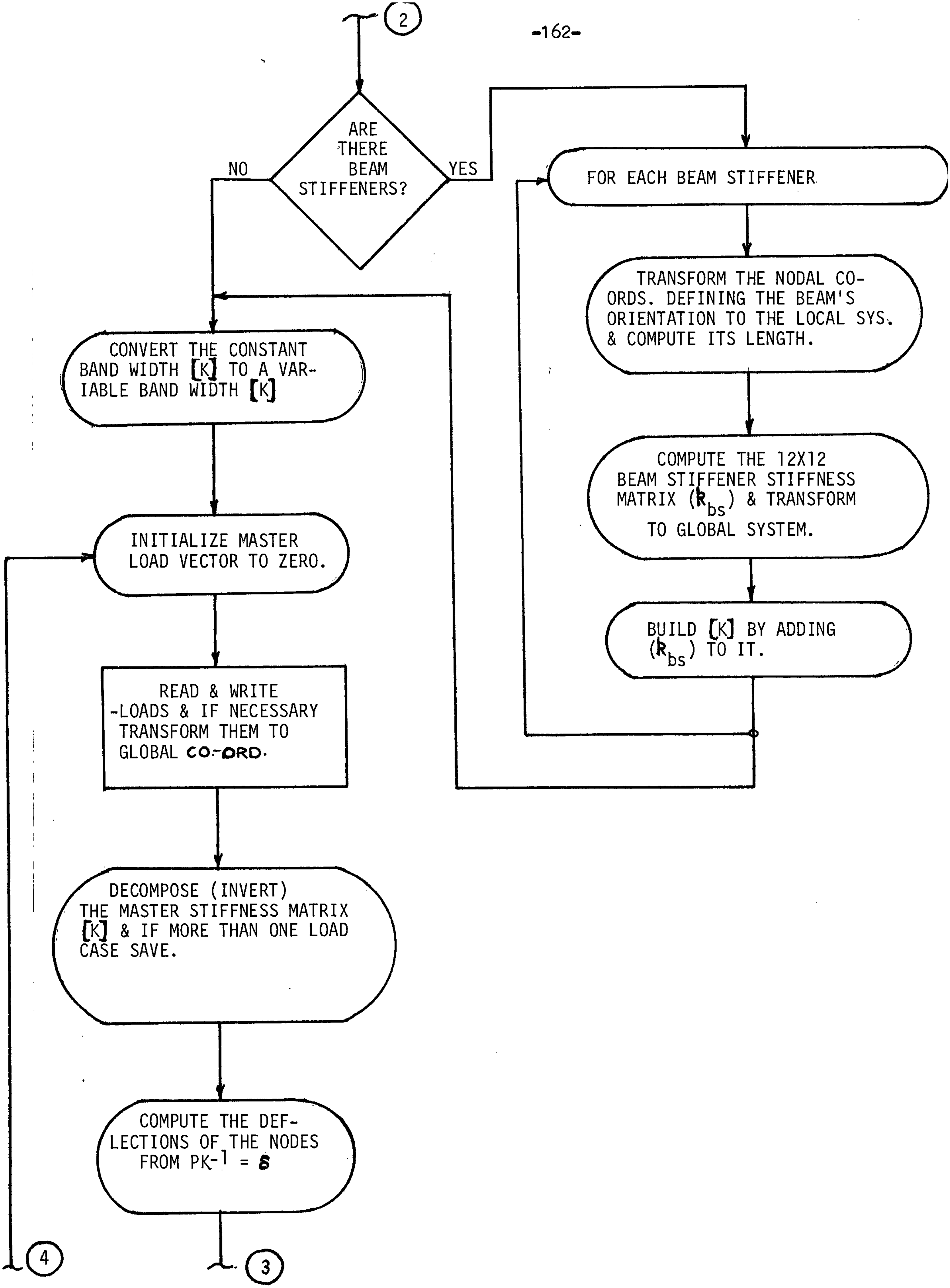
2
ARE THERE BEAM STIFFENERS?
NO
YES
FOR EACH BEAM STIFFENER
TRANSFORM THE NODAL CO-ORDS. DEFINING THE BEAM'S ORIENTATION TO THE LOCAL SYS. & COMPUTE ITS LENGTH.
COMPUTE THE 12X12 BEAM STIFFENER STIFFNESS MATRIX (k_{bs}) & TRANSFORM TO GLOBAL SYSTEM.
BUILD [K] BY ADDING (k_{bs}) TO IT.
CONVERT THE CONSTANT BAND WIDTH [K] TO A VARIABLE BAND WIDTH [K]
INITIALIZE MASTER LOAD VECTOR TO ZERO.
READ & WRITE -LOADS & IF NECESSARY TRANSFORM THEM TO GLOBAL CO-ORD.
DECOMPOSE (INVERT) THE MASTER STIFFNESS MATRIX [K] & IF MORE THAN ONE LOAD CASE SAVE.
COMPUTE THE DEFLECTIONS OF THE NODES FROM $PK^{-1} = \delta$
4
3

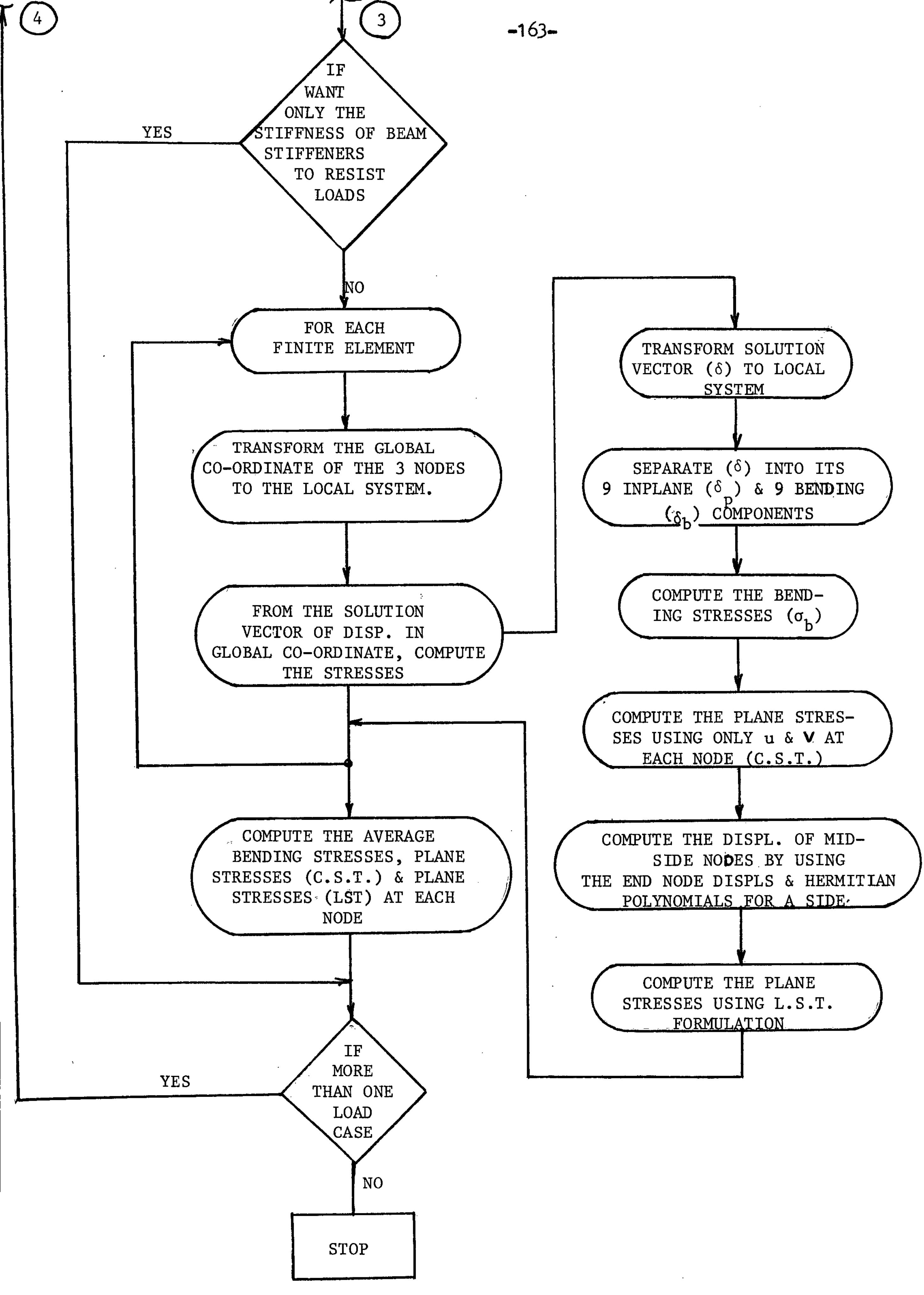
4
3
IF WANT ONLY THE STIFFNESS OF BEAM STIFFENERS TO RESIST LOADS
YES
NO
FOR EACH FINITE ELEMENT
TRANSFORM THE GLOBAL CO-ORDINATE OF THE 3 NODES TO THE LOCAL SYSTEM.
FROM THE SOLUTION VECTOR OF DISP. IN GLOBAL CO-ORDINATE, COMPUTE THE STRESSES
TRANSFORM SOLUTION VECTOR (δ) TO LOCAL SYSTEM
SEPARATE (δ) INTO ITS 9 INPLANE (δ_p) & 9 BENDING (δ_b) COMPONENTS
COMPUTE THE BENDING STRESSES (σ_b)
COMPUTE THE PLANE STRESSES USING ONLY u & V AT EACH NODE (C.S.T.)
COMPUTE THE DISPL. OF MID-SIDE NODES BY USING THE END NODE DISPLS & HERMITIAN POLYNOMIALS FOR A SIDE
COMPUTE THE PLANE STRESSES USING L.S.T. FORMULATION
COMPUTE THE AVERAGE BENDING STRESSES, PLANE STRESSES (C.S.T.) & PLANE STRESSES (LST) AT EACH NODE
IF MORE THAN ONE LOAD CASE
YES
NO
STOP

BIBLIOGRAPHY

1) Beavers, J.E., "Theoretical and Experimental Investigations of Non-Prismatic Folded Plate Structures", Ph.D. Thesis presented to Vanderbilt University, Nashville, Tennessee, 1974.

2) Cook, R.D., "Concepts and Applications of Finite Element Analysis", John Wiley and Sons, Inc., Toronto, 1974.

3) Cowper, G.R., Lindbert, G.M., Olson, M.D., "A Shallow Shell Finite Element of Triangular Shape", International Journal of Solids and Structures, Vol. 6, 1970, pp. 1133-1156.

4) Cowper, G.R., Kosko, E., Lindberg, G.M., Olson, M.D., "A High Precision Triangular Plate Bending Element", NRC No. 10621, Ottawa, 1968.

5) Johnson, C.D., and Lee, T.T., "Experimental Study of Non-Prismatic Folded Plates", Journal of the Structural Division, ASCE, No. ST6, June 1968, pp. 1441-1455.

6) Olson, M.D., "Analysis of Arbitrary Shells Using Shallow Shell Finite Elements", Thin-Shell Structures: Theory, Experiment and Design, Fung, Y.C. and Sechler, E.E., Prentice-Hall, Inc., New Jersey, 1974.

7) Olson, M.D., "Compatibility of Finite Elements in Structural Mechanics", Proceedings of World Congress on Finite Element Methods in Structural Mechanics", Bournemouth, England, Oct. 12-17, 1975.

8) Timoshenko, S., "Strength of Materials", D. Van Nostrand Co., New York, 1958.

9) Zienkiewicz, O.C., "The Finite Element Method in Engineering Science", Second Edition, McGraw-Hill Book Co., London 1971.

10) Clough, R.W., Johnson, R.J., "A Finite Element Approximation for the Analysis of Thin Shells", Int. J. Solids Struc., No. 4, pp. 43-60, 1968.